Aus dem
Veterinärwissenschaftlichen Department
der Tierärztlichen Fakultät der Ludwig-Maximilians-Universität München
Lehrstuhl für Anatomie, Histologie und Embryologie
Vorstand: Prof. Dr. Dr. Fred Sinowatz
Arbeit angefertigt unter der Leitung von Dr. Renate Weller, PhD, MRCVS

The Anatomy and Function of the equine thoracolumbar Longissimus dorsi muscle

Inaugural-Dissertation
zur Erlangung der tiermedizinischen Doktorwürde
der Tierärztlichen Fakultät der Ludwig-Maximilians-Universität München

Vorgelegt von
Christina Carla Annette von Scheven
aus
Düsseldorf

München 2010

Gedruckt mit der Genehmigung der Tierärztlichen Fakultät
der Ludwig-Maximilians-Universität München

Dekan:	Univ.-Prof. Dr. Joachim Braun
Berichterstatter:	Priv.-Doz. Dr. Johann Maierl
Korreferentin:	Priv.-Doz. Dr. Bettina Wollanke

Tag der Promotion: 24. Juli 2010

Für meine Familie

Table of Contents

ADP	adenosinediphosphate
ATP	adenosinetriphosphate
C	cervical vertebra
CY	coccygeal vertebra
EMG	electromyography
FL	fascicle length
Fmax	maximal isometric force
GM	middle gluteal muscle
IC	iliocostal muscle
L	lumbar vertebra
LD	Longissumus dorsi muscle
LF	left forelimb
LH	left hindlimb
LT	latissimus muscle
M	multifidus muscle
N	Newton
PA	pennation angle
PCSA	physiological cross-section area
R	rib
RA	rectus abdominal muscle
RF	right forelimb
RH	right hindlimb
S	sacral vertebra
SP	spinal muscle
Stdev	standard deviation
StE	standard error
T	thoracic vertebra
Vmax	maximal contraction velocity

I. Introduction

Musculoskeletal disorders of the back are very common in humans and their aetiopathogenesis, clinical presentation and treatment are well researched (Demoulin *et al.* 2007a; Demoulin *et al.* 2007b; Lu *et al.* 2002; van Roy *et al.* 2001). Back problems are also very common in horses and have been described in the literature as early as 1876 (Lupton 1876), but unlike in humans their aetiopathogenesis, diagnosis and treatment are one of the least understood disorders of the horse and present a challenge to the veterinary practitioner. Increasing demands on and expectations of horses as well as the recognition of poor performance in association with back pain has increased awareness of back problems among owners, riders and veterinarians. Intensive use of the horse as an athlete and in year-round intensive competition by riders with various grades of experience may lead to a higher incidence of predisposition to back injuries (Jeffcott 1979).

Several studies have investigated the anatomy of the equine vertebral column and its adjacent collagenous structures (ligaments) (Denoix 1999b; Haussler 1999; Jeffcott and Dalin 1980; Townsend *et al.* 1986) and the static and dynamic function of the equine back through kinematic and electromyographic studies (Faber *et al.* 2001a; Faber *et al.* 2002; Faber *et al.* 2000; Gomez Alvarez 2007; Haussler *et al.* 2001; Jeffcott *et al.* 1985; Licka *et al.* 2001a; Licka *et al.* 2004; Peham *et al.* 2001; Peham and Schobesberger 2006; Pourcelot *et al.* 1998; Tokuriki *et al.* 1997). However there is still a paucity of knowledge about the functional capacity of the back musculature of the horse.

Instability of the spine may play an important role in the development of back pain in humans (Panjabi, 2003), and it has been shown that spinal stability is related to recruitment and control of the paraspinal muscle stiffness (Moorhouse 2005). Clinical analysis indicated that unstable structural behaviour of the spine caused, for example, by sudden loading or unloading of the spine, may contribute to long-term material damage. Therefore the paraspinal muscle stiffness is important to prevent damage to the para- and intervertebral tissue which again can induce pain, further reduced spinal stability and a higher risk of injury or reinjury (Panjabi 1992a, b).

In humans, muscle strain of the epaxial musculature is the most common reason to develop back pain (Alexander 1985; Chiou *et al.* 1994). In horses suffering from back pain, a definite diagnosis is often only reached once skeletal changes have occurred (Jeffcott and Haussler 2004; Ross and Dyson 2002). The evaluation of back muscle structure and the detection of insufficient paraspinal muscle stiffness are important at an early stage before instability of the spine results in more advanced skeletal changes. Hence the development of a diagnostic

method which allows an early treatment of muscle problems results in less skeletal changes and therefore a good prognosis. In humans ultrasonography is used to visualise changes in back muscle morphology and EMG to evaluate muscle function and in this study I am adapting these techniques to the horse.

The varying and often controversial opinions with regards to the appropriate diagnostic and therapeutic methods in investigating and treating back problems in horses suggest that further evidence must be obtained to evaluate the importance of epaxial muscle function in sound horses and horses with back problems. Muscle morphology determines muscle function (Gans 1982; Sacks and Roy 1982) and in depth knowledge of the morphology of the epaxial musculature is a prerequisite in understanding how musculature is adapted to specific movement patterns during its normal functioning and how this changes with pathology. This knowledge will contribute to understanding the pathogenesis of back disorders and will provide the basis for the development of new diagnostic and therapeutic techniques.

The aim of this thesis is to determine the morphology and function of the largest muscle of the equine back, the Longissimus dorsi (LD).

The objectives of the study are

- To illustrate the gross anatomy of the equine LD by performing detailed dissections of pony and horse specimens

- To quantify the function of the equine LD in different gaits and different surfaces by measuring activation pattern electromyographically

- To establish the ultrasonographic anatomy of the equine LD by comparing ultrasonographic images to frozen sections

- To determine the intra- and interoperator reliability of ultrasonographic assessment of the equine LD

II. Literature review

II.1 Macroscopic anatomy

The back as part of the body axis forms the connection between front and hind limbs. As part of the trunk the back maintains body posture and supports the centre of gravity during locomotion by maintaining the equilibrium of the body (Boszczyk *et al.* 2001; Ritter 1995; Wada *et al.* 2006a). The function of the body axis is integrated in various locomotion activities with other body parts such as limbs, head, neck and tail but it is also exposed to the passive dynamic forces of the internal organs. These internal and external forces are transmitted onto the axis of the body and cause parts of it to bend, stretch, shorten, twist and shear (Koob and Long 2000). These movements act to transfer momentum from the body to the environment resulting in locomotion. During evolution the structure of the body axis adapted to different environments as different locomotor demands influenced the anatomical structure.

The following paragraph reflects briefly on the different role of the body axis throughout evolution and provides an understanding of the adaptation of the back to different locomotor demands between species.

II.1.1 Comparative evolution of the body axis

The body axis is the part of the musculoskeletal system, which maintains posture and transmits force between the limbs and the trunk (O´Reilly *et al.* 2000). It is composed of the bony vertebral column, the epaxial and hypaxial musculature, ligaments and other soft tissues. Depending on the primary modes of locomotion and the position of the limbs in relation to the body axis, the body axis shows specific features to accomplish specific movement patterns. Length and shape of vertebrae, muscles and soft tissue have been modified to adapt to specialised motion.

In tetrapods**,** for example, vertebrae and axial muscles show more specific modifications to adapt to their specific environment compared to the more simple axial structure of fish. For the survival on land the vertebrae became adapted to a wider range of motion. In the first terrestrial animals (amphibians, reptiles) the inherited lateral, undulating flexion of the fish is still apparent in combination with a symmetrical diagonal sequence of limb movement (Gambaryan 1974). The movement of these animals is more constricted to a horizontally

orientated plane than to a vertically orientated plane due to their limb posture. The limb posture is characterised by a lateral orientation of the long axis of the limb and a foot placement well to the side of the body (Rockwell *et al.* 1938). The myomeric structure of the epaxial musculature still produces lateral bending (Pabst 2000) whereas activity patterns of the predominantly myomeric hypaxial musculature shows bilateral and uniphasic activation pattern which in addition, suggests a stabilising function of this muscle group.

In mammals the vertebral axis supports the head, the neck and the trunk where the head attaches cranial to the cervical vertebral column and the trunk is suspended between front and hind limbs. The limbs are characterised by being more quadrupedal erect where the feet are placed more directly under the body (Rewcastle 1983). This posture allows asymmetrical movements in sagittal planes and changes the functional properties of the vertebral column where the trunk undergoes little or no lateral bending during locomotion (Hildebrand 1974). During evolution the axial musculature progressively abandoned the myomeric muscle construction as the appendicular musculature became more developed. The epaxial musculature is organised in three longitudinal tracts, the multifidus, longissimus and iliocostalis (Walker and Liem 1994). Muscle fascicles retain in a serial arrangement within each of the three muscle tracts reminiscent of the myomeric muscle morphology of fish and lower tetrapodes (Pabst 2000). Bilateral and biphasic muscle activity support the postural function of the epaxial muscle and stabilises the vertebral column against the ground reaction force (English 1980). The stiffer vertebral column acts also as an attachment site for surrounding muscles and transmits their forces to other parts of the body.
The construction of the body axis varies between mammals and is adapted to the overall body shape and to the special locomotor needs of different types of locomotion, such as cursorial locomotion, high speed locomotion, hopping, jumping and climbing, to mention just a few specialisations. These locomotor specialisations are revealed in the structure of the vertebrae, the musculature and the tendinous and ligamentous structures (Gambaryan 1974). The vertebral axis is not only part of the frame-work which stiffens the body but also protects internal organs and the spinal cord. In some vertebrae the body axis is stiffer due to a supportive role of withstanding gravity and external forces. In others mammal higher vertical and horizontal back mobility leads to an increase in stride length and therefore contributes to an increase in speed (Hildebrand 1959).

II.1.2 Axis of the equine body

The general description of the body axis showed variations of the anatomical structure and axial function during phylogenetic history. In this thesis I focus on the body axis of one of the largest terrestrial animals, the horse, specialised in both long distance and speed. In the following paragraphs the structure and function of the vertebral column, axial musculature and spinal ligaments of the horse is described in more detail.

II.1.2.1 Vertebral column of the horse

The equine body axis consists of the vertebral column which includes seven cervical, 18 thoracic, six lumbar, and five sacral and 15-21 coccygeal vertebrae, which are connected by ligaments, joints, the epaxial and hypaxial muscles and their tendons (Fig. 1).

The following paragraph describes the vertebrae in the thoracic, lumbar and sacral region which are the regions of particular interest to this study.

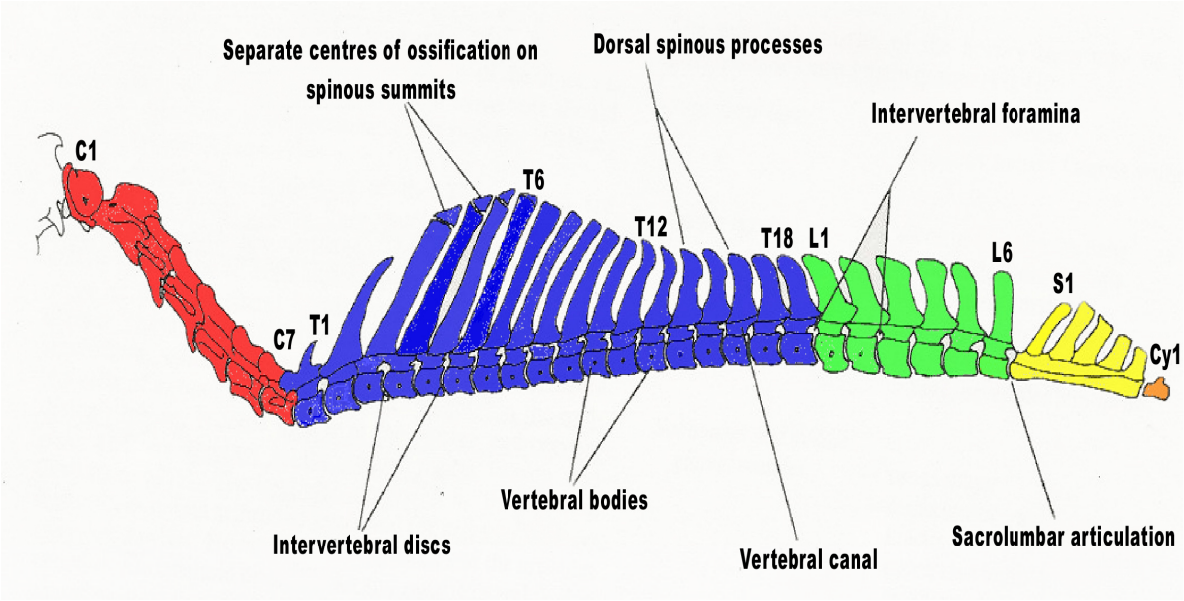

Fig. 1 Diagram of the equine vertebral column. Cervical vertebrae (C, red); thoracic vertebrae (T, blue), lumbar vertebrae (L, green), sacral vertebrae (S, yellow) and coccygeal vertebrae (CY, orange) (modified from Jeffcott and Dalin, 1980)

All vertebrae can be divided into three basic parts: vertebral body, vertebral arch and vertebral processes. These basic structures are adapted to the function of different body regions and therefore vary in their shapes.

Each vertebral body has a convex cranial and a concave caudal surface. They are separated from one another by fibrous intervertebral discs, forming fibrocartilaginous joints. The intervertebral discs contribute to weight bearing, axial shock absorption, and maintenance of vertebral flexibility. In the midthoracic region the intervertebral discs are the thinnest. From there thickness of the intervertebral discs increases in cranial and caudal direction. At the lumbosacral junction a wider intervertebral disc provides an increased range of dorsoventral motion in contrast to the thinner intervertebral discs at the thoracic region which have less mobility (Haussler 1999; Jeffcott and Dalin 1980). The vertebral arch surrounds the spinal cord which is secured by cerebrospinal fluid, the meninges, fat, and the vascular plexus. From the vertebral arch the arising spinous processes vary in their length and in their orientation along the spine. They act as serial levers for the attachments of muscles and ligaments. In the cranial thoracic vertebral column spinous processes resist forces from the head, neck and forelimbs transmitted by the nuchal and supraspinous ligament and adjacent muscles and aponeurosis. In the caudal thoracic and lumbar part of the spine they are exposed to forces from the hind limbs during locomotion. The attaching epaxial and hypaxial muscles flex, extend and rotate the spine by contraction while ligaments limit excessive motion (Gambaryan 1974; Nickel *et al.* 1984).

Bilateral cranial and caudal articular processes are located dorsally at the vertebral body and form intervertebral synovial joints (facet joints) between adjacent vertebrae. The orientation of the articular surfaces changes along the spine. This contributes to a different range of motion and support of the vertebral column. Due to their orientation they limit dorsoventral flexion in the thoracic spine whereas in the lumbar and sacrolumbar part lateral flexion and rotation is restricted.

The transverse processes have different sizes and orientations. They are used as horizontal levers for the attaching epaxial musculature which maintains posture and implies lateral flexion and rotation (Haussler 1999). The transverse processes of the last two or three lumbar vertebrae and the lumbosacral junction have intertransverse synovial joints which are involved in transferring propulsive forces from the hind limbs to the vertebral column and limit the lateral flexion and rotation (Haussler 1999).

The thoracic vertebral column (T) of the horse contains 18 vertebrae. The size of the vertebral body decreases from T1 to T11 and then increases again. Well defined ventral crests arise on

the ventral aspect of the vertebral bodies and provide attachment sites for ligaments and the hypaxial muscles.

The dorsal spinous processes are long and narrow. Their length increases up to T4-T6 (the highest point at the withers) and then decrease again to T13. Following thoracic dorsal spinous processes maintain the similar length. Their orientation changes in a characteristic way. At the thoracic vertebral column the orientation of the dorsal spinous processes incline in a caudal direction (T1-T15). At T16, which is the anticlinal vertebra, the dorsal spinous process points in vertical direction. The dorsal spinous processes of the following vertebrae (T17-T18) angle in a dorsocranial direction (Haussler 1999). The articular processes are orientated horizontally and create synovial joints between the cranial articular processes of one vertebra with the caudal articular process of the preceding vertebra. This arrangement of their articular surface leads to restricted lateral flexion and rotation in the thoracic region. The thoracic vertebral body has a cranial and caudal *fovea costalis cranialis* and *caudalis* where the heads of the ribs articulate with the vertebrae. The foveae articulares flatten towards the caudal thoracic spine and hence permit an increased range of motion of the ribs in caudal direction. Local variations in osteoarticular morphology relate to different ranges of mobility along the thoracic vertebral column. The height of the dorsal spinous processes as well as the articulation of the first ribs with the rib cage limits dorsoventral motion at the cranial thoracic region. In contrast shorter dorsal spinous processes, relatively thick intervertebral discs of the last thoracic vertebrae and the articulation with the asternal ribs allow relatively large movements around the thoracolumbar junction.

The five to seven lumbar vertebrae of the horse have larger, more massive vertebral bodies than those of the thoracic vertebral column. A prominent crest is located ventrally for the attachment of the hypaxial muscles. Their dorsal spinous processes are thin, wide bony plates of similar length. They have widened apeces and are orientated in a dorsocranial direction which results in minimal interspinal distances. The lumbar transversal processes are situated in a horizontal plane and become wider towards their ends. The orientation of the transverse processes of L1-L3 is in a lateral direction whereas the last three transverse processes are more craniolaterally orientated. There is a synovial articulation between the last two processes called the synovial intertransverse joint, which is a characteristic of the horse. The smaller lumbar vertebral processes such as the *processus articulares craniales* and *caudales* as well as *processus mamillares* are located at the base of the vertebral arch. The articular processes lie

in a vertical plane where the dorsally concave articular surface of the cranial process articulates with the ventrally convex surface of the caudal process.
The different anatomical features account partly for the relative stiffness of the lumbar region. Width and height of the spinous processes combined with narrowness of interspinous ligaments restrict the range of dorsoventral, lateral and rotational movement. In addition the size of the vertebral bodies, the prominent ventral crest and the strong ventral longitudinal ligament also contribute to the specific function of this section. The articular processes stabilise the vertebral column and also act as supplementary rigid devices against lateral flexion and axial rotation. In general, the lumbar vertebral column has a progressively decreasing range of motion in the caudal direction (Denoix 1999b; Haussler 1999; Hildebrand 1974; Nickel *et al.* 1984).

The lumbar sacral junction between L5-S1 shows anatomical particularities which allow the greatest range of dorsoventral movement (up to 20°) between the first thoracic and the last sacral vertebrae. The fact that the vertebral disk is thick and high, the dorsal spinous processes of L6 and S1 are widely divergent, the interspinous ligament is relatively weak and articular processes are orientated in a vertical direction contributes to the great amount of flexion and extension. However, excessive flexion is inhibited by soft tissue structures such as the strong aponeurosis of the longissimus dorsi muscle, the interosseous sacroiliac ligament and the ventral intertransverse lumbosacral ligament. Limiting factors for excessive extension are tension of the ventral intertransverse lumbosacral ligament, the ventral part of the intervertebral discs and locking of the articular processes.

The sacrum is composed of three to five sacral vertebrae which are joined and ossified into a single unit. The five vertebrae increase their length in the cranial to caudal direction. At the age of three to four years all five vertebrae are adhered to each other. The first sacral vertebra articulates with the last lumbar vertebra by the synovial intertransverse joint, the lumbosacral joint. The transverse processes are adhered to the lateral part of the sacrum which articulates with the transverse process of the last lumbar vertebrae in the intertransverse vertebral joint. The dorsal spinous processes incline in a caudal direction.

The number of coccygeal vertebrae varies between 15 and 21 vertebrae. The vertebrae are connected by thick intervertebral disks. The size of dorsal spinous processes and transverse

and articular processes diminish in caudal direction to little bony bumps or disappear (Nickel *et al.* 1984).

II.1.2.2 Axial musculature

The axial muscles are the skeletal muscles of the trunk and the tail. As this study focuses on the epaxial musculature a more detailed description of their embryonic development is included to explain how muscle structure and function develop. Due to their embryonic origin the epaxial muscles are arranged in multiple segments. The muscle segments arise from the embryonic source of the paraxial mesoderm, a cell layer formed during embryogenesis. The paraxial mesoderm differentiates into two different types of cell blocks, somites (trunk) and somitomeres (head). The somites become anatomically separated and arranged segmentally next to the neural tube, where they differentiate into myotomes, cells which build the musculature of the body walls. As functional musculature they grow along the vertebral column, the ribs and the body wall. A horizontal septum divides the myotomes in the dorsal region of the epaxial musculature and the ventral region of the hypaxial musculature.

II.1.2.2.1 Hypaxial musculature

The hypaxial musculature lies ventral to the transverse processes and is innervated segmentally by the ventral branches of the spinal nerves. It is classified in three groups. The first group is the subvertebral group. It is located ventral to the transverse processes of the vertebrae. The major function of this muscle group is the dorsoventral and lateral flexion of the spine. The second group, the rectus abdominis group, connects the cranial and caudal part of the body by running lengthwise along the ventral body wall. It supports the visceral cavity and also provides ventroflexion of the body. The third group contains the external oblique, internal oblique, transversus and intercostal muscles. They compose the lateral body wall of the body and aid lung ventilation.

II.1.2.2.2 Epaxial musculature

The epaxial muscles are located bilateral to the vertebral axis and lie dorsal to the transverse processes and the ribs. They form four different groups: the longissimus, the spinal, the iliocostal and the intervertebral muscle group, which consists of the multifidi muscles. Each segment of the epaxial muscles is innervated by a dorsal branch of the spinal nerves. A more detailed description of the structure and arrangement of the different epaxial muscles are given below.

The thoracolumbar longissimus dorsi muscle (LD) is the largest epaxial muscle and is important for back movement and stabilisation. It spans from the ilium all the way to the seventh and sixth cervical vertebrae. The dimension of the caudal LD at the lumbar region is massive but it reduces continuously in cranial direction. The original phylogenetic segmented structure of the muscle is reflected in many tapered muscle bundles which are orientated in the cranioventral and lateral direction and overlap each other. These muscle bundles originate from the tuber, the crest and the ventral surface of the ilium, the first three sacral vertebrae as well as the transverse and mammillary processes of the thoracolumbar spine. The LD is covered by the strong fascia thoracolumbalis which joins the supraspinous ligament and connects to the dorsal spinous processes of the thoracolumbar and sacral spine, the tuber coxae and sacrale of the ilium as well as to the iliac crest (Nickel *et al.* 1984). In the cranial part LD is also covered by the spinalis muscle. At the caudal end the cranial extension of the middle gluteal muscle overlies the LD and inserts onto the aponeurosis of the LD as far forward as T18.

The iliocostal muscle is relatively small and is located lateroventrally to the longissimus dorsi muscle. The caudal part of the iliocostal muscle fuses with the longissimus lumborum muscle in the lumbar region. The numerous muscle bundles of the thoracic and lumbar ilicostal muscle end cranioventrally in multiple tendons. These tendons bridge two to four intercostal spaces and insert on the caudal edge of the 1st-15th rib and on the last cervical vertebra. The iliocostal muscle act as a stabiliser of the spine and contributes to lateral bending (Nickel *et al.* 1984).

Each multifidus muscle is composed of five segmental multifidus fascicles with high tendinous portions. This muscle retains a primitive metameric structure and extends between vertebrae. The muscle bundles originate from the lateral aspect of the dorsal spinous processes and the pars lateralis of the sacrum running craniocaudally and insert on the articular, mamillary and transverse processes of the thoracic and lumbar vertebrae (Haussler 1999; Stubbs *et al.* 2006). The multifidi muscles produce dorsoventral motion (Stubbs *et al.* 2006) and support segmental stabilisation, proprioception and posture (Haussler 1999).

II.1.2.3 Spinal ligaments

The interaction of short and long spinal ligaments plays an important role in stabilising the vertebral column during posture and movement. There are three longitudinal ligaments: the

nuchal and supraspinous ligament, the dorsal longitudinal ligament and the ventral longitudinal ligament. The nuchal ligament originates at the occipital bone and inserts onto the first dorsal spinous processes of the thoracic vertebrae and the cervical vertebrae. It continues as the supraspinous ligament along the thoracolumbar spine and inserts on to the tips of the dorsal spinous processes until it ends at the dorsal spinous processes of the sacrum. The dorsal longitudinal ligament runs within the vertebral canal and the ventral longitudinal ligament attaches to the ventral aspect of the vertebral body, connecting the dorsal and ventral aspect of the vertebral bodies respectively. The short intervertebral ligaments such as the interspinous and intertransverse ligaments connect respective processes whereas the *ligamenta flava* span spaces between the vertebral laminae. The multiple interconnections between the vertebral structures stabilise the vertebral column and protect the spinal cord.

II.1.2.4 Function of the body axis of the horse

In the last two decades the knowledge of the functional anatomy and biomechanics of the vertebral column has been enhanced by a series of *in vitro* and *in vivo* studies (Audigie *et al.* 1999; Denoix 1999b; Faber *et al.* 2001a; Faber *et al.* 2001b; Faber *et al.* 2000; Gomez Alvarez 2007; Haussler 1999; Haussler *et al.* 2001; Jeffcott and Dalin 1980; Jeffcott *et al.* 1982; Licka *et al.* 2008; Licka *et al.* 2001a; Licka *et al.* 2004; Townsend *et al.* 1983). The knowledge of the fundamental kinematics along the vertebral column and the understanding of the influence of limb and neck movement on back motion are necessary to evaluate abnormalities of motion of the vertebral column.

II.1.2.4.1 In vitro kinematic evaluation of the back

A series of *in vitro* experiments were performed on the isolated equine vertebral column or on the whole axial skeleton, including rib cage and sternum. Moving the spine with and without the rib cage showed that the range of movement around different axis (dorsoventral, latero-lateral and rotational movement) varied between regions along the thoracolumbar vertebral column (Denoix 1999b; Jeffcott and Dalin 1980; Townsend and Leach 1984).

The greatest overall movement takes place in the lumbosacral joint (Denoix 1999b; Gambaryan 1974; Jeffcott and Dalin 1980; Townsend *et al.* 1983) followed by the first thoracic joint (Townsend *et al.* 1983). The regional range of dorsoventral motion was greatest between T9 and T18 compared to lesser movement at the regions T2-T8 and L2-L5. Lateral bending varied significantly between the different regions of the thoracolumbar vertebral

column. In the thoracic spine lateral flexion was always coupled with rotation around the longitudinal axis of the spine or vice versa. In contrast, in the lumbar spine rotation is rather limited and not associated with lateral flexion. The greatest lateral flexion and rotation was found between T9 and T14 (Townsend *et al.* 1983). However in the cranial part of the thoracic spine (T2-T9) the presence of the sternal ribs, the height of the dorsal spinous processes and the strong supraspinous ligament limit these movements. Also functional particularities of the lumbar spine, such as the shape, size and orientation of articular processes and frequent fusions of the lateral joints, restrict lateral and rotational movements between L4-L6 (Denoix 1999b; Schlacher *et al.* 2004; Townsend and Leach 1984). Due to the regional stiffness of the lumbar vertebral column it is more likely that different movements induce higher stresses (especially compressions) on bony structures of this region. In contrast, soft tissue strains on ligaments and joint capsules may occur predominately in the thoracic spine where the range of motion is greater.

In order to show detailed dynamic interaction between the anatomical structures precise measurements of the vertebral movement and the intervertebral mobility were performed (Denoix 1999b). Forces were applied to the vertebral column which imitated the physiological action of several trunk muscles via elastic straps. The behaviour of the different vertebral structures during flexion and extension as well as laterolateral flexion and rotation is displayed in Fig. 2 and Fig. 3 Table 1 and Table 2.

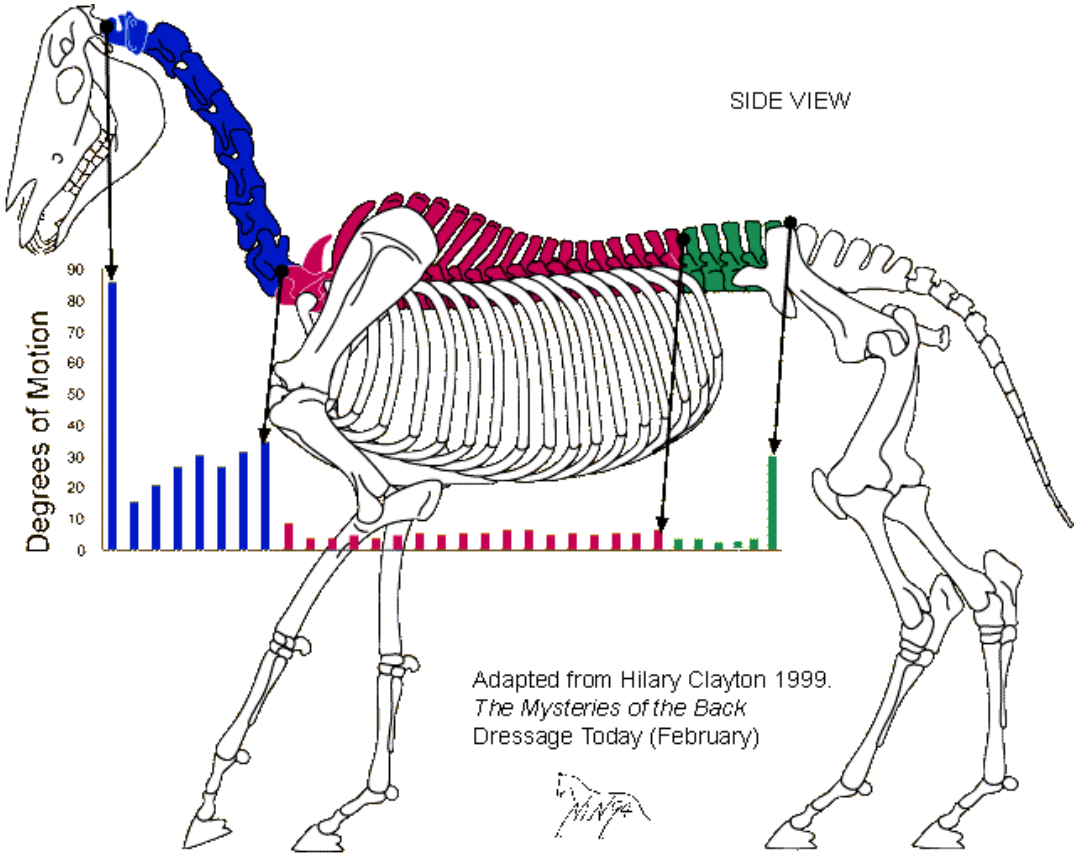

Fig. 2 The range of dorsoventral motion of the equine vertebral column (adapted from Clayton 1999)

Table 1 Mechanical behaviour of different anatomical structures of the equine vertebral column during flexion and extension.

Flexion	Extension
Shearing of the discs	Shearing of discs
Shearing and tension of the dorsal longitudinal ligament	Tension of ventral longitudinal ligament
Shearing of the ventral longitudinal ligament	Relaxation of dorsal longitudinal ligament
Cranial slide of the caudal articular process which leads to tension of the joint capsule and decreased pressure on the articular surface	Caudal slide of the caudal articular process leads to relaxation of the joint capsule and increases pressure on the articular surface
Cranioventral sliding of the spinous process which increases tension of the supraspinous ligament and induces shearing and tension in the interspinous ligaments	Caudodorsal slide of the dorsal spinous processes increases interspinous space and leads to relaxation of supraspinous, interspinous and flavum ligaments.
Tension of flavum ligament	

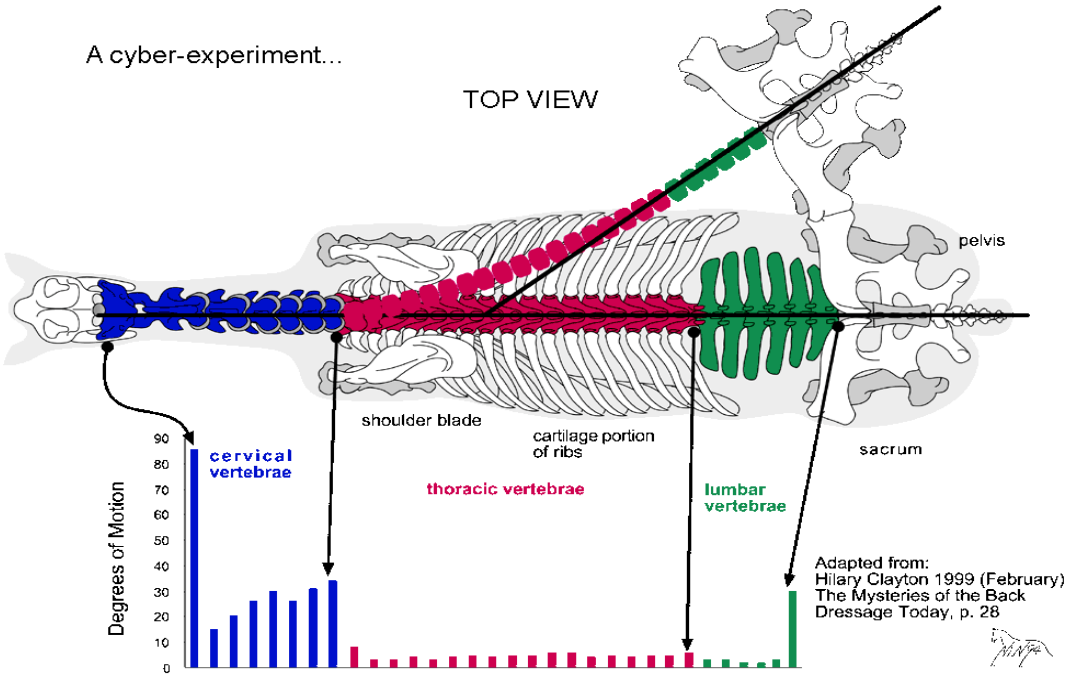

Fig. 3 The range of laterolateral motion of the equine vertebral column adapted from (Clayton 1999)

Table 2 Mechanical behaviour of different vertebral structures of the thoracic and lumbar vertebral column during left lateral bending and rotation.

	Right side of the thoracic vertebral column	**Left side of the thoracic vertebral column**
Left lateral flexion	Separation of the articular processes Craniomedial sliding of the caudal articular processes Tension of the articular capsule Increased mobility of the ribs	Left sliding of the caudal left articular processes Moderate tension of the articular capsule Locking of the ribs
Left rotation	Separation of the articular processes Lateral sliding of the caudal articular processes Tension of the articular capsule	Right sliding of the caudal left articular processes Tension of the articular capsule
	Right side of the lumbar vertebral column	**Left side of the lumbar vertebral column**
Left lateral flexion	Separation of the lateral part of the articular processes Craniomedial sliding of the caudal right articular processes Tension of the articular capsule	Covering and compression of the lateral part of left articular processes Caudal sliding of caudal left articular processes Relaxation of the articular capsule
Left rotation	Lateral compression of the lateral part of the right articular processes Craniolateral sliding of the caudal right articular processes Relaxation of the articular capsule	Separation of the lateral part of the articular processes Medial sliding of the caudal left articular processes Tension of the articular capsule

II.1.2.4.2 In vivo kinematic evaluation of the back in different gaits

In vivo kinematic studies focused on quantifying motion of the equine back during normal, physiological movements and abnormal back movements during different gaits (Audigie *et al.* 1999; Back and Clayton 2001; Cassiat *et al.* 2004; Faber *et al.* 2001a; Faber *et al.* 2001b; Faber *et al.* 2000; Gomez Alvarez 2007; Haussler *et al.* 2001; Holm *et al.* 2006; Johnston *et al.* 2004; Licka and Peham 1998; Licka *et al.* 2001a; Licka *et al.* 2001b; Pourcelot *et al.* 1998; Robert *et al.* 2001a; Robert *et al.* 2002; Wennerstrand *et al.* 2004).

To quantify the rather complex and often subtle motion of the vertebral column computerised motion analysis systems are commonly used. This involves the use of infrared cameras that register light reflected from markers fixed to bony landmarks of the spine and the pelvis and identify the position of those markers in three dimensions. Assessment of the spine on live horses is complicated by skin movement and overlying muscles which restrict the direct observation of the spine. However, some studies were performed with markers inserted into the dorsal spinous processes to avoid marker movement with the skin (Faber *et al.* 2001a; Faber *et al.* 2001b; Faber *et al.* 2000; Haussler *et al.* 2001). Comparisons of skin markers with bone pin markers showed skin markers to be a sensitive and accurate tool to measure back kinematics. The collected kinematic data was processed to angular movement patterns which describe the time of movement versus the angle of three different axes in relation to foot placement. This results in specific movement patterns around the three-dimensional axis of the spine during a stride cycle for each gait. In general, the largest magnitudes of flexion and extension were detected in the lumbosacral joint (Faber *et al.* 2001a; Faber *et al.* 2001b; Faber *et al.* 2000; Haussler *et al.* 2001). Between T14-T16 less flexion and extension occurred although the magnitude for lateral bending and axial rotation were large in all gaits. The smallest amount of movement in all gaits appeared between L1-L3 (Haussler *et al.* 2001).

Walk

During walk back flexion and extension run through two full oscillations per stride cycle. When the left hind limb contacts the ground, T10 rotates clockwise and S3 counter-clockwise which leads to the extension of the back. Flexion is produced by counter-clockwise rotation of the thoracic region and the clockwise rotation of the pelvic region and occurs always whenever the forelimb contacts the ground and the ipsilateral hind-limb is in early swing phase (Faber *et al.* 2000). Peak maximal flexion is obtained slightly earlier at the lumbosacral junction from where it continues in a cranial direction along the spine (Haussler *et al.* 2001). The mean (±stdev) range of dorsoventral motion increases in a craniocaudal direction and represents 4.2° (±1.6°) at T6, >8° at T10 and T13 and 6.5°-7.0° for the region caudal to T13.

The limited range of flexion and extension is due to the construction and orientation of the dorsal spinous processes. Especially in the thoracic region, tangential facet joints restrict dorsoventral mobility.

Lateral bending is a single periodic motion during the stride cycle where T10 rotates to the opposite side of S3. In L1 almost no rotation is detectable. The maximal and minimal bending angles are more distinct at T6 whereas in the sacral area they are less obvious. The sacral region bends towards the side of the respective hindlimb, for example left hindlimb, long before the actual hoof contact with the ground occurs. The thoracic region rotates to the opposite side (clockwise) which results in bending towards the right side. The range of motion was less than 3° for the caudal thoracic and cranial lumbar region. There was 6° of laterolateral motion in the pelvic area.

During axial rotation all vertebrae between T13 and the pelvis act as one segment. The mean (±stdev) range of axial rotation increases in a cranial 4.3° (±1.2°) to caudal 13.1° (±1.2°) direction. The thoracic part, being closest to the forelimb, acts as point of rotation (Faber *et al.* 2000). Maximal axial rotation to the left occurs when the right forelimb is close to hoof contact. In reverse maximal rotation to the right happens when the left forelimb is close to hoof contact (Haussler *et al.* 2001).

In walk the measurable laterolateral and rotational mobility along the vertebral axis corresponded to the *in vitro* measurements although the magnitude of the range of motion was much smaller in vivo (Faber *et al.* 2000).

Trot

In trot flexion and extension show a bimodal sinusoidal pattern per stride cycle. Thoracic and sacral vertebrae move out-of-phase by 180° where L1 moves out-of-phase by only 90° in transition to both ends of the vertebral column. Starting from the foot contact of the left hind limb T10 rotates in a clockwise and S3 in a counter-clockwise direction resulting in extension of the back. Extension lasts until mid-stance then T10 starts to move counter clockwise and S3 to the opposite direction inducing back flexion. When the right hind limb contacts the ground the movements reverse and the back extends again (Audigie *et al.* 1999; Faber *et al.* 2001a; Haussler *et al.* 2001; Pourcelot *et al.* 1998). The mean (±stdev) range of dorsoventral vertebral motion has the lowest angular value at T6 and S3 2.8° (±0.8°) and (±0.9°) and the highest at T10 4.9° (±1.4°). A slightly different result was reported for a study using skin markers where the highest dorsoventral motion occurred at T16 (Licka *et al.* 2001a) and at the thoracic and lumbosacral angle (3.9°) respectively (Audigie *et al.* 1999). These differences may be due to variations in the experimental set up, data processing and analysis. Movement

of the head has been reported to influence the rotation of the thoracic vertebrae (Gomez Alvarez 2007; Rhodin *et al.* 2005).

Lateral bending is a single periodic movement in trot. As in walk, T10 and L3 rotate out-of-phase by 180°. At hoof contact of the left hind limb L1 and S3 rotate clockwise while T10 moves in the opposite direction. These rotations induce bending towards the non-supporting hind limb (clockwise rotation of the horse). At midstance at the moment of maximal propulsion L1 followed by S3 rotates in a counter clockwise direction while T10 changes to clockwise rotation after the left hind limb lifts off. Now the vertebral column is pushed towards the right side of the horse (counter clockwise bending). This sideway force is absorbed by musculature which promotes a forward movement. The range of motion is 4.6°-5.8° for all vertebrae except T10 and T13. They have a smaller range of motion 3.1°-3.3°.

During axial rotation T10 rotates counter clockwise when the left hind limb and right fore limb hit the ground. By the progressive loading of the right forelimb the cranial dorsal part of the trunk moves towards the unsupported left side. At midstance when the right forelimb starts to push off and the left hind protracts T10 rotates clockwise and clears the way for the protracting leg. After maximal propulsion T10 rotates counter clockwise again when the left hindlimb is about to contact the ground.

The caudal part of the vertebral column (S3) moves counter clockwise during the first part of the stance phase toward the supporting hindlimb. At the end of the concussion phase axial rotation changes towards the unsupported side to which side also the pelvis drops. After midstance the pelvis is rotated towards the supporting side by the push-off forces and hip extensors. This means counter clockwise rotation and clearance for the opposite hindlimb during protraction. In the suspension phase S3 moves in clockwise direction while the right hindlimb reaches forward to contact the ground (Faber *et al.* 2001a; Haussler *et al.* 2001; Licka *et al.* 2001a).

Canter

Canter is an asymmetric gait and with a rather complex movement pattern. In comparison to walk and trot a greater amount of segmental vertebral motion occurs during canter (Faber *et al.* 2001b; Haussler *et al.* 2001).

In canter flexion and extension show a unimodal movement pattern of the back during one stride cycle which is closely related to limb placement. The thoracic region of the vertebral column moves differently to the sacral region in terms of peak maximal and minimal angles and timing. Starting from the hoof contact of the trailing hind limb the back is extended and T10 rotates clockwise (looking at the left side). At the end of the stance phase of the diagonal

limbs T10 rotates counter clockwise and the back begins to flex. This rotation reverses again at the end of the support phase of the leading front limb. The cranial part of the body is elevated by the upward direction of the impulse of the leading forelimb and the active LD and the back extends. In contrast flexion and extension of the caudal end of the back coincide with the foot contact of the trailing hind limb and leading forelimb respectively. When the hoof of the trailing hind limb hits the ground the leg acts as a pillar and the body rotates forward over the limb while the sacral area rotates counter clockwise. After the leading fore limb contacts the ground the equine body rotates over the front limb, the sacrum rotates in a clockwise direction while the caudal part of the body moves under the horse. The mean (±stdev) range of motion for flexion and extension is 12.1° (±2.1°) at T6, decreases to 6.4° (±0.8°) towards the lumbar region and increases again to 15.8° (±1.3°) at the caudal lumbar region (Faber *et al.* 2001b).

Only for the cranial part of the thoracolumbar spine lateral bending is a single periodic pattern for every stride cycle. The clockwise rotation of T10 is initiated by the forward movement of the body when the trailing forelimb contacts the ground. The reverse rotation is induced by forward movement of the body when the leading forelimb hits the ground. The counter clockwise rotation continues throughout the suspension phase and the single support phase of the trailing hind limb. In contrast, L1 and S3 have a biphasic movement pattern throughout the stride cycle. The pelvis rotates clockwise when the hoof of the trailing hind limb touches the ground. The direction of the rotation changes to counter clockwise when the diagonal limbs contact the ground and maximal forward propulsion exerts an oblique force on the vertebral column. After the maximal propulsion of the leading hind limb S3 rotates clockwise. During the suspension phase S3 rotates counter clockwise away from the trailing hind limb. This assists protraction of the trailing hind limb.

Axial rotation appears in two periods per stride cycle when all vertebrae rotate simultaneously. The first period starts when the trailing hind limb contacts the ground and the vertebral column rotates counterclockwise towards the trailing hind limb. At midstance of the trailing hind limb the rotation reverses towards the unsupported side. This movement is induced by the forward and upward movement of the body during push off. The second period begins when the leading forelimb touches the ground and continues until the end of the stride cycle which corresponds to the push-off phase of the leading front limb and the suspension phase. In the second period vertebrae move independently from each other.

II.1.2.4.3 Factors influencing kinematic studies

Kinematic studies show that the interaction between movements of the limbs and the vertebral column leads to efficient locomotion (Faber *et al.* 2001a). Changes in the interaction with speed, lameness and back pain or factors like age, breed and training status can influence movement pattern and efficiency of locomotion (Cassiat *et al.* 2004; Jeffcott *et al.* 1982; Johnston *et al.* 2002; Licka *et al.* 2001a; Robert *et al.* 2001a; Robert *et al.* 2002).

Increasing speed has been shown to alter the sinusoidal movement pattern of the back in horses trotting on a treadmill. Influenced by higher stride frequency and decreased stance time within a stride cycle the peak values of vertical displacement of the vertebral column occurred significantly earlier in the stride cycle when speed increased (Back and Clayton 2001; Drevemo *et al.* 1980; McLaughlin *et al.* 1996). Although the angles of thoracic and thoracolumbar flexion decreased significantly maximal angles for extension remained unchanged. This resulted in a decrease in the overall range of back motion. In contrast the peak vertical displacement for the lumbosacral region did not change (Robert *et al.* 2001a).

Horses with back pain showed alterations of the angular movement pattern of the spine. A comparison between horses with back dysfunction and sound horses showed significant differences in the range of motion predominantly at the thoracolumbar spine. In affected horses flexion and extension was significantly reduced during walk and trot at the thoracic and thoracolumbar vertebral column. Other significant findings for horses with back dysfunction were increased lateral bending at the thoracic spine and reduced axial rotation of the pelvis. Back pain also affected the stride length which was significantly shorter at walk although there was no difference in trot. The alterations of the range of motion at the thoracic spine and the pelvis have been discussed as adjustments through neuromuscular control mechanisms to avoid pain. This study concluded that horses trying to avoid back pain by reducing dorsoventral flexion and extension and thus limit the movement between the segments of the thoracolumbar part (Wennerstrand *et al.* 2004). In another study increased back stiffness with a slight convexity towards the pain-free side was demonstrated by induced unilateral back pain. These horses were unable to maintain their top speed after back pain induction (Jeffcott *et al.* 1982).

This result stands in contrast to findings of increased back motion after unilateral pain induction (Gomez Alvarez 2007). An increase of lateral spinal motion towards the painful side was observed and explained by reduced muscle function due to muscle pain. The reverse

movement pattern towards the non-affected side suggested stiffening of the painful muscle and abnormal muscle function (Gomez Alvarez 2007). A previous study of induced back pain demonstrated only a slight convexity of the back but showed increase rigidity and an inability to perform at high speed (Jeffcott *et al.* 1982).

Other factors which seemed to have an impact on the mobility of the back are breed and age. Dressage horses, for example, tend to have longer lumbar backs than show jumping horses (Cassiat *et al.* 2004; Johnston *et al.* 2002). The length of the thoracic back has been shown to correlate positively with the amount of laterolateral motion of the lumbar spine in walk and trot. As a consequence these horses may be prone to a higher risk of caudal back injuries (Johnston *et al.* 2002). A significant negative correlation was found between age and the range of flexion and extension. Older horses tended to have stiffer backs and therefore reduced dorsoventral flexion in the thoracolumbar area caused by degenerative changes of articular and spinous processes (Johnston *et al.* 2004).

II.1.2.4.4 Trunk muscle activity

Trunk musculature has already been described as an important body part which contributes to maintaining stability, balance and locomotion of the equine body. Superficial epaxial muscles, such as the LD, are dynamic and play a role in regional vertebral motion, whereas deep epaxial muscles, for example multifidus, have a more static function and are active in segmental stabilisation, proprioception and posture. The epaxial muscles extend the back during bilateral activation and produce lateral flexion and rotation when activated unilaterally (Nickel et al, 1986). Several studies have been performed to evaluate the role of different trunk muscles by using electromyography (EMG) to record muscle activity during movement (Licka *et al.* 2008; Licka *et al.* 2004; Peham *et al.* 2001; Robert *et al.* 1999; Robert *et al.* 2001b). EMG is a technique which is widely used to measure excitation patterns of muscles. The electrical activity emitted by active muscle fibres is received by special sensors and recorded as the electrical activity pattern of local muscle fibres (Lieber 2002).

Two of the major muscles involved in trunk movement are the LD and the Rectus abdominis muscle (RA). They have antagonistic activity and function. During walk LD showed only weak activity bursts in the middle of the stance phase of both hind limbs while RA was not active throughout the stride cycle (Tokuriki *et al.* 1997). In trot, RA is active during extension while LD is active during flexion of the back. The activation pattern for both muscles shows two activity bursts per stride cycle. RA is active during the first part of the diagonal stance phase when initial forward and downward movement of the body and acceleration of visceral

organs continue. These observations lead to the opinion that extension is a passive phenomenon (Robert *et al.* 1998; Tokuriki *et al.* 1997). The function of RA, and also of the active obliquus externus abdominis muscle, is thought to oppose the forces exerted by the moving visceral mass and abdomen and therefore limit the passive thoracolumbar extension. The LD and also the multifidi muscles have a reciprocal activity to RA and oliquus externus abdominis. During the second half of the diagonal stance phase the LD is activated until the early swing phase. This is the time when the back is flexed due to trunk acceleration and due to released energy from the strong thoracolumbar fascia, ligaments and fibrous tissue (Alexander *et al.* 1985). The active LD is presumed to stabilise the back and counterbalance back flexion during that phase (Robert *et al.* 1998; Tokuriki *et al.* 1997). During canter the LD is active on both sides of the back from early or middle stance phase to the end of the swing phase of the leading hind limb. LD is thought to stabilise the back and to support the hind limb during the suspension phase (Tokuriki *et al.* 1997).

Corresponding to vertebral column locomotion, the associated muscle activity of the RA and LD shows an increase of activity with higher speeds at trot. In compliance with the movement pattern of the back the activity bursts of RA and LD occur earlier in the stride cycle. The duration of the first burst of RA activity is decreased while the second burst remains the same. This can be explained by the shortened stance phase of the ipsilateral hind limb. The required force counterbalancing the inertial force of the abdomen and visceral mass is reduced and therefore the activity of RA is shortened. As the velocity of the horse increases the LD exerts higher forces to stabilise the back by holding the vertebrae together. The two activity bursts appear during the swing phase. The swing phase duration is not as obviously affected by speed as the stance phase therefore the LD activity duration remains unchanged (Robert *et al.* 2001a). The suggestion was made that both muscles act mainly to restrict excessive motion along the vertebral column and the trunk which would provide a stiffer platform for fast swinging legs which again transmit propulsion (Rooney 1982).

EMG data from trotting horses on an incline revealed a significant increase of LD activity duration and the tendency of RA activity to be longer (Robert *et al.* 2001a). It was suggested that higher muscle activity is required to stiffen the back and neck during propulsion when paravertebral muscles work concentrically (Denoix and Pailloux 2001). Increased stability of the body also facilitates raising the body up an incline against gravity.

II.2 Microscopic anatomy

Skeletal muscles perform dynamic and static work which permits locomotion and maintains body posture and/or position. To understand the biomechanics of the LD function, it is

essential to know the basic microscopic structure of the muscle, the gross anatomical arrangement and the basic muscle mechanics. This chapter provides a brief description of the composition and structure of skeletal muscle and gives a short introduction to muscle mechanics and force production.

II.2.1 Skeletal muscle morphology

Each muscle belly is composed of a multitude of muscle fascicles which are surrounded by a fibrous fascia, the epimysium. The muscle fascicles are enclosed by a dense connective sheath, the perimysium. Muscle fascicles are composed of muscle fibres which are again surrounded by loose connective tissue, the endomysium, as well as nerves, capillary blood vessels and the sarcolemma, a delicate plasma membrane. Each fascicle contains numerous contractile elements, the myofibrils, which can again be subdivided in the smallest functional units of the contractile muscle system, the sarcomeres. Epi-, peri-, endomysium and sarcolemma act as parallel elastic structures and are continuous with the muscle tendons which attach to the skeleton. These structures transmit the force produced by muscle contractions onto the bone. The layers of collagen fibres also provide a structural frame work for the contractile components of the muscle and facilitate economic force transmission (Nordin and Hirsch-Frankel 2001).

II.2.1.1 The Sarcomere

The sarcomere is the basic functional unit of the muscle. The repeated serial arrangement of sarcomeres in the myofibril gives the skeletal muscles the typical striated pattern which is visible under the light microscope. The borders of the sarcomeres are defined by the so-called Z-lines (Zwischenscheiben). Each sarcomere is composed of thin and thick protein molecules, so-called actin and myosin filaments, which are arranged parallel to each other. The parallel myosin (thick) filaments are located in the centre region of the sarcomere. Their ends connect to the Z-line by titin strands, a highly elastic protein (Alexander 2003). Myosin filaments are responsible for the dark pattern of the striated muscle which is called A-(anisotropic)-zone whereas the actin (thin) filaments make up the light pattern of the striated muscle (I-zone). Actin filaments are attached to the Z-line at either end of the sarcomere. From the Z-line they extend towards the centre where they overlap with the myosin filaments.

Each myosin filament represents hundreds of myosin molecules which are bundled together. Every myosin molecule has a long shaft, the “tail” portion, and a head on one end of the tail,

called the cross-bridge. The head contains a binding site for actin and an enzymatic site to catalyse the hydrolysis of ATP (Adenosinetriphosphate) which provides the energy for muscular contractions. According to the cross-bridge theory (Huxley 1957), the myosin heads contact with the actin filaments and pivot around their fixed position on the surface of the myosin filaments. This movement produces the sliding of the actin filaments towards the centre of the sarcomere until the cross-bridges detach and reattach itself to another site further along the actin filaments. During continuing muscle shortening this whole circle of cross-bridge attachment, pull and detachment repeats every 5 nm further along the actin filaments (Kitamura *et al.* 1999). The repetitions result in a force transmission along the filaments which again is transmitted onto the tendon.

The contraction velocity of sarcomeres is determined by the metabolic pathway and the rate at which energy is made available for these sarcomeres. Enzymatic splitting of adenosinetriphosphate (ATP) into adenosinediphosphate (ADP) provides the energy to move myosin cross-bridges during their attachment to actin filaments. Observations have led to the identification of three distinct metabolic rates of muscle fibres which then were divided into three major muscle fibre types, Type-I muscle fibres, Type IIa muscle fibres and Type IIb muscle fibres.

II.2.1.2 Neuromuscular control

The performance of muscle contraction is controlled by the smallest functional unit of the skeletal muscle, the motor unit.

Skeletal muscles are innervated by somatic motor neurons which propagate electrical signals (action potentials) from the central nerve system (CNS) to the muscles. At the muscle the alpha motor neurons divide into multiple branches from which each terminal branch connects with a single muscle fibre and forms the neuromuscular junction (Prentice and Voight 2001).

The functional connection between a motor neuron and the corresponding muscle fibre is a chemical synapse, called the end-plate. This neuromuscular synapse contains many vesicles of a neurotransmitter, acetylcholine. Action potentials travelling along the presynaptic membrane of the motor neuron release acetylcholine which depolarizes the postsynaptic membrane of the muscle fibre. Once the postsynaptic membrane is depolarised to its threshold an action potential propagates along the membrane of the muscle fibre. The acetylcholine is rapidly hydrolysed by acetylcholinesterase so that the muscle fibre is ready to respond to the next action potential (Kandel *et al.* 2000).

An alpha motor neuron and all corresponding, innervated muscle fibres form a single motor unit represent the smallest functional unit of the skeletal muscle. The whole muscle contains many motor units which can be made to contract independently (Prentice and Voight 2001). Electrical signals, which stimulate the motor neuron, sufficiently activate all corresponding muscle fibres in the motor unit. They contract either maximally or not at all as response to stimulation.

The size of the motor unit depends on the size and the function of the muscle. The motor units of small muscles which perform a high degree of coordination contain only a small number of muscle fibres whereas in large muscles the number of muscle fibres per motor unit can be up to 1000-2000 fibres. This means that motor units which contain more muscle fibres can exert larger forces per nerval stimulation. The size and functional properties of motor units vary not only between muscles but also within a muscle. The electrical currents resulting of all activated muscle fibres of a motor neuron generate an electrical signal. The pattern of this electrical signal reflects the relative timing and amplitude and can be recorded as an electromyogram (EMG) (Kandel *et al.* 2000). EMG studies have demonstrated that some muscles have discrete compartments which are innervated by different motor nerve branches and contain different corresponding muscle fibre types. Despite the fact that they are in the same muscle they can show different muscle activation patterns (Lieber 2002). Nevertheless there are muscles which are predominately designed for a specific activity and therefore they are composed of a higher percentage of either slow-twitch or fast-twitch muscle fibres. Such differences can be found, for example, between the soleus muscle and the medial and lateral gastrocnemius of the cat. The soleus muscle which comprises mainly of slow-twitch fibres maintains postural control and is active during walk. In contrast lateral and medial gastrocnemius muscles consist of fast-twitch fibres and are active during faster gaits to provide more rapid and forceful ankle extension (Biewener 2003).

II.2.2 Structural arrangement of skeletal muscle

The internal structure of the muscle belly and the muscle fibre arrangement has a huge influence on muscle function and force generation.

II.2.2.1 Muscle architecture

Muscle can be divided into parallel-fibred, fusiform and pennate-fibred muscles (Fig. 4-Fig. 6) depending on the arrangement of the muscle fibres.

In parallel fibred muscles, muscle fibres run from origin to insertion, parallel to the pull of the tendon and force transmission. These muscles are characterised by relatively long muscle fibres with little or no tendon. In contrast, pennate muscles have longer tendons and an additional internal tendon or aponeurosis. The muscle fibres run at an angle to these tendinous structures that means at an angle to the line of force transmission. Pennate muscles have generally shorter muscle fibres than parallel fibred muscles. During contraction the change of muscle fibre length is less than the muscle length change.

Fig. 4 The equine sartorius muscle as an example for a parallel fibred muscle. Muscle fibres extend the full length of the muscle belly. The force transmission to the tendon is parallel to the muscle fibre arrangement. (Courtesy of Dr. R. Payne, The Royal Veterinary Collage).

Fig. 5 The cranial tibialis muscle as an example for a bi-pennate muscle. Muscle fibres are arranged in an angle to the central tendon and therefore are orientated at an angle to the line of pull. (Courtesy of Dr. R. Payne, The Royal Veterinary Collage)

Fig. 6 The equine superficial digital flexor muscle as an example for a multi-pennate muscle. Muscle fibres orientated at an angel to the multiple tendon branches. The multipennate muscle contains more muscle fibres and therefore produces larger forces. (Courtesy of Dr. R. Payne, The Royal Veterinary Collage)

II.2.2.2 Muscle architectural parameter

Architectural measurements are widely used to estimate the force generating capacity of a muscle. These include muscle mass, volume, length, pennation angle and fibre length and angle and can be obtained by dissection of cadavers or by ultrasound in live specimens.

Muscle mass

Muscle mass is obtained by weighing the muscle belly (Payne *et al.* 2004).

Muscle volume

Muscle volume is either measured directly or can be calculated from muscle mass divided by muscle density ($1.06 gcm^{-3}$) (Mendez and Keys 1960).

Muscle length

Muscle length describes the entire length of the muscle. It is defined as the length from the origin of the most proximal muscle fibres to the insertion of the most distal muscle fibres. (Lieber 2002).

Muscle fibre length

Muscle fibre length can only be determined by microdissection. Values reported as muscle fibre length generally refer to the length of muscle fibre bundles or muscle fascicles, which can also be assessed ultrasonosgraphically (Maganaris *et al.* 1998). Muscle fibre length depends on the number of sarcomeres in series (Felder *et al.* 2005) and is directly proportional to the maximum contraction velocity (Zajac 1989). Consequently longer muscle fibres of the same fibre type can shorten more rapidly and exert force over a greater range than shorter

fibres (Wickiewicz *et al.* 1983). Muscles with shorter fibres are usually stronger due to more muscle fibres and therefore a higher number of sarcomeres in parallel.

Pennation angle

The pennation angle **(**α) describes the angle at which the muscle fibre inserts onto the tendon or aponeurosis. In parallel fibred muscles muscle fibres orientate in the direction of the tendon hence parallel to the axis of the force transmission. In these muscles the pennation angle is zero (α=0) (Alexander and Vernon 1975; Gans 1982; Zajac 1989) .
In contrast pennate muscles have generally shorter muscle fibres which insert at an acute angle (α > 0) onto the tendon (Biewener 2003). Consequently muscle fibre orientation affects the physiological cross-sectional area of the muscle since more muscle fibres can fit in the same muscle volume than in parallel muscle fibres and therefore transmit more force to the tendon. Nevertheless, pennate muscles experience some loss of force transmission due to their angle of insertion. Muscle fibres inserting, for example, at an angle of 20 degrees transmit only 95% of their muscle force onto the tendon (i.e. $Ft=Fm_{cos}$ (20) = 0.94 Fm) (Biewener 2003; Wickiewicz *et al.* 1983).

From measurements of the architectural parameters the following functional parameters can be calculated: physiological cross-sectional area, muscle volume, maximal isometric force, maximal contraction velocity and power

Physiological cross-sectional area

The physiological cross-sectional area (PCSA) determines the cross section of a muscle when all muscle fibres are cut at right angles. The PCSA describes the number of parallel sarcomeres and is directly related to the amount of force that a muscle can exert.
The PCSA can be calculated with the following equation (Alexander and Vernon 1975; Gans 1982; Narici 1999)

$$PCSA= (M_m \cos\theta) / \rho \times FL$$

M_m= muscle mass (g),
Cos θ = pennation angle,
ρ= muscle density 1.06gcm^{-3},
FL = fibre length (cm)

The pennation angle of the muscle fibres influences the force transmission of the muscle to the tendon. The cosine of pennation angles ≤ 20° are close to one and therefore has little

effect on the estimation of PCSA. Furthermore the complex three-dimensional structure of the muscle and subsequently the pennation angle is known to change during contraction. Therefore in several anatomical muscle studies the following equation is used to calculate PCSA (Payne *et al.* 2006; Payne *et al.* 2005; Smith *et al.* 2006).

$PCSA = V_m / FL$

V_m = muscle volume,
FL = fibre length (cm)

A parallel fibred muscle with a given muscle mass has a smaller PCSA and longer muscle fibres than a pennate muscle of equal mass. A pennate muscle of the same muscle mass has a larger PCSA and hence transmits more force to its tendon, but has lesser shortening capacity due to shorter muscle fibres. This is in contrast to the parallel-fibred muscle which has a smaller cross-sectional area, longer muscle fibres and provides a greater range of motion with increased contraction velocity (Biewener 2003).

The performance of a muscle can be expressed by maximal isometric force (Fmax) and maximal contraction velocity (Vmax).

Maximal isometric force

Maximal isometric force (Fmax) is determined by multiplying physiological cross-sectional area by the maximum isometric stress of vertebrate skeletal muscle (0.3 MPa) which means that maximal isometric force is proportional to the PCSA hence the number of sarcomeres in parallel (Medler 2002; Wells 1965; Woledge *et al.* 1985; Zajac 1989).

Maximal contraction velocity

Maximal contraction velocity **(**Vmax) depends on the number of sarcomeres and the degree of overlap between actin and myosin filaments. Muscles with longer muscle fibres have greater contraction velocity due to a higher number of sarcomeres in series. Contraction velocity is influenced by the load against the muscle contracts. With decreased load muscle contraction velocity increases hence maximal contraction velocity is reached when the muscle contracts against no load.

II.3 Muscle function and mechanics

The main muscle function is to provide body posture and locomotion. This is achieved y different types of muscle contraction.

II.3.1 Types of muscle contraction

There are different forms of muscle contractions depending on whether the muscle fibres shorten or elongate or keep the same length. According to the length change of the muscle fibres the contractions are called isometric, concentric and eccentric contractions.
The isometric contraction is characterised by an activated muscle without any muscle length, muscle fibre length or sarcomere length change (Rassier *et al.* 1999). The resultant mechanical work is zero. Isometric contractions are often used to stabilise joints or other muscles. In contrast, muscle contraction that permits the muscle to shorten is defined as concentric contraction. Concentric contraction occurs when the muscle exerts enough force to overcome the resistance of the load which is less than the maximum isometric force. This results in shortening of the muscle. As the load which the muscle is required to lift decreases, contraction velocity increases. The muscle does positive work. During eccentric contractions the muscle can not exert enough force to overcome the resistance of the load. The muscle lengthens while it is contracting due to the high external load. In eccentric contraction mechanical work is negative.

The muscle mechanics describe the amount of force a muscle can exert. This is influenced by several factors such as the type of contraction, the speed of contraction and the length of contraction. The following relationships show these factors theoretically.

II.3.2 Force-length relationship

Length-tension relationship describes the relationship between muscle length and force generation**Fehler! Verweisquelle konnte nicht gefunden werden.**. The force developed during isometric contractions varies with the starting length of the muscle and the actin and myosin overlap in the sarcomere (Gordon *et al.* 1966).
If muscle and consequently sarcomeres fibres are highly stretched the overlap between actin and myosin filaments is missing. The muscle develops no active force. With decreased sarcomere length force generation increases. Maximal isometric tension is reached when actin and myosin filaments overlap along their entire length and the number of cross-bridges is

maximal. However, if the sarcomere length decreases below a certain length the actin filaments from one side overlap with the opposite actin and myosin filaments which cause interference of the cross-bridge formation. This results in a reduction of muscle output.
In contrast to active muscle tension during muscle contraction passive tension occurs when the muscle is stretched to various lengths without muscle stimulation. At the optimal sarcomere length passive tension is almost zero. With increased stretching passive tension increases due to passive tension of elastic components of the myofibrils (Labeit and Kolmerer 1995; Magid and Law 1985). These passive components are giant proteins called titin which origin from the Z-line and anchor to the thick filament and the M-Line. Titin is thought to provide the force to re-establish the thick and thin filament-overlap after the sarcomere was stretched beyond the point cross-bridge attachments become impossible (Herzog 2000). Therefore passive tension can play a role in providing resistive force also during absent muscle activity (Labeit and Kolmerer 1995; Magid and Law 1985).

II.3.3 Force-velocity relationship

The force-velocity relationship describes the force generated by a muscle as a function of velocity under conditions of constant load (Lieber 2002). Muscles were stimulated to contract against a load which was less than the maximum isometric tension it could generate. The muscle began to shorten (concentric contraction). If the load decreases contraction velocity increases and force generation decreases. As the load on the muscle increases and exceeds the point of maximum isometric tension the external force on the muscle is greater than the force that the muscle can generate. The muscle is forced to lengthen (eccentric contraction). During eccentric contraction the absolute muscle tension is high relative to the maximum isometric tetanic tension and the contraction is independent of the contraction velocity.

II.4 Pathological changes of the equine back

Back problems in horses have been recognised for a long time. In 1876, injuries of the equine back were already described as common problems (Lupton 1876). Aetiopathogenesis is still not completely understood today and diagnosis and treatment remains challenging in the horse.

II.4.1 Aetiopathogenesis and clinical signs

Many back problems seem to be associated with chronic and persistent injuries and multiple lesions are common in horses with back problems (Jeffcott and Haussler 2004). However, in general, there appears to be a correlation between the conformation of the horse, sex, breed or type of use and the type of injury which is sustained (Jeffcott 1979, 1980). A whole range of underlying causes can affect the vertebral column and adjacent structures. They can be separated into three major categories: primary back problems, which can be subdivided in soft tissue injuries, osseus injuries, neurologic disorders and tack related problems; secondary back problems and presumed back problems. The specific lesions and problems associated with the different categories are displayed in Table 3 (Jeffcott and Haussler 2004).

Table 3 Differential diagnoses for horses with back problems (by Jeffcott and Haussler, 2004)

Type of back problem	General category	Specific lesion or problem
Primary back problems	Soft tissue injury	Longissimus muscle strain
		Supraspinous ligament sprain or desmitis
		Dorsal sacroiliac ligament sprain or desmitis
		Exertional rhabdomyolysis
		Non-specific soft tissue injury
	Osseous injury	Conformational or developmental abnormality
		Over-riding or impinged dorsal spinous processes
		Osteoarthritis (e.g. articular processes)
		Vertebral fracture
		Spondylosis
		Diskospondylitis
		Spinal neoplasia
	Neurogenic disorders	Equine protozoal myeloenecephalitis (EPM)
		Equine degenerative myeloencephalopathy (EDM)
		Equine herpesvirus myeloencephalitis (EHV-1)
		Equine motor neuron disease (EMND)
	Tack associated	Poor saddle fit or excessive pressure
Secondary back problems		Hindlimb lameness
		Forelimb lameness
		Neck problem
		Acute sacroiliac injury
		Chronic sacroiliac disease
		Pelvic fracture
Presumed back problems		Bad temperament
		Lack of ability (rider or horse)
		Lack of fitness
		Improper tack fit or use
		Dental problems

The clinical symptoms for these lesions and problems vary widely in their nature and severity. Depending on the underlying reason horses are presented to the veterinarian because of poor performance, intolerance of exercise, stiffness of the back and hindlimbs and back pain.

Soft tissue injuries usually occur as a result of slips, falls or poorly performed jumps which may be caused by fatigue or inadequate fitness of the horse. These incidences can lead to uni- or bilateral strains of the epaxial muscles and ligaments. Clinical signs of muscle strain may include an acute onset of poor performance accompanied by changes of the horses temperament, localised heat and swelling. Gait abnormalities such as stiffness of the hindlimb and the back, disunited canter and frequent breaking of strides are commonly seen in horses with back pain. There can be a marked reduction of thoracolumbar flexion and obvious pain palpating this area. In some acute cases an elevated level of muscle-derived enzymes can be measured after mild exercise. Metabolic disorders of the back muscles show similar clinical signs but are usually characterized by high levels of muscle-derived enzymes (CK and AST) after exercise or characteristic levels of metabolic substances seen in longissimus dorsi muscle biopsy samples (Quiroz-Rothe *et al.* 2002). Back muscle tension or strain may also be diagnosed secondary to lameness. Other soft tissue injuries such as strain of spinal ligaments are usually caused by the same traumatic reasons as muscle strain. A common site of injury is the supraspinous ligament which is adherent to the summits of the thoracic and lumbar dorsal spinous processes. Clinical signs are similar to those caused by back muscle strain. However, additional signs that may be visible include swelling, pain on palpation, and reduced lateral flexion. Severe injuries to spinal ligaments are characterised by complete ligamentous disruption and joint laxity (Jeffcott and Haussler 2004).

Osseous pathology of the vertebral column and the sacroiliac articulation can also be a major cause of chronic poor performance in horses (Gills 1999; Jeffcott 1980; Jeffcott *et al.* 1985; Jeffcott and Haussler 2004). The most common locations for degenerative changes of the spine are the facet joints and the sacroiliac articulation (Denoix, 1999a; Denoix, 1999b; Haussler et al, 1999). These synovial joints undergo progressive stages of degeneration: dysfunction, instability and degeneration. They are characterised by restricted mobility, localised pain and inflammation which can cause hypertonicity of the paraspinal muscles. With continuing joint immobilisation bone demineralisation, capsular adhesions and loss of ligamentous strength take place. Initial musculotendinous contractures are followed by capsular, periarticular and intra-articular adhesions. The dysfunctional joint is unable to sustain normal biomechanical stress. Consequently changes of subchondral bone, cartilagenous, capsular and ligamentous deformation and degeneration result in joint

instability which again affects proprioception and the central neuromotor control of movement and posture. Radiographic findings often include osteophyte formation, spinal ligament ossification, spinal ankylosis and other signs of advanced osteoarthritis (Jeffcott and Haussler 2004; Ross and Dyson 2002).

Impinged or over-riding dorsal spinous processes (kissing spines) were reported to be another frequent cause of back pain in horses and occur commonly between T10 and T18 (Denoix 1999a). However, a high percentage of horses with no clinical signs of back pain also show radiographic osseous changes of the dorsal spinous processes which complicate precise diagnostic (Ross and Dyson 2002). A higher prevalence of spinous process impingement was observed in Thoroughbreds due to narrower interspinous spaces and misshapen dorsal apices (Jeffcot L 1979, Townsend et al, 1986). Competitive jumping horses also seemed to have a higher incidence of pathological changes of the spine induced by increased dorsoventral flexion and demanding spinal manoeuvres (Jeffcott 1979).

Conformational deformities of the spine such as scoliosis, lordosis and kyphosis can be congenital. Lordosis can also be found in aged horses or brood mares after several foals. The alterations of the spinal curvature can lead to an extra stress on the vertebral column and adjacent soft tissue structures which can result in soft tissue strain and alteration of the vertebral bones (Ross and Dyson 2002).

In humans, the pain element of a back problem is considered to be as important as the original injury or disease. Primary back pain is caused by the irritation of spinal nerve roots, branches of the spinal nerves and their communicating receptor system (nociceptive receptors). The nociceptive receptors are represented as freely ending nerve fibres distributed throughout all kinds of tissue (skin, muscle, joint and viscera). These nerve endings are activated by chemical, mechanical and traumatic factors. Unlike in humans the unspecific nature of clinical signs associated with back problems contribute to the challenge of diagnosing back pain in horses.

To evaluate the factor pain in horses with back problems, back pain was induced by injections of concentrated lactic acid into the equine back. This resulted in local pain, stiffness and noticeable reduction in performance but did not induce lameness (Jeffcott *et al.* 1982). A more recent study, however, found an increase in back motion after pain induction on one side (Gomez Alvarez 2007).

II.4.2 Diagnostic methods

The clinical examination remains a challenging task in horses with back pain. The majority of horses are presented with impaired performance. Locating and quantifying back pain is difficult especially as some horses perform satisfactorily in spite of low-grade back pain and some horses appear to be hypersensitive along the back which can falsely be interpreted as a sign of pain (Jeffcott and Haussler 2004). Collection of the detailed history of onset and progression of the back problem is important and helpful to isolate the cause of back pain as well as to discover any related schooling and equestrian problems. A thorough clinical examination is necessary to rule out any underlying limb lesion which could account for secondary back pain before proceeding with more advanced diagnostic imaging techniques. The following paragraphs describe the systematic examination of horses with back problems.

II.4.2.1 Clinical examination

The clinical examination starts in general with a visual inspection of the horse in stance to assess any abnormalities in behaviour and posture, as well as any swelling or asymmetry of the spine, epaxial musculature, pelvis or tail. This is followed by palpation to determine pain along the back. Gentle, superficial and firm deep palpations can detect pain, heat or swelling along the tips of the dorsal spinous processes, the supraspinous ligament, the epaxial muscles or the saroiliacal region and help to identify supraspinous desmopathy and deformation or malalignment of the spinous processes. Focal muscle spasm can point to the presence of significant lesions (Ross and Dyson 2002). Skin stimulation of the dorsal and lateral aspects of the neck and the trunk is also used to manipulate the horse and induce dorsoventral movements of the cervical and thoracolumbar spine and the lumbosacral junction. The response in form of restriction or intolerance of motion helps to isolate potential sources of pain (Ross and Dyson 2002). However, different degrees of sensitivity between horse breeds contribute to the confusion over evaluating sites of pain. For example thin-skinned thoroughbred-type horses may give the false impression of a painful back by guarding the back and having protective spasm of the epaxial musculature. In contrast, more stoical cob-type horses may have a lack of sensitivity and an inherently restricted range of motion.

Examination during motion is performed to assess abnormalities of gaits. The horse is exercised on a straight line as well as on circles in different gaits. Gait abnormalities, restricted movement of the back, stiffness and restricted hind limb action can be presented in horses with back pathology. Examination of the horse being ridden is useful to detect any

influence of the rider and tack because some horses show signs of back pain only when they are ridden. At times alterations of behaviour and temperament of the horse can be observed when the horse is tacked or mounted. For example, horses with seemingly sensitive backs will often dip the back when saddled or mounted by the rider, but this is not necessarily a sign of back pain. After identifying the site of pain local anaesthesia is performed to asses the clinical significance of this particular area. Infiltration of painful areas of soft tissue, articular or osseous structures of the back and pelvis with local anaesthesia is supposed to block out the pain and alter the range of motion and/or gait. The injection of local anaesthesia in narrowed interspinous spaces can assess the significance of the over-ridden or impinged spinous processes. Injection of deeper structures along the vertebral column should be performed under ultrasonographic guidance. Intra-articular injections of the articular processes are difficult to perform due to the narrow joint space and small joint cavity and therefore deeper injections are effectively intramuscular injections. The close location to the intervertebral foramen and hence the neurovascular structures may influence the interpretation of the result of the local anaesthesia (Jeffcott and Haussler 2004; Ross and Dyson 2002). It was also demonstrated that local anaesthetic injection in sound horses influenced the range of back motion and resulted in an increase of flexion and extension as well as lateral bending during walk. In trot a decreased range of motion was detected at L3 (Holm *et al.* 2006).

II.4.2.2 Diagnostic imaging

A number of different diagnostic imaging methods are available to identify certain pathological changes of the equine back. Radiography, nuclear scintigraphy and ultrasonography are widely used in equine practice. Each of these techniques is suited to certain conditions of back pathologies and is briefly described in the following paragraphs.

II.4.2.2.1 Radiography

Radiography generally includes laterolateral and oblique projections of the vertebral column with the horse standing square. Due to the difference in radiographic density of the more dorsal compared to the more ventral parts of the spine, it is often necessary to acquire two sets of radiographs with different exposures. High-output x-ray generators are necessary and it is often difficult to acquire images of diagnostic quality, especially in the lumbar region of heavy horses. In a slightly dorsoventral oblique view the articular facets of the vertebrae (between T7-T17) can also be projected. This technique is useful to show overriding dorsal spinous processes, ventral spondylosis and osteoarthritis of the dorsal articular facets.

Interpretation of radiographic appearance of the facet joints is often difficult due to superimposition and scatter induced noise (Weaver *et al.* 1999).

II.4.2.2.2 Nuclear scintigraphy

Nuclear scintigraphy with Technetium^{99m}-phosphonates is commonly used in the horse to assess musculoskeletal structures and reflects vascularisation and bone turnover. It has shown to be useful in detecting active overriding dorsal spinous processes, ventral spondylosis, osteoarthritis of the dorsal articular facets, spinal fractures and sacroiliac joint pathology. However it has also been shown that scintigraphic changes are present in horses with no clinically apparent back disorders (Erichsen *et al.* 2004).

II.4.2.2.3 Ultrasonography

In general, ultrasonography is used to determine soft tissue alterations. It is useful for the examination of ligaments, tendons, musculature, joint surface and joint capsules (Denoix 1999c). Different kinds of tissue vary in their ability to return ultrasound signals of an ultrasound beam generally described as their echogenicity.
The normal image of back muscles is similar to the image of other muscle groups. Muscle is less echogenic compared to fat and tendinous structures. The transverse images show disorganized fine echoes scattered throughout the muscle. In the longitudinal view the muscle is characterized by homogeneous, multiple, fine, parallel echoes (Fig. 7). This sonographic appearance is due to multiple muscle bundles (fascicles) surrounded by fibroadipose septa (perimysium). Connective tissue fascia and fat overlying the muscle appears as a bright echogenic outer margin (Rantanen and McKinnon 1997).

Although superficial structures such as the supraspinous ligament, the longissimus dorsi muscle and the dorsal sacroiliac ligament around the equine back are easy to document by ultrasonography, the interpretation of the images needs a certain degree of experience (Henson 2005). Pathological alterations like insertional desmopathy, avulsion fractures of the insertion of the supraspinous ligament, kissing spines, hypoechogenic changes in the ligaments with lesions or hyperechogenic changes from calcification can be observed with ultrasonogaphic imaging (Denoix 2006). Muscle injuries such as muscle strain are difficult to detect but severe cases of muscle fibre tearing can be identified ultrasonographically. Ultrasound images show increased echogenicity of the muscle tissue with thickening of the connective tissue septae or haematomas in the back muscles (Jeffcott and Haussler 2004; Reef 1998).

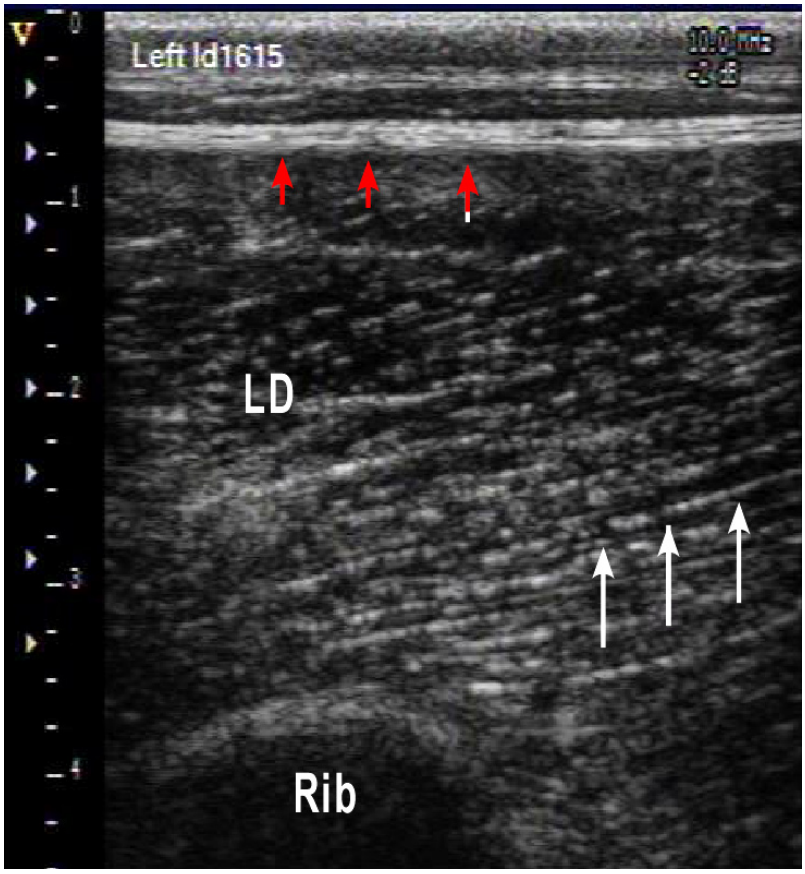

Fig. 7 Ultrasound image of the equine LD. Showing the hyperechoic muscle septa (white arrows), the hyperechoic superficial thoracolumbar fascia (red arrows) and the hyperechoic bony surface of the rib. Muscle tissue is displayed as hypoechogenic structure.

II.4.2.2.4 Electromyography

Electromyography (EMG) records the electrical activity of muscle fibres by surface or needle electrodes (Licka *et al.* 2001b; Robert *et al.* 1998, 2001b; Tokuriki *et al.* 1997; Wijnberg *et al.* 2004; Wijnberg *et al.* 2003). Muscle activation is provided by the electrical impulse, so-called action potential, conducted from a nerve along the muscle into the corresponding muscle fibres. The summation of the local muscle fibre action potentials is recorded and displayed as electrical activity pattern. In horses EMG has been mainly used to show the activity pattern of muscles in combination with kinematic data. Duration and intensity of muscle activity in relation to body motion under different conditions (gait, speed, incline) demonstrated the function of muscles during locomotion (Licka *et al.* 2001b; Robert *et al.* 1998, 2001b; Tokuriki *et al.* 1997). However, in humans it was demonstrated that alterations in muscle activity pattern can predict myogenic or neurogenic changes (Fuglsang-Frederiksen *et al.*

1976; Kimura 2001; Wijnberg *et al.* 2003) but systemic quantative EMG analyses have been performed only on a limited number of horses and needs to be further evaluated (Wijnberg *et al.* 2003).

III. Own investigations: Novel insights into the anatomy and function of the equine thoracolumbar Longissimus dorsi muscle

III.1 Gross anatomy of the equine thoracolumbar Longissimus dorsi muscle

III.1.1 Introduction

The back forms the dorsal part of the equine body and joins front and hind limbs. It plays an important role in supporting the trunk and transmits propulsion from the hindlimbs to the rest of the horse. The back is composed of the vertebrae, numerous ligaments and strong musculature covered and incorporated by fascia (see chapter II for a detailed description). The largest muscle of the epaxial musculature is the thoracolumbar Longissimus dorsi muscle (LD). The muscle originates at the last cervical and the first thoracic vertebrae. It lies bilateral to the dorsal spinous processes and dorsal to the ribs and transverse spinous processes and it inserts onto the ribs, the transverse and mammillary processes of the thoracolumbar spine as well as to the tuber, the crest and the ventral surface of the ilium and the first three sacral vertebrae.

The knowledge of normal epaxial muscle architecture provides understanding of back function as muscle architectural parameters (muscle fibre length, pennation angle, muscle volume, physiological cross-sectional area) determine functional and mechanical properties of muscles (Gans 1982; Sacks and Roy 1982). The length of muscle fibres and the arrangement of muscle fibres between tendons or tendon plates determine the capacity of the muscle for length change and the ability of the muscle to generate force (Biewener and Roberts 2000).

Several anatomical studies have revealed differences of the architectural arrangement between muscles. These morphological distinctions influence performance and function of the muscles (Brown *et al.* 2003a; Lieber and Blevins 1989; Payne *et al.* 2004; Payne *et al.* 2005; Sacks and Roy 1982; Van Eijden *et al.* 1997; Wickiewicz *et al.* 1983). Differences of fibre length and pennation angle with respect to muscle volume and physiological cross-section area (PCSA) explain the preference of muscles for either force production or velocity contraction and excursion. The analysis of architectural features in limb muscles of different species has revealed several specific skeletal muscle adaptations (Brown *et al.* 2003a; Brown *et al.* 2003b; Lieber and Blevins 1989; Payne *et al.* 2004; Payne *et al.* 2005; Wickiewicz *et al.* 1983). The epaxial musculature acts as antigravity muscles which contribute to the postural stability of the trunk by reducing the overall trunk movement during vertical movement in the centre of mass of the body (Carlson 1978; English 1980; Tokuriki 1973b, 1974; Tokuriki *et al.* 1997).

However, kinematic and electromyelographic studies have shown that the LD has to be capable of fullfilling different functions, therefore it seems reasonable to assume that this is reflected in a variation of muscle morphology along its length.

Anatomical studies of the equine back published to date have concentrated on the skeletal and ligamentous structures only. Knowledge about the morphology and function of the equine back musculature is limited. The epaxial muscles have been studied mainly functionally (Licka *et al.* 2008; Licka *et al.* 2004; Peham *et al.* 2001; Robert *et al.* 2001; Robert *et al.* 2002; Tokuriki *et al.* 1997) without detailed data on fibre length, cross-sectional area, moment arms and hence force generating capacity.
The aim of this study was to describe the muscle morphology of the LD in detail. The objectives included the quantification of fascicle length, pennation angle, PCSA, muscle mass and muscle volume. It was hypothesised that the equine LD muscle shows differences in fibre length, PCSA and pennation angle along the muscle and hence varying capacity of force production and contraction velocity.

III.1.2 Material and Methods

III.1.2.1 Subjects

Twenty-one LD of seven horse and six pony cadavers were dissected and were examined in this study. The cadavers were obtained from horses that had been euthanased for reasons unrelated to this study and came from ten geldings and three mares, of different breeds (two Shetland ponies, four Welsh section A ponies, four Welsh Cobs and three Warmbloods). The cadavers were selected to present a range of different ages (six months to 32 years, mean±stdev 13±13 years). They had no history of musculoskeletal pathology and had been subjected to euthanasia for reasons unrelated to back pathology.
In three cadavers only one LD was obtainable and measured as the muscles of the contralateral side were damaged during the routine post mortem examination. In one horse the LD muscles were dissected to demonstrate the innervations pattern of the LD.

III.1.2.2 Experimental protocol

After removal of the thoracic and abdominal contents, limbs and parts of the rib cage were removed from the carcass. The skin of the back was separated from the trunk along with

connective tissue, cutaneous and superficial muscles (latissimus dorsi, serratus dorsalis and ventralis, trapezius muscle).

The dorsal spinous processes of T12 - T18 and L 2 were identified and marked with pins (5 star office push pins, 24mm). The pins were used as landmarks to relate LD segments to corresponding vertebrae and ribs. The relative position of the thoracic and lumbar LD in relation to the bony landmarks and to the middle gluteal, spinalis and iliocostal muscle was identified and documented by taking digital photographs (Nikon coolpixel P1, Nikon Corperation, Tokyo, Japan). In the first three cadavers the lateromedial width of LD was measured between the 12^{th} rib and 2^{nd} lumbar vertebrae to identify the dimensions of the muscle in relation to the overlying and surrounding muscles. In the following dissections measurements of muscle width were discarded to focus on the architectural parameters as the quality of fibre length and pennation angle measurements were affected by progressing post-mortem decay.

The LD was separated from the spinalis, middle gluteal, iliocostal and multifidus muscle as well as surrounding fascia. Finally it was removed from the spine and the ribs. Muscle mass (g) and muscle length (cm) of the whole muscle were determined. The muscle was weighed on a single-pan scale to obtain the muscle mass. Muscle length was determined by measuring the beginning of the most proximal muscle fibres to the end of the most distal fibres with a flexible tape measure (cm). Muscle fascicle length (cm) and pennation angle (º) were quantified at different sections. For these measurements the muscles were subdivided in three sections along the muscle: cranial section T1-T12, middle section T13-T18 and caudal section T18-L6. These subdivisions were based on kinematic findings showing an increased range of motion in the cranial thoracic spine and less spinal motion in the caudal vertebral column (Haussler *et al.* 2001; Townsend *et al.* 1983). The respective sections were also subdivided in dorsal and ventral areas by dividing the corresponding section horizontally in half (Fig. 8). Muscle fascicle length was obtained by cutting along the length of the muscle belly in a 90° angle to the internal tendon or by making incisions through the muscle belly until the plane of the muscle fascicles had been detected. With a clear plastic ruler muscle fascicle length were measured in mm. The measurements were repeated a minimum of ten times in randomly selected samples at each location and depth.

The resting pennation angles were determined by measuring the angle between the aponeurosis or internal fascia and the fascicles with a clear plastic protractor in the same muscle sections as the muscle fascicle length was measured. These measurements were also repeated a minimum of ten times.

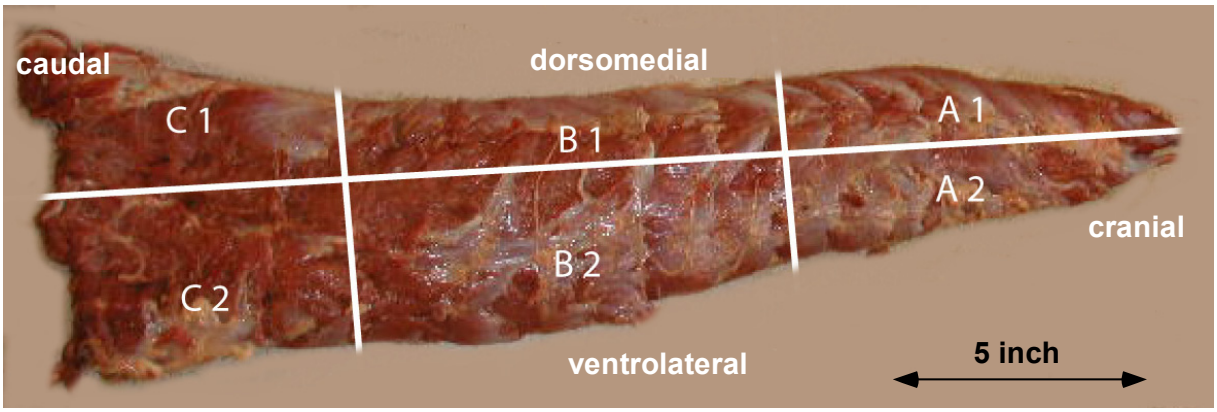

Fig. 8 Thoracic and lumbar Longissimus dorsi muscle of a pony illustrating the subdivisions used for muscle fascicle measurements (5 inch = 12.7 cm). Subdivisions were based on the different range of movement along the back and were identified by anatomical landmarks.
A1 = craniodorsal section, A2 = cranioventral section, B1 = middle, dorsal section, B2 = middle, ventral section, C1 = caudodorsal section, C2 = caudoventral section.

The overall muscle volume was calculated by dividing muscle mass by muscle density (1.06g cm^{-3}, Mendez and Key, 1960). Due to the changing shape of the muscle and missing muscle mass measurements for the individual cranial, middle and caudal section of the subdivided LD, muscle volume for these areas were calculated using unpublished muscle volume data of a CT study in three equine thoracic and lumbar longissimus dorsi muscles (personal conversation with Pattama Ritruechai, 2006). Data of this study showed that the percentage of muscle volume of the three sections is the same between horses (Coefficient of variations, < 0.01). Therefore the volume was calculated for the cranial part (T1-T11), middle part (T12-T18) and the caudal part (L1-L6) of the LD.

The physiological cross-section area (PCSA) was calculated for the cranial, middle and caudal part of the subdivided LD with following equation: muscle volume (cm^3) was divided by the mean of muscle fibre length (cm) for the respective muscle sections. The pennation angle was not included in this calculation because the pennation angle undergoes substantial changes through contraction (see below). Therefore architectural measurements can not represent the changes occurring in the 3D real muscle (Otten 1988, Zajac 1989). The maximum isometric force (F_{max}) is proportional to the physiological cross-sectional area and is estimated by multiplying physiological cross-section area by maximum isometric stress of the vertebral skeletal muscle (0.3 MPa) (Medler 2002; Wells 1965; Woledge *et al.* 1985; Zajac 1989).

In two of 21 LD muscles the innervation pattern of the dorsal rami of the spinal nerves were examined through gross dissection and documented with digital photographs.

III.1.2.3 Statistical analysis

The collected data was calculated and processed in Excel (Microsoft Office 2003, Microsoft Cooperation, Redmond, USA). For further statistical analysis the data was exported to SPSS (Version 14.0, SPSS Inc., Chicago, IL, USA). The data was tested for normal distribution using the Kolmogorow-Smirnov test. A univariate linear model was used to assess the effect of horses and ponies, right and left LD and different sections of LD on muscle parameters. P value was set at 0.05 for all tests.

III.1.3 Results

III.1.3.1 Descriptive Anatomy

Fig. 9 Ventral view of the left thoracic and lumbar Longissimus dorsi muscle of a pony (5 inch = 12.7 cm). The diameter of the cranial muscle is smaller than of the caudal muscle.

The LD is located bilaterally to the dorsal spinous processes and dorsally to the ribs and the transverse processes. The muscle originates at the last cervical (C7) and the first thoracic vertebrae (T1 and T2) via short, flat tendons. It spans along the thoracolumbar vertebral column and inserts onto the ilial crest, craniomedial to the ilial wing and the sacrum. Along

the vertebral column the LD inserts also to the mammillary, transverse and dorsal spinous processes as well as to the ribs. The mediolateral dimension of the muscle body is smaller in the cranial thoracic region and increases its size over the whole length of the thoracolumbar area up to its broad insertion to the ilial wing

(

Fig. 9). Mean ±stdev muscle width increased between T14 and L2 from 15 ± 3 cm to 18 ± 3 cm. The cranial thoracic LD is covered by the spinalis muscle which extends caudal to T13. In the lumbar area the cranial extension of the middle gluteal muscle is overlying the LD up to T 18 (Fig. 10).

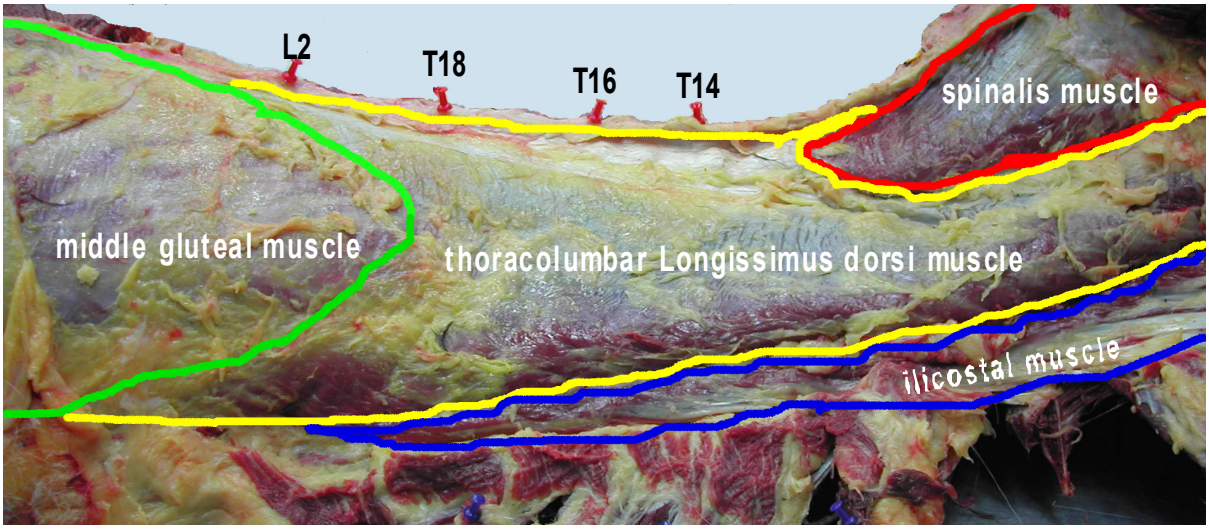

Fig. 10 The thoracolumbar longisssimus dorsi muscle in relation to the iliocostal muscle (blue), the overlying tongue of middle gluteal muscle (green) and the spinalis muscle (red).

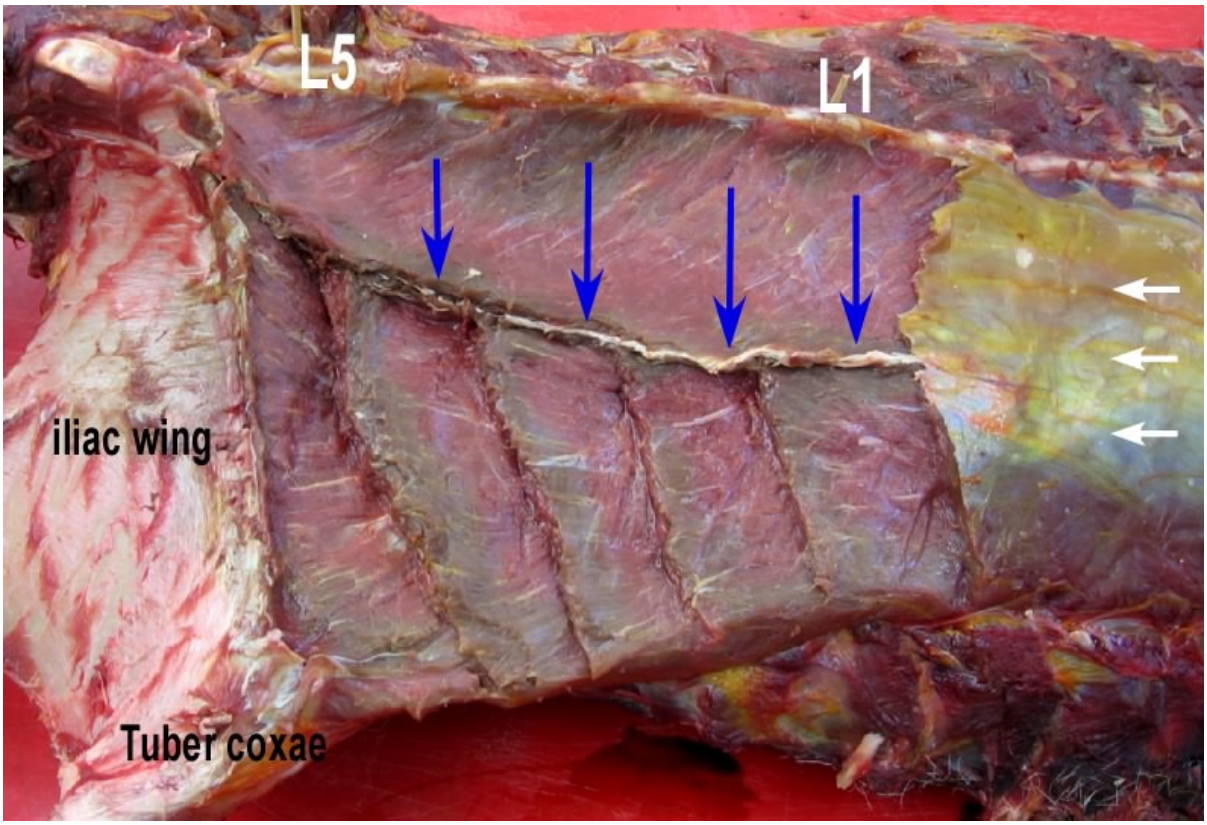

Fig. 11 Caudal section of thoracolumbar LD inserting onto the iliac wing and the dorsal spinous processes of the lumbar vertebrae and the sacrum. The strong superficial thoracolumbar fascia (white arrows) is visible in the cranial part of the image covering LD and the internal fascia (blue arrows) is visible as a white line in the musculature. Ventral to the thoracolumbar fascia LD was dissected in cascading pattern to show the orientation of muscle fibres.

Strong fascia and aponeuroses surround and divide the LD. The muscle is covered by the strong superficial thoracolumbar aponeurosis, which joins the supraspinous ligament in the midline of the back. In the caudal part of the muscle between T17- L5 an internal fascia is released from the thoracolumbar aponeurosis into the muscle and divides it in two layers, medial and lateral (Fig. 11-Fig. 13).

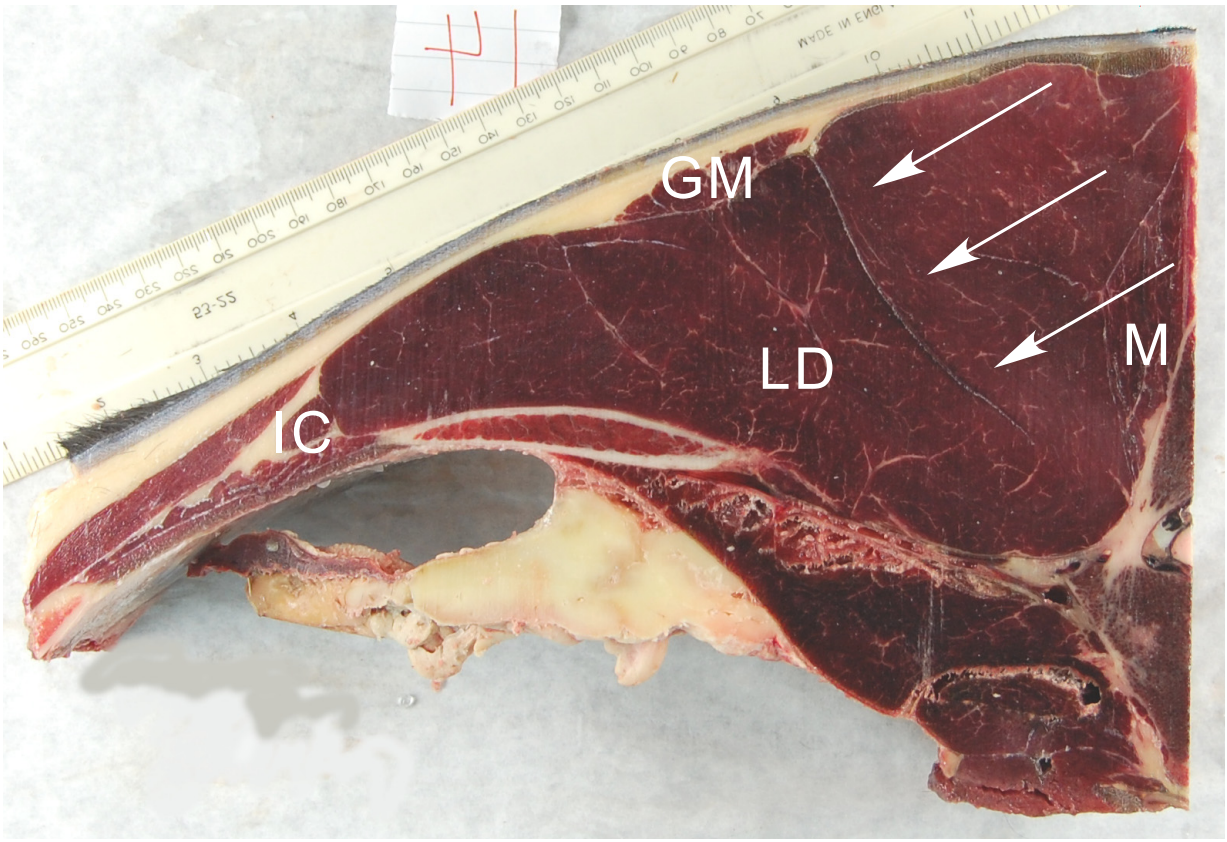

Fig. 12 Shows the internal fascia (white arrows) released by the superficial thoracolumbar fascia which separates the longissimus dorsi (LD) and the middle gluteal muscle (MG) at the level of T18 in an adult horse.

The internal structure of the thoracolumbar LD shows multiple muscle bundles (Fig. 14). These muscle bundles taper and insert to the bone or with very short aponeurotic sheets which insert onto the ribs and the mammillary and transverse processes of the thoracic and lumbar vertebrae. In the caudal part of the thoracolumbar LD the segmental organisation is not clearly visible due to a strong fascia and a number of very thin fascia running through the muscle. In this area the muscle fibres attach very tightly to the transverse processes of the lumbar vertebrae and the deep layer of the thoracolumbar fascia.

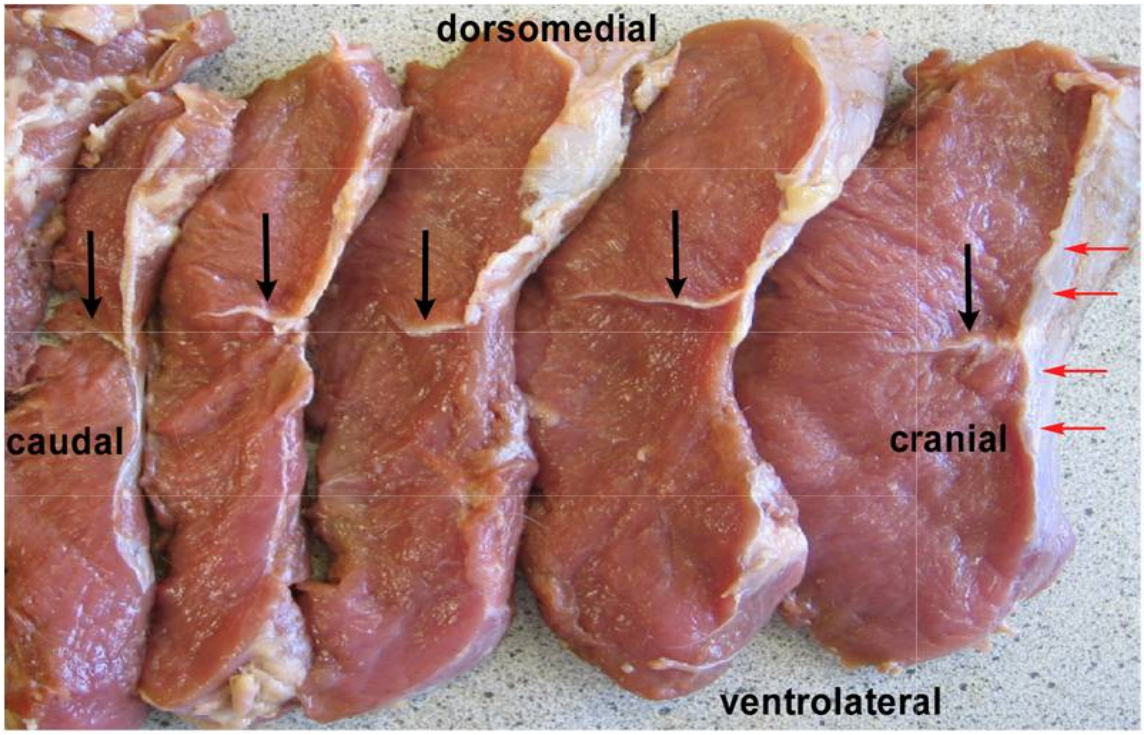

Fig. 13 Caudal section (T17-L5) of the right LD of a six-month-old pony dissected and cut in five transverse muscle slices. The internal fascia (black arrows) which is released by the superficial thoracolumbar fascia (red arrows) is visible as a white structure.

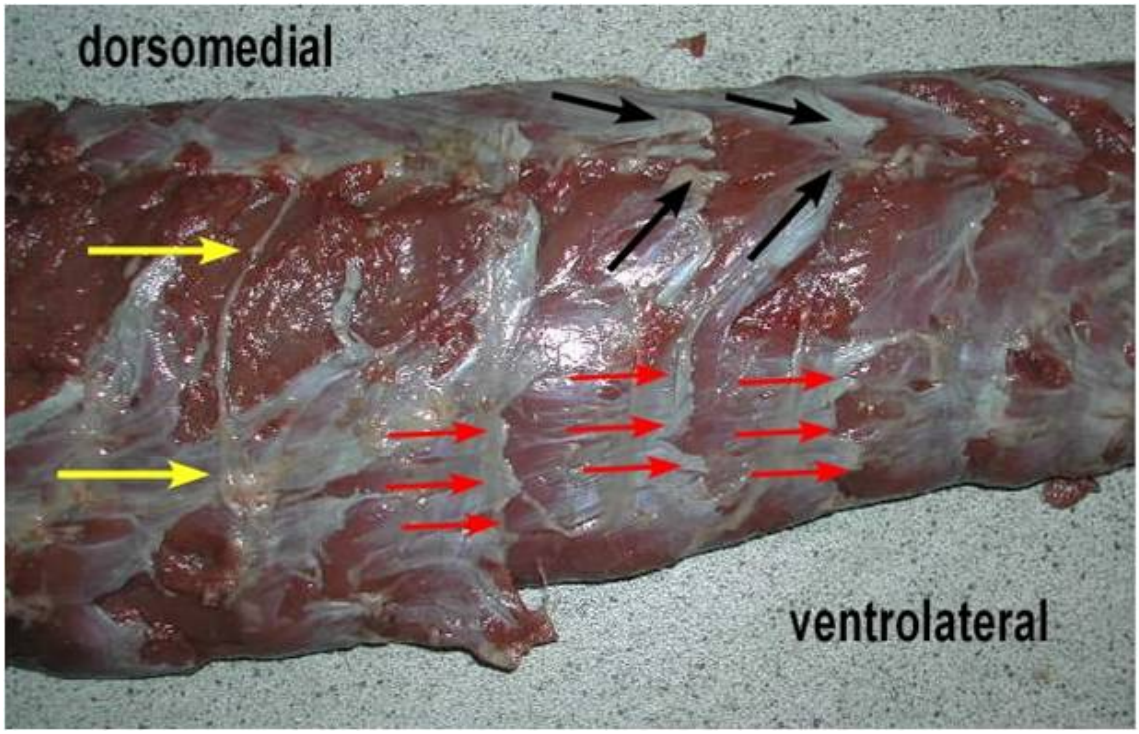

Fig. 14 Ventral view of LD. The removed aponeurosis and fascia from the bony attachments are visible and indicate the attachment of muscle bundles onto the ribs (red arrows) and mamillary and dorsal spinous processes (black arrows). The yellow arrows indicate the innervation of LD by the dorsal rami of the spinal nerve.

Orientation of the muscle fibres in the muscle bundles varies widely along the muscle. In the cranial thoracic part long muscle fibres (mean ±stdev FL 85 ±27 mm) insert with a relatively small pennation angle (mean ±stdev PA 35 ±12°) (Fig. 16). They are arranged parallel to the spinal column (Fig. 15). Towards the caudal part of the thoracic LD and in the lumbar LD muscle fibres decrease in length and their pennation angle increases (mean ± stdev FL 52 ±11 mm; mean ± stdev PA 48 ±15°) (Fig. 17). Muscle fibres dorsal to the internal fascia are orientated from caudoventral laterally to craniodorsal medially. The muscle fibres ventral to the internal tendinous sheet in the caudal part of the lumbar LD run in the opposite direction. They are orientated from cranioventral to caudodorsal (Fig. 18)

The LD of the equine back is innervated segmentally. These segments are equal to the spaces between the ribs and the transversal spaces of the lumbar spinal region (Fig. 19).

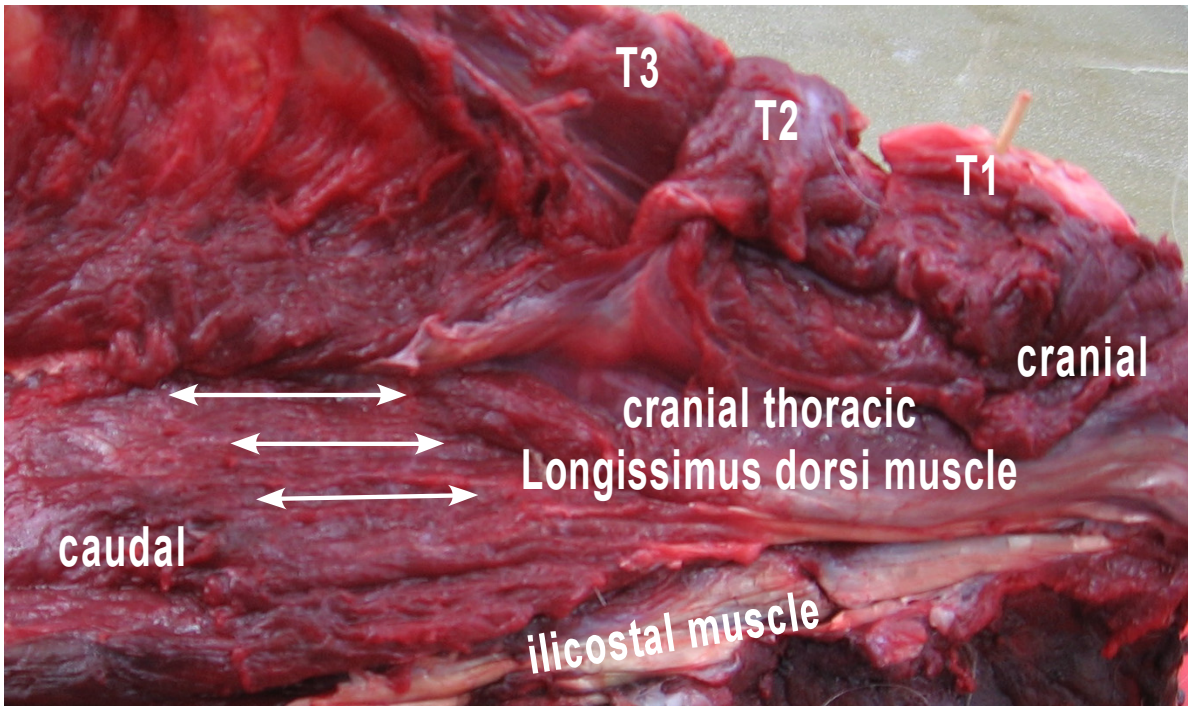

Fig. 15 Lateral view of the cranial thoracic longissimus dorsi muscle (T2-T5). Muscle fibre orientation is almost horizontal and parallel to the axis of the vertebral column.

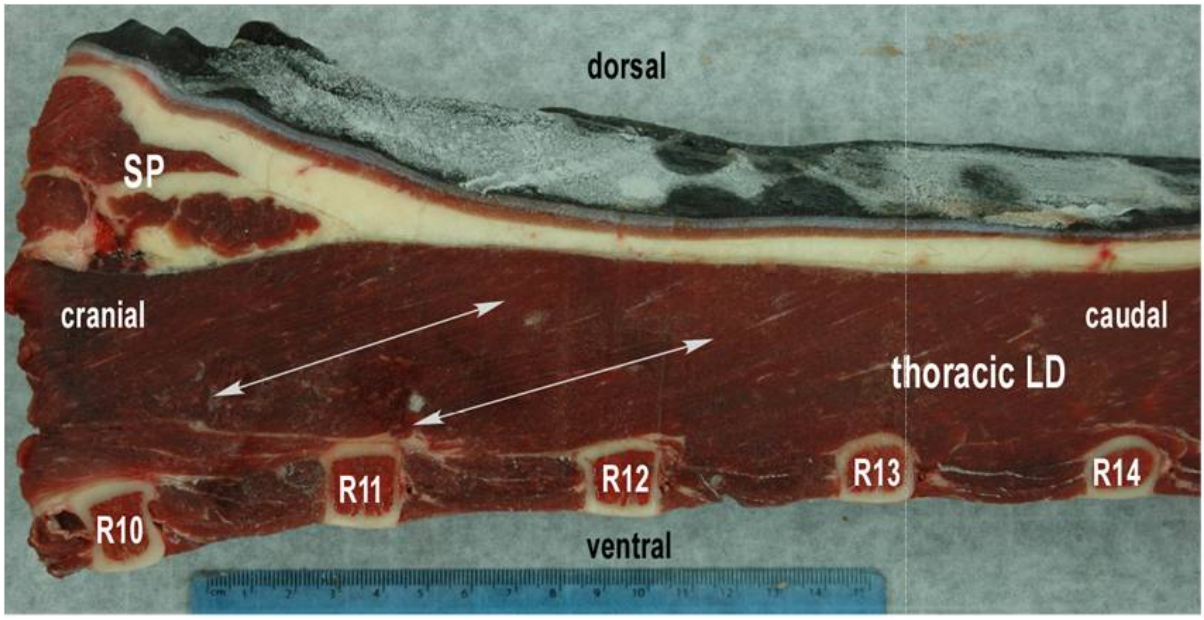

Fig. 16 The cranial-middle section of the thoracic LD (T10-T14) 15 cm lateral to the midline. LD lies dorsal to the ribs (R) and is covered cranial by the spinal muscle (SP). The muscle fibre orientation is indicated by white arrows.

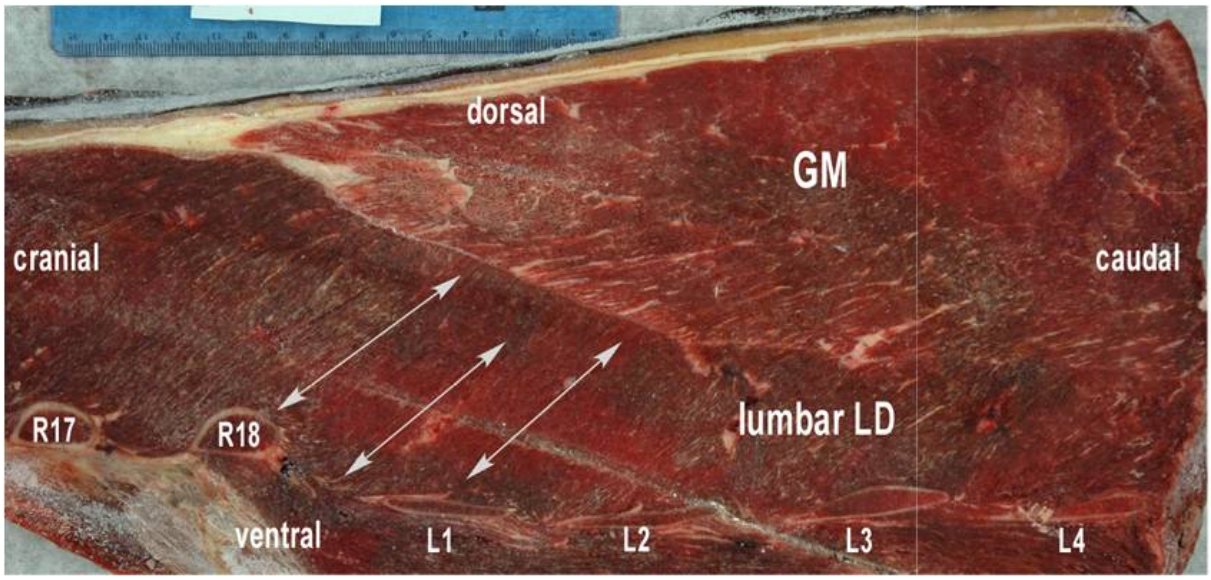

Fig. 17 In a distance of 10cm lateral to the midline the lumbar LD lies dorsal to the ribs (R) and the lumbar transverse processes (L) and ventral to the middle gluteal muscle (GM). Muscle fibre orientation of the lumbar LD is indicated by white arrows.

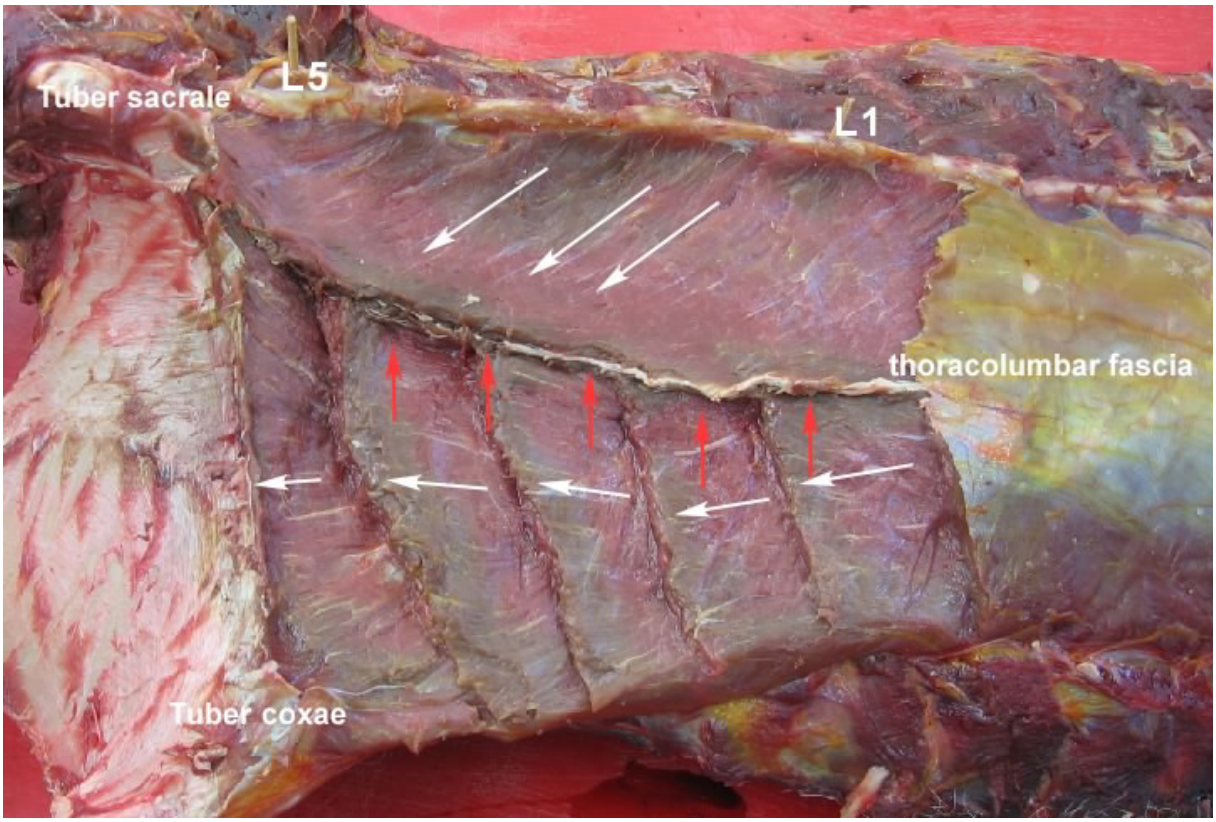

Fig. 18 Caudal section of LD (T16-Sacrum) demonstrating the insertion of the muscle to the iliac crest (caudal), the dorsal spinous processes of the lumbar vertebrae (dorsomedial) and to the sacrum. The muscle fibre orientation (white arrows) and internal aponeurosis (red arrows) of the lumbar LD (T18-L6). In the thoracic section LD is covered by the superficial thoracolumbar fascia.

Fig. 19 Ventral view of LD showing segmental innervation of the equine LD. White arrows indicate *rami dorsales* of the spinal nerve which innervate the corresponding muscle segment.

III.1.3.2 Architectural measurements

The dissected thoracic and lumbar LDs of the 13 cadavers were grouped according to their breeds in six ponies and seven horses for the descriptive statistical tests.

Muscle mass, overall muscle length and muscle volume

The muscle mass in the dissected horses ranged from 5260 g to 10400 g with a mean ±stdev muscle mass of 7088 ±1537g. Muscle length ranged from 92 cm to 130 cm with a mean ±stdev of 112 ±14 cm. Muscle volume ranged from 4157 cm^3 to 9801 cm^3. The mean ±stdev volume was 6555 ±1601 cm^3.

Muscle mass, muscle length and muscle volume of the LD in ponies were significantly lower than for horses (muscle mass p=0.0001, muscle length p= 0.03 and muscle volume p=0.0001). The muscle mass of the ponies ranged from 1247 g to 4200g with a mean ±stdev of 2222 ±1226g. Muscle length had a minimum value of 53 cm and a maximum of 110 cm. The mean ±stdev was 75 ±20 cm. Muscle volume ranged from 1173 cm^3 to 3958 cm^3 with a mean ±stdev of 2104 ±1150 cm^3. All values are presented in Table 4-Table 6.

Right and left LD showed no significant differences in muscle mass and muscle length between both sides (muscle mass p= 0.9, muscle length p=0.8 and muscle volume p=0.9) (Table 7-Table 9)

Table 4 Mean values, standard deviation, minimum and maximum values of LD muscle mass measurements (g) in horses and ponies.

Muscle mass (g)	N	Mean	Stdev	Minimum	Maximum
Horse	12	7088	1537	5260	10400
Pony	9	2222	1226	1247	4200

Table 5 Mean values, standard deviation, minimum and maximum values of LD muscle length measurements (cm) in horses and ponies.

Muscle Length (cm)	N	Mean	Stdev	Minimum	Maximum
Horse	12	112	14	92	130
Pony	9	75	20	53	110

Table 6 Mean values, standard deviation, minimum and maximum values of LD muscle volume measurements (cm^3) in horses and ponies.

Muscle Volume (cm^3)	N	Mean	Stdev	Minimum	Maximum
Horse	12	6555	1601	4157	9801
Pony	9	2104	1150	1173	3958

Table 7 Right and left muscle mass (g) for horses and ponies showing mean values, standard deviation, minimum and maximum values.

Muscle mass (g)		N	Mean	Stdev	Minimum	Maximum
Horses	right	5	6740	1327	5700	8900
	left	5	6652	1229	5260	8500
Ponies	right	3	2343	1523	1390	4100
	left	3	2360	1598	1304	4200

Table 8 Right and left muscle length (cm) for horses and ponies showing mean values, standard deviation, minimum and maximum values

Muscle length (cm)		N	Mean	Stdev	Minimum	Maximum
Horses	right	5	109	15	95	130
	left	5	114	16	92	129
Ponies	right	3	79	21	65	104
	left	3	79	27	59	110

Table 9 Right and left muscle volume (cm^3) for horses and ponies showing mean values, standard deviation, minimum and maximum values

Muscle volume (cm^3)		N	Mean	Stdev	Minimum	Maximum
Horses	right	5	6358	1252	5377	8396
	left	5	6275	1159	4962	8019
Ponies	right	3	2210	1437	1311	3868
	left	3	2227	1508	1230	3962

Muscle fascicle length

In horses the mean ±stdev value of the muscle fascicle length was 7.7 ±2.4 cm. The mean ±stdev value of the muscle fascicle length in ponies was 6.8 ±2.6 cm. There was no significant difference in fascicle length between horses and ponies (p=0.2).

In the subdivided LD the fascicle length varied between the cranial (T1-T12), middle (T13-T18) and caudal (L1-L6) section. Muscle fascicle length decreased from cranial to caudal in horses and ponies (Fig. 20).

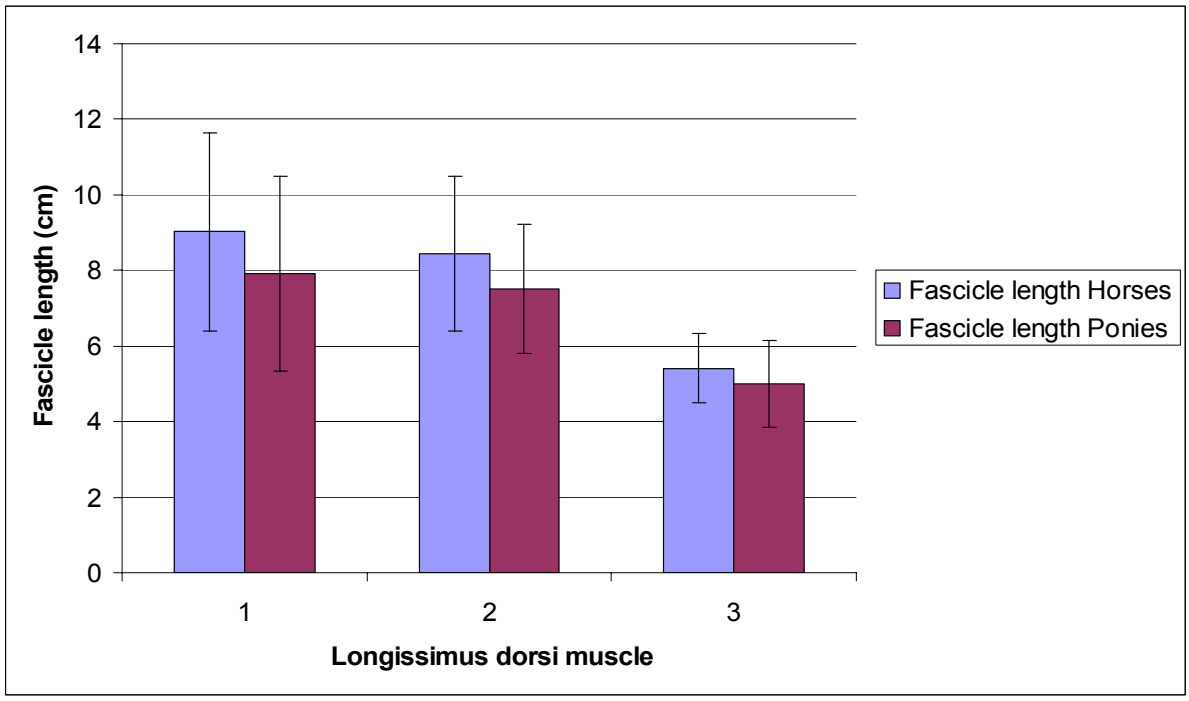

Fig. 20 Mean (± stdev) muscle fascicle length (cm). Horses and ponies show the same trend of decreasing muscle fascicle length in cranial to caudal direction (cranial=1, middle=2, caudal=3)

Minimum and maximum fascicle length in horses differed from 4.8 cm and 13.8 cm in the cranial part to 6.2 cm and 13.3 cm in the middle part and from 3.5 cm and 6.7 cm in the caudal part. The mean ±stdev fascicle length decreased from 9.0 ±2.6 mm (cranial), to 8.4 ±2.0 cm (middle) and to 5.4 ±0.9 cm (caudal) (Table 10, Fig. 21).

In the ponies, minimum and maximum fascicle length ranged from 3.8 cm to 11.3 cm in the cranial part, 4.9 cm to 9.8 cm in the middle and 3.0 cm to 6.4 cm in the caudal part. The mean (±stdev) fascicle length decreased in cranial to caudal direction from 7.9 ±2.5 cm (cranial) to 7.5 ±1.7 cm (middle) to 4.6 ±1.1 cm (caudal) (Table 11, Fig. 22).

Table 10 Mean values, standard deviation, minimum and maximum values of muscle fascicle length (cm) for the cranial, middle and caudal LD in the horse

Fascicle Length (cm)	N	Mean	Stdev	Minimum	Maximum
Cranial	12	9.0	2.6	4.8	13.8
Middle	12	8.4	2.0	6.2	13.3
Caudal	12	5.4	0.9	3.5	6.7

Table 11 Mean values, standard deviation, minimum and maximum values of muscle fascicle length (cm) for the cranial, middle and caudal LD in the pony

Fascicle Length (cm)	N	Mean	Stdev	Minimum	Maximum
Cranial	9	7.9	2.5	3.8	11.3
Middle	9	7.5	1.7	4.9	9.8
Caudal	9	4.6	1.1	3.0	6.4

Fig. 21 and Fig. 22 show a consistent trend of muscle fascicles length to decrease between the middle and the caudal section of LD. The changes of fascicle length between the cranial and the middle part were not uniform and showed even an increase of fascicle length in some of the muscles. There was a significant decrease of muscle fascicle length between the middle and the caudal section in horses (p= 0.0001) and in ponies (p=0.001) and also between the cranial and the caudal section in the horse (p= 0.0001) and ponies (p= 0.0001). There was no significant difference in fascicle length between the cranial and middle section in horses (p= 0.7) as well as in ponies (p=0.9). Also no significant difference was found between dorsal and ventral measurements of fascicle length in both horses and ponies (p= 0.9). The mean ±stdev value of the dorsal and ventral fascicle length was 7.8 ±1.8 cm and 7.6 ±2.1 cm in the horse and 6.6 ±1.5 cm and 6.5 ±2.2 cm in the pony.

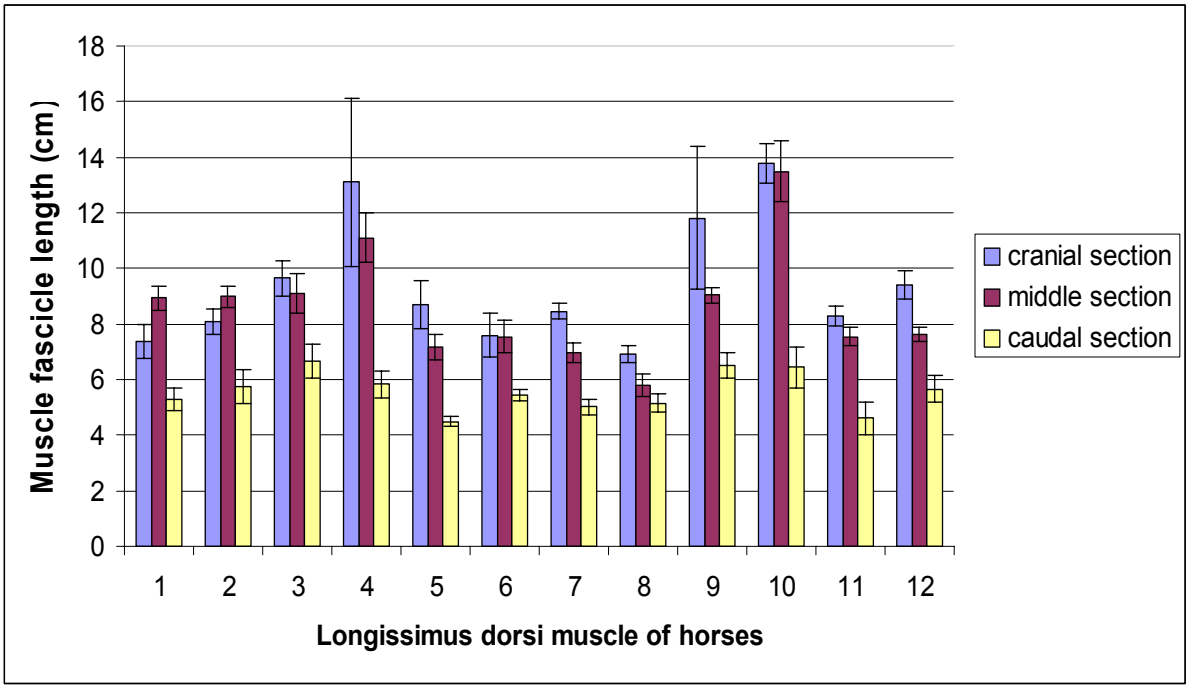

Fig. 21 Mean (± stdev) muscle fascicle length (cm) in the cranial, middle and caudal section of twelve LDs of horses. Mean values of fascicle length decrease in cranial to caudal direction. Columns present the mean values, whiskers the standard deviation.

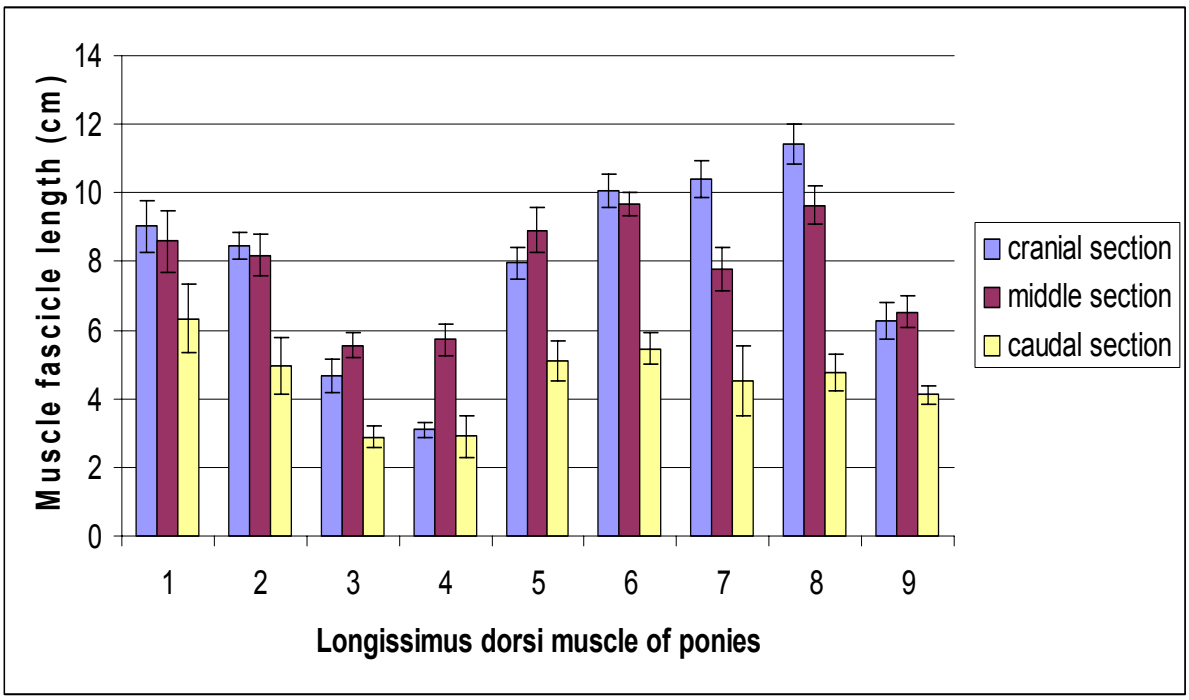

Fig. 22 Mean (± stdev) muscle fascicle length (cm) in the cranial, middle and caudal section of nine LDs of ponies. Mean values of fascicle length decrease in cranial to caudal direction. Columns present the mean values, whiskers the standard deviation.

Normalised muscle fascicle length

The normalised muscle fascicle length (cm) describing the ratio of muscle fascicle length (cm) to muscle length (cm) showed a mean (±stdev) value of 0.07 ±0.02 cm in the horse and 0.09 ±0.03 cm in the pony (Table 12). Muscle fibre length normalised for whole muscle length was significantly longer (p=0.005) in ponies compared to horses.

Table 12 Mean values, standard deviation, minimum and maximum values of the normalised muscle fascicle length (cm) in horses and ponies

Norm. Fascicle Length (cm)	N	Mean	Stdev	Minimum	Maximum
Horse	57	0.07	0.02	0.03	0.13
Pony	56	0.09	0.03	0.03	0.17

In the subdivided LD of the horses minimum and maximum fascicle length normalised for whole muscle length differed from 0.07 cm and 0.09 cm in the cranial part to 0.06 cm and 0.09 cm in the middle part and to 0.03 cm and 0.06 cm in the caudal part. The mean ±stdev normalised fascicle length decreased from 0.08 ±0.02 mm (cranial), to 0.07 ±0.02 cm (middle) and to 0.05 ±0.01 cm (caudal) (Table 13, Fig. 24).

In the ponies, minimum and maximum normalised fascicle length ranged from 0.08 cm to 0.11 cm in the cranial part, 0.08 cm to 0.12 cm in the middle part and 0.04 cm to 0.07 cm in the caudal part. The mean ±stdev values decreased in cranial to caudal direction from 0.1±0.03 cm (cranial) to 0.1 ±0.03 cm (middle) to 0.06 ±0.02 cm (caudal) (Table 14 and Fig. 24).

Table 13 Mean values, standard deviation, minimum and maximum values of the normalised muscle fascicle length (cm) for the cranial, middle and caudal LD in horses

Norm. Fascicle Length (cm)	N	Mean	Stdev	Minimum	Maximum
Cranial	12	0.08	0.02	0.07	0.09
Middle	12	0.07	0.02	0.06	0.09
Caudal	12	0.05	0.01	0.03	0.06

Table 14 Mean values, standard deviation, minimum and maximum values of the normalised muscle fascicle length (cm) for the cranial, middle and caudal LD in ponies

Norm. Fascicle Length (cm)	N	Mean	Stdev	Minimum	Maximum
Cranial	9	0.1	0.03	0.08	0.11
Middle	9	0.1	0.03	0.08	0.12
Caudal	9	0.06	0.02	0.04	0.07

The normalised fascicle length showed no significant difference between the cranial and the middle section in horses (p=1.0) or ponies (p=1.0). In both horses and ponies, however, there was a significant decrease of muscle fascicle length between middle and the caudal section (p= 0.0001) and also between the cranial and the caudal section (p= 0.0001). Also no significant difference was found between dorsal and ventral normalised fascicle length (p=0.7). The mean (±stdev) value of the dorsal and ventral normalised fascicle length was 0.6 ±0.2 cm and 0.7 ±0.3 cm in horses and 0.8 ±0.2 cm and 0.7 ±0.3 cm in ponies respectively.
Fig. 23 and Fig. 24 show that the trend of decreasing muscle fascicle length along LD was similar between the normalised muscle fascicle length and non-normalised muscle fascicle length. Fig. 24 also displays the significantly longer normalised muscle fascicle length (p= 0.005) in ponies compared to horses, although in the caudal section of LD the mean value for the normalised fascicle length is similar between horses (0.05 ±0.01 cm) and ponies (0.06 ±0.02cm).

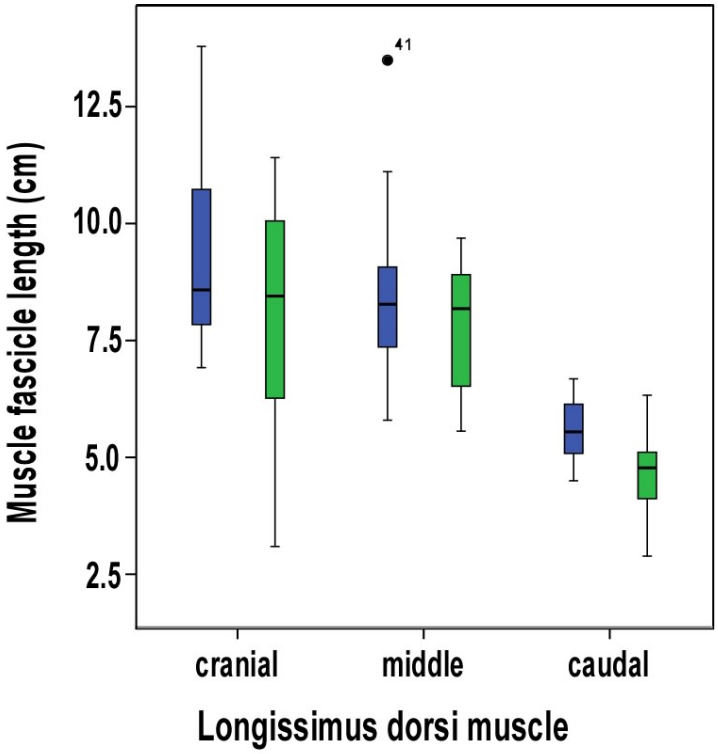

Fig. 23 Box and whisker plot presenting muscle fascicle lengths in horses (blue) and ponies (green) for the cranial, middle and caudal section. The middle line presents the median, the box the interquartile range, the whiskers the maximum and minimum and the dot an outlier.

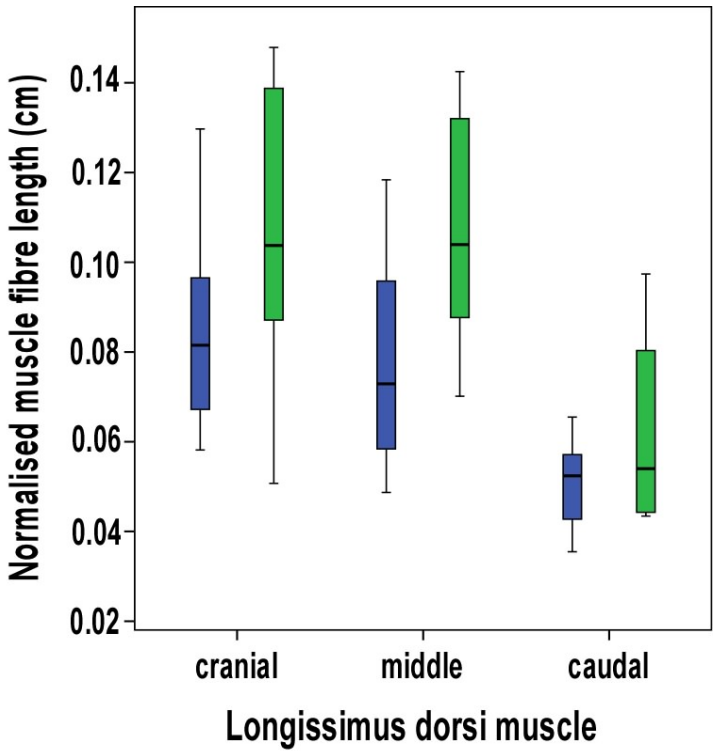

Fig. 24 Box and whisker plot presenting muscle fascicle lengths normalised for whole muscle length in horses (blue) and ponies (green) for the cranial, middle and caudal section. The middle line presents the median, the box the interquartile range and the whiskers the maximum and minimum.

Pennation angle

The mean ±stdev value of the pennation angle was 43 ±14° in horses and 38 ±14° in ponies. Minimum and maximum values ranged from 13° to 81° in horses and from 10° to 38° in ponies (Table 15). There was no significant difference (p=0.06) between the pennation angle of horses and ponies.

Table 15 Mean values, standard deviation, minimum and maximum values of pennation angle (°) in horses and ponies

Pennation angle (°)	N	Mean	Stdev	Minimum	Maximum
Horse	48	43	14	13	81
Pony	43	38	14	10	75

In the subdivided LD pennation angle showed an increase in cranial to caudal direction.

In horses the minimum and maximum pennation angle was 18° and 60° (cranial), 31° and 71° (middle) and 26° and 81° (caudal). The mean ±stdev pennation angle decreased from 35 ±11° in the cranial sector to 45 ±11° in the middle sector to 51 ±15° in the caudal sector (Table 16, Fig. 25).

In the ponies the variation of the pennation angle in the cranial, middle and caudal sections ranged from 10° to 44° (cranial), 18° to 74° (middle) and 32° to 75° (caudal). The means ±stdev pennation angles were 30 ±9° in the cranial part, 41 ±14° in the middle and 48 ±12° in the caudal part (Table 17, Fig. 26).

Table 16 Mean values, standard deviation, minimum and maximum values of pennation angle (°) for the cranial, middle and caudal LD in the horse

Pennation angle (°)	N	Mean	Stdev	Minimum	Maximum
cranial	11	35	11	18	60
middle	11	45	11	31	71
caudal	11	51	15	26	81

Table 17 Mean values, standard deviation, minimum and maximum values of pennation angle for the cranial, middle and caudal LD in the pony

Pennation angle (°)	N	Mean	Stdev	Minimum	Maximum
cranial	9	30	9	10	44
middle	9	41	14	18	74
caudal	9	48	12	32	75

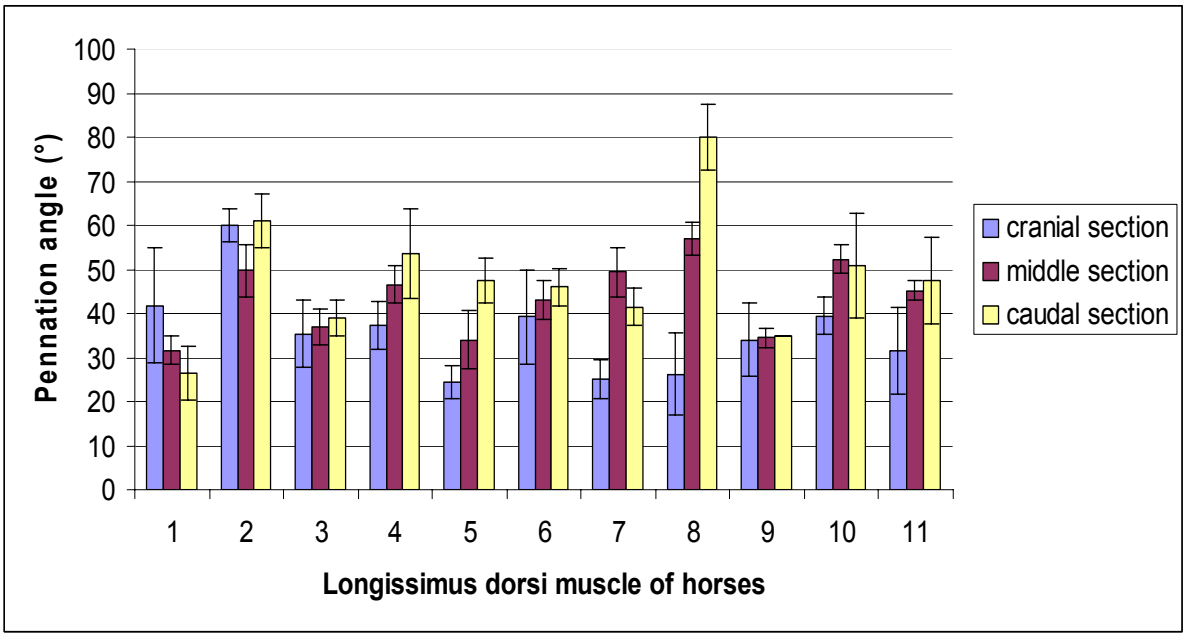

Fig. 25 Mean (± stdev) muscle pennation angle in the cranial, middle and caudal section of eleven LDs of horses. Mean values of pennation angle increase in a cranial to caudal direction. Columns present the mean values, whiskers the standard deviation.

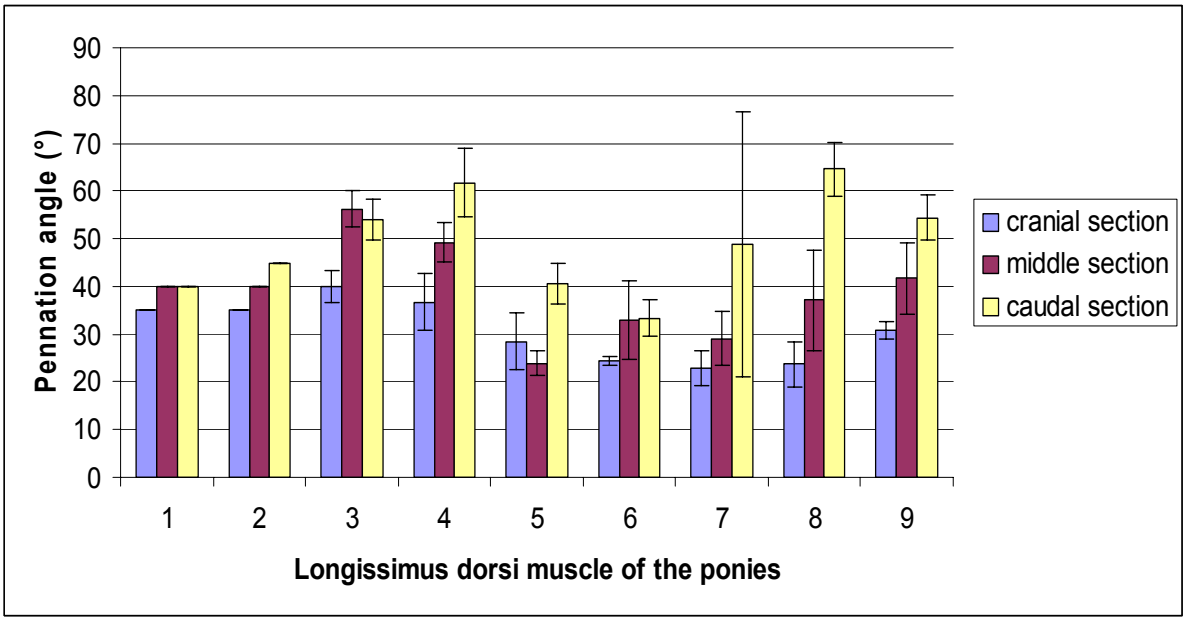

Fig. 26 Mean (± stdev) muscle pennation angle in the cranial, middle and caudal section of nine LDs of ponies. Mean values of pennation angle increase in a cranial to caudal direction. Columns present the mean values, whiskers the standard deviation.

There was a significant difference between the pennation angle of the cranial and middle part for horses (p=0.05) and ponies (p=0.02) as well as between the cranial and caudal part for horses (p=0.004) and ponies (p=0.0001). No significant difference was found between the middle and caudal part for horses (p=0.8) and ponies (p=0.06). No significant difference was found between dorsal and ventral pennation angle in horses (p=0.2) and ponies (p= 0.9). The mean ±stdev of the dorsal and ventral pennation angle was respectively 51° ±8 and 41° ±11 in horses and 41° ±5 and 41° ±12 in ponies.

Physiological cross-section area and maximum isometric force

The physiological cross-sectional area (PCSA) is calculated by dividing muscle volume (cm^3) by muscle fascicle length (cm). The minimum value of PCSA for horses was 642 cm^2 and the maximum value was 1199 cm^2. Mean ±stdev PCSA was 869.6 ±189.6 cm^2. In ponies the minimum value of PCSA was 143 cm^2 and the maximum value 522 cm^2. The mean ±stdev value was 309.2 ±146.2 cm^2 (Table 18). These results show a significantly lower PCSA for ponies than for horses (p=0.0001).

Table 18 Showing mean values, standard deviation, minimum and maximum values of the physiological cross-section area (PCSA) of the whole LD in horses and ponies

PCSA (cm^2)	N	Mean	Stdev	Minimum	Maximum
Horses	12	869.6	189.6	642.0	1199.0
Ponies	9	309.2	146.2	143.0	522.0

The diameter of LD increased in cranial to caudal direction while muscle fascicle length decreased (Fig. 27). Subsequently PCSA was calculated individually for the cranial, middle and caudal sections. Muscle volume measurements were obtained from a previous study (Ritruechai P, 2006). From this study it was emphasised that muscle volume between the cranial part (T1-T12), middle part (T13-T18) and the caudal part (L1-L6) of the LD had almost identical percentages of the total muscle volume. The volume for these areas showed 38.7% (cranial), 31.8% (middle) and 29.4% (caudal) of the overall muscle volume with a coefficient of variation (= standard deviation/ mean) of 0.01. Therefore PCSA of LD was expected to increase in cranial to caudal direction. Based on muscle fascicle changes the following results for horses and ponies confirmed the increase of PCSA between cranial and caudal as well as between middle and caudal sections.

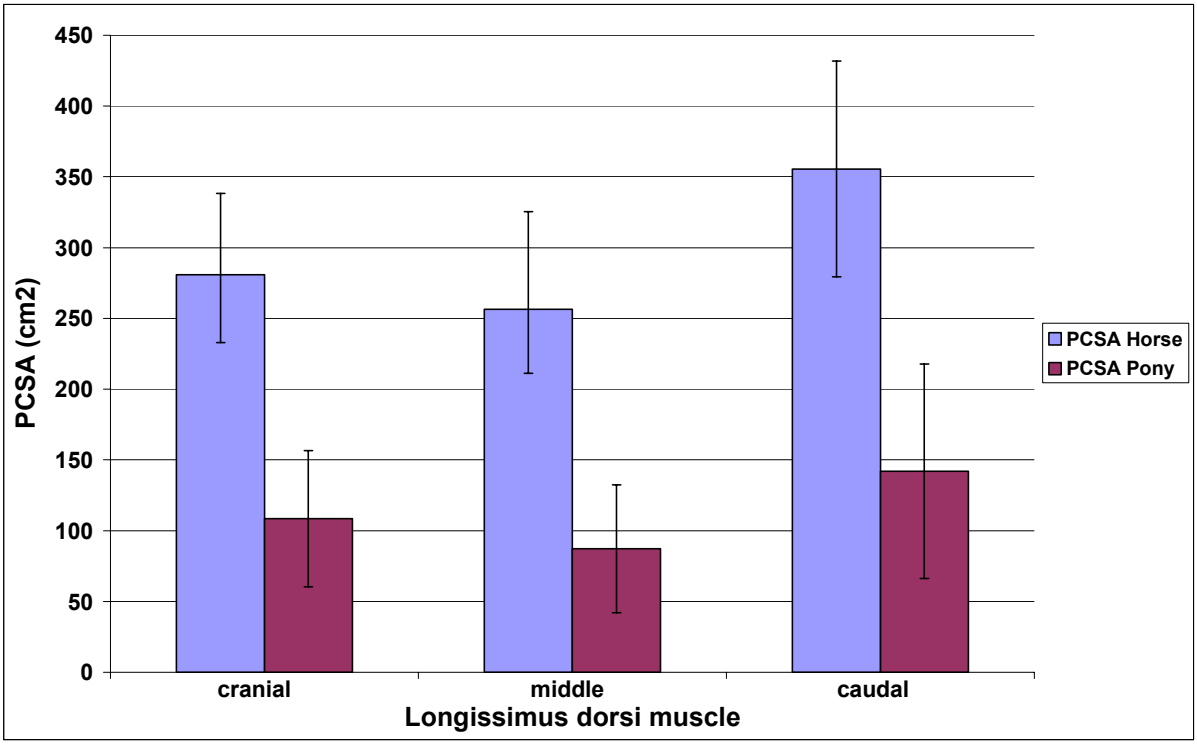

Fig. 27 Mean (± stdev) cranial, middle and caudal PCSA (cm^2) of LD are shown for horses and ponies. Columns present the mean values, whiskers the standard deviation.

In horses mean ±stdev PCSA was 280.9 ±57.4 cm^2 cranial, 256.4 ±68.9 cm^2 middle and 355.3 ±76.5 cm^2 caudal (Table 19, Fig. 28). In ponies the mean values ±stdev of PSCA were 108.5 ±48.0 cm^2 cranial, 87.2 ±45.1 cm^2 middle and 142.0 ±75.8 cm^2 in the caudal section (Table 20, Fig. 29).

Table 19 Mean values, standard deviation, minimum and maximum values of physiological cross-section area (cm^2) for the cranial, middle and caudal LD in the horses

HORSE	N	Mean (cm^2)	Stdev	Minimum	Maximum
Cranial	12	280.9	57.4	198.0	392.0
Middle	12	256.4	68.9	171.0	354.0
Caudal	12	355.3	76.5	254.0	535.0

Table 20 Mean values, standard deviation, minimum and maximum values of physiological cross-section area (cm^2) for the cranial, middle and caudal LD in the ponies

PONY	N	Mean (cm^2)	Stdev	Minimum	Maximum
Cranial	9	108.5	48.0	47.0	180.0
Middle	9	87.2	45.1	40.0	158.0
Caudal	9	142.0	75.8	66.0	251.0

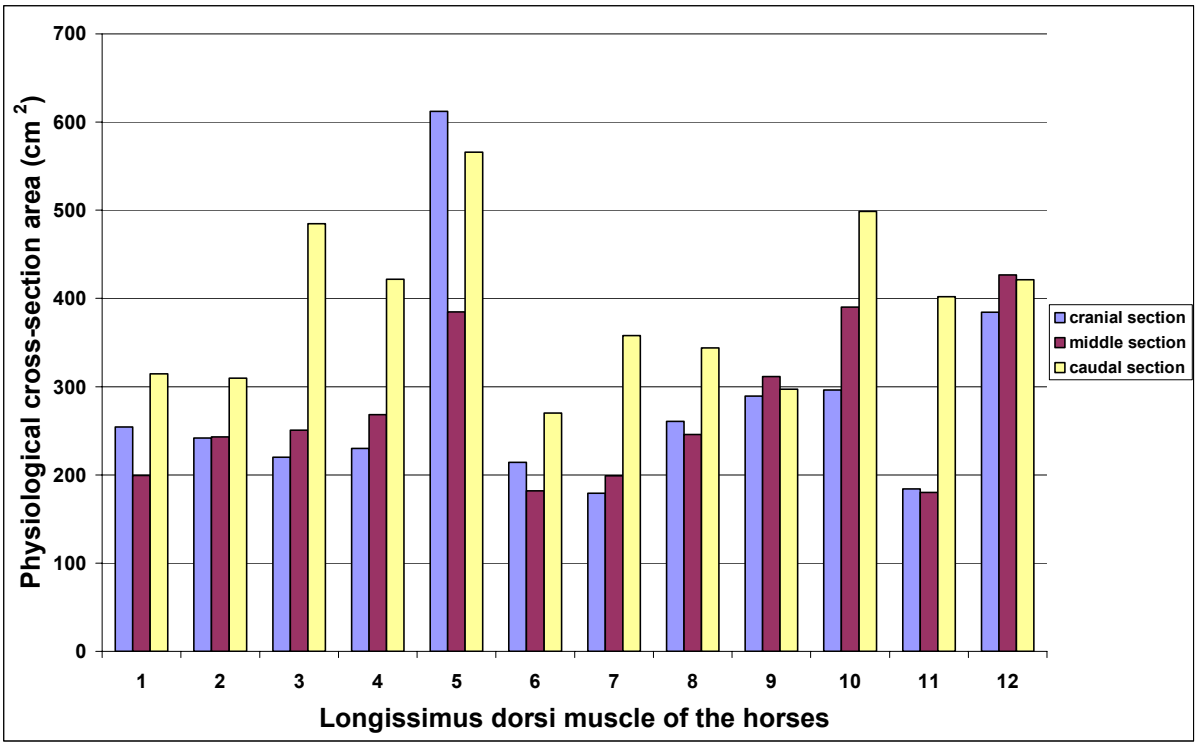

Fig. 28 Mean values of the physiological cross-section area (cm^2) in the cranial, middle and caudal section of twelve LDs of horses. Mean values of physiological cross-section area increase in cranial to caudal direction. Columns present the mean values, whiskers the standard deviation.

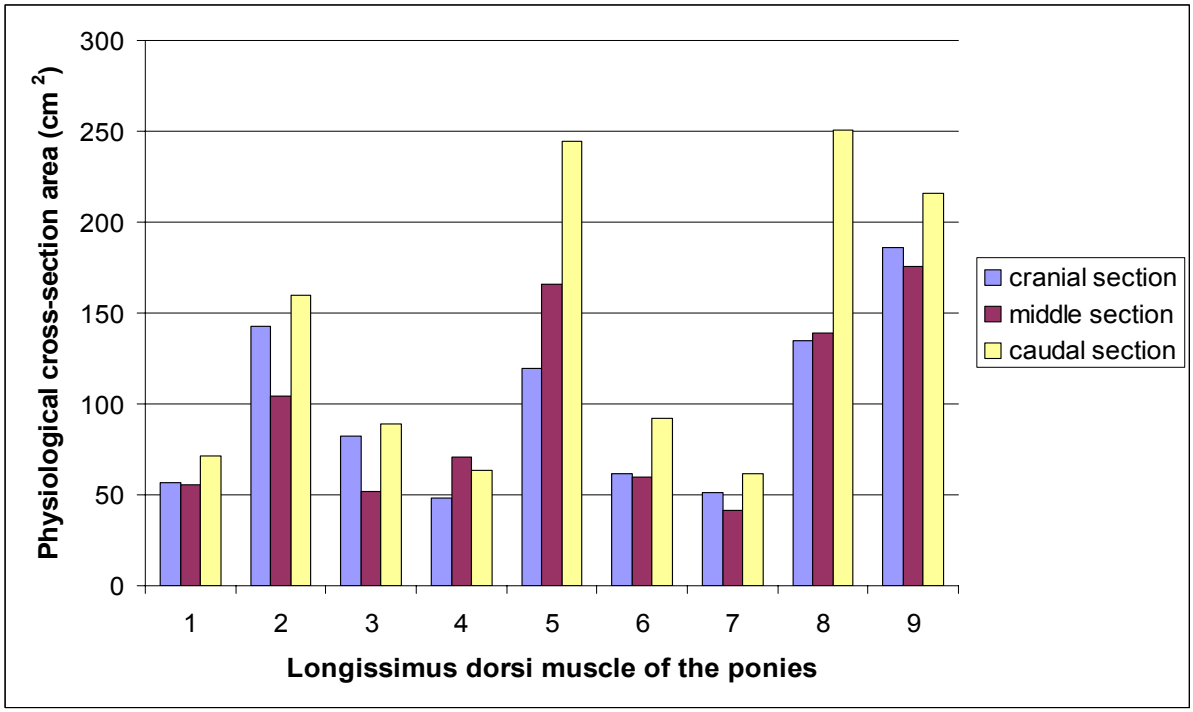

Fig. 29 Mean values of the physiological cross-sectional area (cm^2) in the cranial, middle and caudal section of nine LDs of ponies. Mean values of physiological cross-sectional area increase in cranial to caudal direction. Columns present the mean values, whiskers the standard deviation.

In the horses there was a significant difference between the cranial and the caudal section of LD (p=0.03) as well as between the middle and the caudal section (p=0.03). No significant difference was detected between the cranial and the middle section of LD (p=1.0)
In contrast, in the ponies there was only a significant difference between the middle and the caudal section of LD (p=0.05) but no significant difference was shown between the cranial and the middle section (p=0.3) and between the cranial and the caudal section (p=0.1).

Maximum isometric force (F_{max}.)

Maximum isometric force (F_{max}) is proportional to PCSA. The mean ±stdev maximum isometric force for the whole LD was 26088.4 ±5688.6 N/cm^2 in the horses and 9278.3 ±4386.7 N/cm^2 in the ponies (Table 21). The F_{max} was significantly larger in horses compared to ponies (p=0.0001).

Table 21 Mean values, standard deviation, minimum and maximum values of maximum isometric Force (N/ cm^2) in horses and ponies

	N	Mean (N/ cm^2)	Stdev	Minimum	Maximum
Horse	12	26088.4	5688.6	19285.0	35983.0
Pony	9	9278.3	4386.7	4291.0	15667.0

Maximum isometric force of the LD changes in a craniocaudal direction in horses. The cranial region had a mean ±stdev value of 8427.6 ±1721.4 N/cm^2, the middle region 7691.9 ±2067.8 N/cm^2 and the caudal region 10659.9 ±2296.3 N/cm^2 (Table 22). In the ponies the mean value ±stdev of the maximum isometric force was calculated for the cranial region 3253.9 ±1442.5 N/cm^2, middle region 2615.1 ±1353.9 N/cm^2 and the caudal region 4260.0 ±2275.3 N/cm^2 (Table 23).

Table 22 Mean values, standard deviation, minimum and maximum values of maximum isometric Force (N/cm^2) for the cranial, middle and caudal LD in the horses

Horse	N	Mean	Stdev	Minimum	Maximum
Cranial	12	8427.6	1721.4	5936.0	11773.0
Middle	12	7691.9	2067.8	5137.0	10609.0
Caudal	12	10659.9	2296.3	7625.0	16064.0

Table 23 Mean values, standard deviation, minimum and maximum values of maximum isometric Force (N/cm^2) for the cranial, middle and caudal LD in the ponies

Pony	N	Mean	Stdev	Minimum	Maximum
Cranial	9	3253.9	1442.5	1420.0	5415.0
Middle	9	2615.1	1353.9	1211.0	4749.0
Caudal	9	4260.0	2275.3	1987.0	7531.0

In the horses there was a significant difference between the cranial and the caudal section of LD (p=0.03) as well as between the middle and the caudal section (p=0.03). No significant difference was detected between the cranial and the middle section of LD (p=1.0). In contrast, in the ponies there was only a significant difference between the middle and the caudal section of LD (p=0.05) but no significant difference was shown between the cranial and the middle section (p=0.3) and between the cranial and the caudal section (p=0.1). Fig. 30 shows the the difference in F_{max} between horses and ponies.

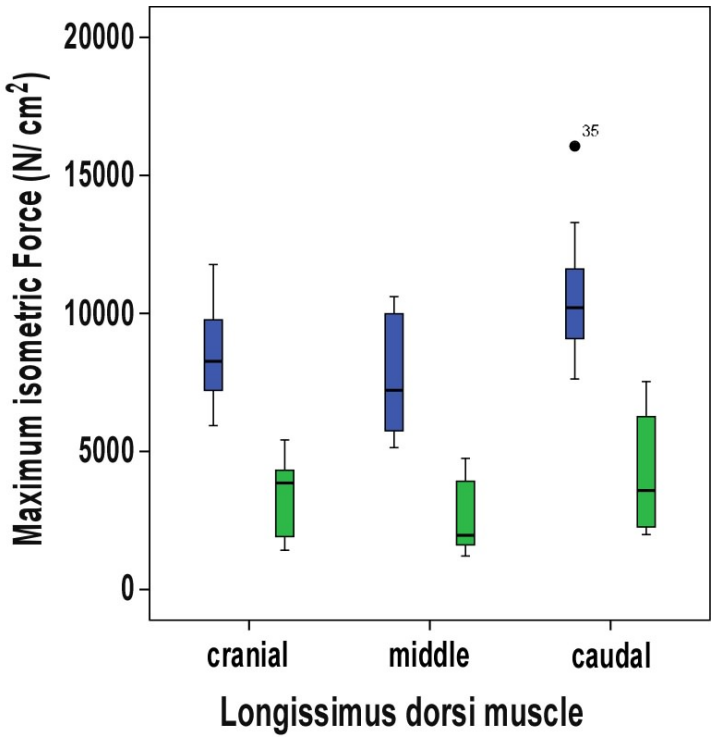

Fig. 30 Box and whisker plot showing the maximum isometric force values (N/cm^2) for horses (blue) and ponies (green) in the cranial, middle and caudal section of LD. The middle line presents the median value, the box the interquartile range, the whiskers the maximum and minimum and the dot an outlier.

III.1.4 Discussion and Conclusion

III.1.4.1 Structure and Function

The knowledge about the functional capacity of the largest muscle of the equine back contributes to understand the pathogenesis of back problems and hence their diagnosis and treatment. This study provides architectural measurements of the equine thoracic and lumbar LD, which contribute to better understanding of the mechanics of the equine back.

The longissimus dorsi muscle as the longest muscle in the horse shows a rather complex structure. Multiple muscle bundles overlapping one another extend over one or more intercostal and intertransversal spaces. They attach with rather short tendons or aponeurotic sheets to the bony structures or insert with muscle fascicles to strong aponeurotic fascia. An internal aponeurosis which seems to be homologous with the lumbar intermuscular aponeurosis of man, cat, dog and monkey (Bogduk 1980) divides the muscle in a more superficial dorsal layer and a deeper ventral layer.
The size and the complexity of LD impact on the calculated values of PCSA, and therefore the calculation of the force generation capacity of the muscle. To increase the validity of the architectural data and to reflect the different functional properties of LD the muscle was subdivided in different sections. The subdivision of muscles with broad attachment sites have been previously performed in studies of other complex muscles (Dumas *et al.* 1991; Sharir *et al.* 2006; Van der Helm and Veenbaas 1991). In this study the equine LD muscle was divided based on vertebral landmarks. The thoracic LD was additionally subdivided based on kinematic findings which were increased range of motion in the cranial thoracic spine and less spinal motion in the caudal vertebrae.

The analysis of the architectural measurements and calculated parameters suggest differences in the functional properties within the LD muscle. The variations in the diameter of the muscle and of the muscle fibre arrangement are reflected in functional variations along the muscle.
The thoracic LD is characterized by long muscle fibres and relatively small pennation angles. The rather small diameter in the area of the first few thoracic vertebrae (T1-T4) and slowly increasing diameter of the thoracic LD from T4-T18 in combination with long muscle fibres suggest a specialization for velocity contractions and high excursion. Especially in the cranial part of thoracic LD the pennation angle is relatively small and therefore has limited influence on the contraction of the muscle. This architectural arrangement of the cranial thoracic LD

indicates the prevalence for motion rather than for stabilization as the main task of this muscle part. This is also supported by the orientation of the muscle fibres. Based on the parallel arrangement of the muscle fibre to the spine the muscle acts preferentially as lateral flexor (Bojadsen *et al.* 2000).

Over the course of the thoracic LD muscle fibre length decreases whereas the pennation angle and the cross-section area increase towards the caudal part of the thoracic spine. In the caudal region of LD the large maximum value of the pennation angle in the horse (81°) is more likely to be an artefact due to post mortem changes of the muscle tissue. However, the larger dimension of the muscle as well as the relatively shorter muscle fibres suggests a tendency for more powerful contractions (Payne *et al.* 2005; Payne *et al.* 2004).

In comparison to the thoracic LD the lumbar LD shows distinct differences in fibre arrangement, with smaller muscle fibre lengths and larger pennation angles. Not all muscle fibres of the lumbar area attach directly to the tendon of insertion. They also attach to the strong lumbar intermuscular aponeurosis and to multiple intrinsic fascia of the muscle which divide the muscle in small pennated parts. Hence the architecture of the muscle fibres is more pennated which results in a rather parallel arrangement of sarcomeres. This design increases the capacity of the muscle to exert large forces and to experience high tension.

The calculated maximal isometric force for the three different parts of the subdivided muscle was significantly different between the cranial and caudal and the middle and caudal part. In the lumbar LD significantly shorter muscle fibres and a significantly larger pennation angle result in a significantly larger physiological cross-section area. Therefore the arrangement of a higher number of sarcomeres in parallel leads to the conclusion that this muscle part is designed to exert larger force (Van Eijden *et al.* 1997).

These results demonstrate obvious differences in functional capacity between the thoracic and lumbar LD. The muscle architecture indicates that the whole LD is well suited to a broad range of tasks. Lateral and dorsoventral flexion in the thoracic LD is made possible by long muscle fibres. The lumbar and caudal thoracic LD stabilize the vertebral column during downwards movement of the visceral mass at stance phase due to multipennated short fibred muscle architecture. Strain energy is stored and utilized in the strong and thick aponeurosis and the lumbar intermuscular aponeurosis, the elasticity of the aponeurosis acting as energy-saving mechanism (Ettema and Huijing 1989). In horses the energy saving mechanism of tendons is well documented. Elastic strain energy is stored when tendinous structure are stretched and then returned when the strain is released. This optimizes the economy of the muscle by reducing the required mechanical work (Alexander 1991).

The functional arrangement of the muscle fibres of LD corresponds with findings of kinematic studies of the equine spine. Results of these *in vitro* and *in vivo* studies showed a higher range of motion, in the cranial thoracic vertebral column (up to T14) and at the lumbar sacral junction (Denoix 1999b; Faber *et al.* 2001a; Faber *et al.* 2000; Haussler *et al.* 2001; Jeffcott and Dalin 1980). The kinematic results correspond to the architectural findings of the thoracic and lumbar LD. The prevalence for larger excursion and velocity contraction of LD in the thoracic area due to the long muscle fibres and small pennation angles reflect the higher range of motion between T1-T14. The stabilising function of the cranial trunk is provided by the strong musculature of the neck and the shoulder gridle, the front limbs and the rib cage contribute to the static support of the cranial trunk and resist against gravity. Although the largest range of dorsoventral flexion was observed in the lumbosacral joint the decreased range of motion of the caudal thoracic and lumbar back can be explained by the characteristics of the LD muscle architecture and the rigidity of the vertebral column. Pennate, short muscle fibres characterize muscles which generate large forces and exert high tension. In contrast to the stability provided by the rib cage in the thoracic vertebral column there is a lack of supporting bony structures at the lumbar spine. Therefore in the lumbar section the stabilisation of the trunk against gravity relies on the relatively small transverse processes of the lumbar vertebrae and the non static epaxial and hypaxial musculature including the strong caudal thoracic and lumbar LD. The lumbar LD may also act as a lever for the overlying tongue of the middle gluteal muscle. The middle gluteal muscle is one of the major propulsion muscles of the hindlimb and its tongue reaches from caudal as far as T18. It inserts to the strong thoracolumbar aponeurosis of LD. Kinematic studies showed a rather rigid lumbar spine with increased range of dorsoventral flexion in the lumbosacral joint (Haussler *et al.* 2001; Townsend and Leach 1984). The lack of the supporting rib cage to resist against gravity and the weight of the visceral organs as well as the role of the lumbar spine in the transition of propulsion from the hindlimbs to the trunk suggests an important stabilising role of the lumbar LD muscle in this area.

The clinical relevance of back lesions as cause for poor performance, back pain and lameness is sometimes difficult to diagnose and the functional relevance of muscle alterations is still unclear. A radiologic and scintigraphic study in clinically sound horses showed an incidence of spinal alterations of 26 horses preferentially in the area between T13 and T18 (Erichsen *et al.* 2004). Muscle wastage of LD was shown to be a common sign in horses with sacroiliac

joint pathology (Ross and Dyson 2002). According to the functional characteristics of LD it can be considered that different pathological alterations are related to certain areas of the back. Further research in terms of evaluation of LD muscle function needs to be done to reveal whether a lack of laterolateral flexibility of the horse is connected to a thoracic LD or and thoracic vertebral column lesion or a lack of hindlimb (propulsion) support is a result of lumbar musculature and vertebral column alteration.

Unfortunately some limitations to the study had an influence on the utilisation of the results. The examined horses and ponies did not reflect the average population because the range of age was very high (between 6 month and 32 years) and the majority of animals were over the age of 20. Studies in humans showed that aging musculature undergoes a remarkable amount of changes. The loss of muscle mass is associated with increasing body fatness (sarcopenia) showing that muscle structure is significantly altered in old age (Narici *et al*., 2003). This could be observed in most of the older horses/ ponies which had visible muscle atrophy and a fare amount of fat incorporation into the muscle tissue and into adjacent connective tissue. The additional fat could have influenced both the architectural arrangement of the muscle and the rate of decay and therefore the accuracy of the measurements.

III.1.4.2 Conclusion

The presented study provides a detailed data of the gross-morphology of the equine LD. The predicted force generation capacity of the LD in combination with the range of spinal motion contributes to the understanding of back related pathological conditions and their impact on the movement and performance of the horse.

Alterations of the cranial part of the thoracic and lumbar LD due to spinal vertebral pathology or primary muscle injuries can lead to an increase in stiffness of the spine and reluctance to bend laterally. The changes in the caudal region of the LD might lead to a lack of stability and weakness which could lead to a restriction of propulsion transformation from the hind limb musculature to the axis of the horse during jumping and forward movements.

Although the architectural results can give an idea of the performance capacity of the thoracic and lumbar LD in healthy and in pathological conditions it is necessary to carry out further tests. Muscle fibre typing and electromyography would complete the functional and anatomical picture and contribute to understand the back as a complete anatomical and functional unit. Muscle fibre type composition could reveal functional differences between LD sections as different fibre types in varying proportions within a muscle represent a certain specification in function. Electromyography provides information of the intensity of muscle

activity and timing in relation to locomotion. Electromyographic activity pattern in the different segments along LD gives an insight of the whole muscle activity during locomotion (Chapter III.2.).

III.2 Muscle activity of the equine thoracolumbar Longissimus dorsi muscle during locomotion

III.2.1 Introduction

Disorders of the equine back are often made responsible for a whole range of unspecific clinical signs, such as reluctance to exercise and poor performance and it is often impossible to reach a definite diagnosis. Radiography of the back and less commonly scintigraphy and ultrasonography are the imaging modalities of choice, but changes are rarely pathognomonic. The extent to which pathological changes of the back musculature such as chronic muscle wastage influences back function and clinical signs is not clear. Hence a thorough knowledge of normal muscle function of the epaxial musculature is essential for the understanding of back function as a whole and is a prerequisite to understand the development of back pathology. The thoracolumbar LD is the largest muscle of the equine back and extends from its origin at the last cervical vertebrae to its insertion at the iliac wing. Its size and the anatomical location alone indicate its pivotal role in back movement. Anatomical studies have (chapter III.1) demonstrated that muscle morphology is not uniform along the muscle. It was found that muscle fibre length and pennation angle vary significantly along the muscle. These results presume variations between different segments in their ability to generate force and hence may indicate different function during locomotion.

The equine vertebral column is a rather inherently rigid structure. *In vitro* studies showed a limited range of motion of the vertebral column and adjacent structures by applying different forces to the vertebral column (Denoix 1999b; Townsend and Leach 1984). These forces simulated the weight of the abdominal contents as well as dynamic forces which impact on the vertebral column during locomotion. Results showed that the magnitude of movements which can take place between vertebrae depends on the direction of the movement and varies along the vertebral column. The greatest range of flexion and extension is shown in the lumbosacral joint followed by the caudal part of the thoracic vertebral column (T14-T18). Lateral bending and axial rotation are present mainly between T9 and T14 whereas at the more cranial and more caudal spine lateral bending and rotation is limited by the ribcage, the heights of the dorsal spinous processes and the intertransverse joints (Denoix 1999b; Schlacher *et al.* 2004; Townsend and Leach 1984).

In vivo studies similarly showed the maximum flexion and extension movement at the lumbosacral junction. Apart from the lumbosacral joint the highest range of flexion and

extension was found between T10-T13. The range of lateral bending was similar for all vertebrae in walk, but a higher range of lateral bending occurred in trot. Axial rotation has a slightly smaller range of motion between T10 and T13. In all orientations the caudal part of the thoracolumbar spine tends to move more or less as a rigid body during locomotion which is due to the morphology of the vertebrae (Faber *et al.* 2001a; Faber *et al.* 2001b; Faber *et al.* 2000).

As back locomotion is an interaction between passive and active structures it is equally important to know the range of spinal motion as well as the influence of epaxial musculature on back motion.

The epaxial musculature presents the largest muscle group of the back and is located dorsally bilateral to the thoracic and lumbar vertebral column and the ribs. It comprises the Multifidus, Iliocostal and Longissimus dorsi muscle (LD) which all receive a multisegmental innervation (Nickel *et al.* 1984). The largest of the epaxial group is the thoracic and lumbar LD. It has been subject of numerous studies in different species due to its size and its anatomical position which is relatively easy to access. The dimension and the position of the muscle suggest an important role during back movement. To evaluate LD function several studies have used electromyography (EMG) to demonstrate muscle activity and relate the EMG activity pattern to kinematic measurements of the spine and the limbs during stride cycles (Licka *et al.* 2008; Licka *et al.* 2004; Ritter *et al.* 2001; Robert *et al.* 1999; Robert *et al.* 2001b; Tokuriki *et al.* 1997; Wada *et al.* 2006a; Wada *et al.* 2006b).

EMG provides information about the neuronal effects on the muscle and contractile activity of the muscle by recording interference pattern of motor unit action potentials from active motor units (MU). Motor units are described as the unit of an alpha motoneuron and the sum of its corresponding muscle fibres. EMG has been used to collect information about the electrical activity pattern of motor units in terms of number, duration, onset time and amplitude of excitations which enables the study of muscle contractions related to movement (Wijnberg *et al.* 2004). EMG is widely used in human medicine and sports science to detect myogenic and neurogenic abnormalities or to monitor muscle changes due to training, fatigue, aging, and disuse (Aagard *et al*., 2001; Abe *et al.* 1997; Caldwell *et al.* 2003; Kawakami *et al.* 1995; Kubo *et al.* 2003b). It also has been used to determine normal values of activation patterns in different muscles to investigate functional interaction of the musculoskeletal system and between synergistic and antagonistic muscle groups.

In animals, especially in horses, EMG was mainly applied to different limb muscles to characterise limb muscle activity in relation to limb movement during motion cycles (Robert

et al. 1999; Tokuriki 1973a; Tokuriki and Aoki 1995; Tokuriki *et al.* 1989; Tokuriki *et al.* 1999). Trunk muscle activity has also been measured by EMG to show the recruitment pattern of the muscles under different conditions such as different gaits, speeds, inclines and jumping (Licka *et al.* 2008; Licka *et al.* 2004; Peham *et al.* 2001; Robert *et al.* 2001b; Robert *et al.* 2002; Tokuriki *et al.* 1997).

The recorded muscle activity pattern showed that LD is active during dorsal flexion. As a major extensor muscle this led to the suggestion that LD stabilises the thoracolumbar spine by restricting excessive dorsal flexion (Robert *et al.* 2001b; Robert *et al.* 2002; Tokuriki *et al.* 1997). To control the impact of decelerating, vertical and accelerating forces on the trunk during the stance phase and also to coordinate locomotion it is believed that epaxial muscle function resists these forces and therefore provides postural stability (Carlson 1978; English 1980; Ritter 1995; Thorstensson *et al.* 1982; Tokuriki 1973a, b). With higher dynamic forces through increased speed the onset time of LD activity increased in coordination with hind limb activity in order to oppose the larger inertial forces on the trunk (Rooney 1982; Tokuriki *et al.* 1997). These conclusions were obtained by analysing the results of LD, EMG and kinematic assessment of the spine and limb motion.

In walk the activity pattern of the equine LD showed two small EMG bursts during the middle of stance phase of both hindlimbs (Tokuriki *et al.* 1997). A similar pattern with two EMG bursts per stride cycle was observed in trot. EMG bursts occurred bilaterally and lasted from the late stance phase to the early swing phase of each hindlimb (Robert *et al.* 2001b; Robert *et al.* 2002; Tokuriki *et al.* 1997). The amplitude of the first EMG burst during foot-off of the ipsilateral hind limb was larger than the second EMG burst recorded during foot-off of the contralateral hind limb (Licka *et al.* 2004). In canter both sides of LD were active only once per stride cycle between the early or mid swing phase and the end of the swing phase of the leading hind limb (Tokuriki *et al.* 1997).

The influence of speed and incline was reflected by significant changes of the muscle activity pattern of LD. Compared to slower speed the foot-on time of the hind limbs was earlier in a stride cycle with increased speed. Consequently the onset time of each EMG burst of LD was also significantly earlier. In trot speed affected the activity duration of the first EMG burst by increasing the activity duration while the second burst remained the same. Also muscle activity showed a significantly higher activity level with increased speed. Changes in incline did not change the stride and stance phase duration in trot but influenced EMG activity in the LD. The duration of muscle activity of the LD increased significantly. Onset and offset time of muscle activity per stride cycle changed with increased incline in terms of later onset time

of the first activity burst and a later offset time of both EMG activity bursts. Also the integrated EMG showed a linear increase of the activity level with increasing incline (Robert *et al.* 2001b).
The pattern of muscle activity led to the assumption that LD stabilises the thoracolumbar spine by restricting lateral and dorsoventral flexion. In coordination with hind limb activity the onset of LD muscle activity was earlier and muscle activity level increased with higher dynamic forces of increased speed to oppose larger inertial forces on the abdomen/ trunk (Rooney 1982; Tokuriki *et al.* 1997).

Several studies of the equine LD used only one electrode which do not reflect the overall activity of this large muscle (Robert *et al.* 2001b; Robert *et al.* 2002; Tokuriki *et al.* 1997) but the previous anatomical study (Chapter III.1) showed that muscle architectural parameters such as muscle fibre length and pennation angle are not uniform along LD and varies in some parts of LD significantly. Longer muscle fibres and small pennation angles in the cranial thoracic part of LD characterise a specialisation for velocity contractions and for high excursion. Short muscle fibres with large pennation angle at the lumbar part of LD reflect the specialisation to exert large forces. Differences in architectural structure may influence muscle activity under different conditions which may lead to distinct muscle recruitment pattern in certain areas and variation between the intensity of muscle activity. These variations suggest an influence on the intensity and the pattern of muscle activity. To show the neuromuscular control of the back along LD an elaborate study in cats was performed recently (Wada *et al*., 2006a,b). In this study EMG activities were recorded at the same time along different levels of the feline LD during walk and walk on incline and decline. Muscle activity during level walk showed the same activity patterns with two EMG bursts per stride cycle as reported previously at different LD levels for horses, dogs and cats (English 1980; Licka *et al.* 2004; Ritter *et al.* 2001; Robert *et al.* 2001b; Robert *et al.* 2002; Wada *et al.* 2006a; Wada *et al.* 2006b). The bilateral activity pattern of LD was suggested to increase the stiffness of the vertebral column and therefore to decrease the overall spinal movement. However, on incline the two main bursts of the feline LD often contained two additional EMG bursts whereas on the down slope EMG bursts could hardly be detected and were only observed at steeper grade. Not only the amplitude and duration of EMG bursts increased with increasing upslope but the results of this study also indicated that the timing of EMG onset was influenced by walking conditions. The EMG bursts synchronised their onset time with increasing incline (Wada *et al.* 2006a). The results of this study in cats indicate that muscle

activity along the equine LD might vary between conditions of locomotion and between segments of LD.

Based on anatomical findings in the previous chapter the main hypothesis of this study is that muscle activity pattern and EMG intensity is different between locations along the equine LD. It is also hypothesised that different conditions such as walking and trotting at different speeds and walking on a 5% and 10% incline influence the muscle activity pattern and intensity of muscle activity at the different muscle segments.

III.2.2 Material and Methods

III.2.2.1 Subjects

Six horses (five geldings and one mare) weighing 482 to 578 kg (mean ±stdev 529.5 ±38.9 kg) were used in this experiment. The horses were of mixed breeds (Lippizan, Angoloarab, Irish sport horse, Welsh Cob, Welsh Cob Thoroughbred cross and Thoroughbred). The age of the horses ranged from five years to 17 years (mean 9.8± 4.2 years). All horses were actively ridden and owned by equine science students of Hartpury College who were informed and gave written permission for the use of their horses in this project. The horses were trained and fully habituated to treadmill exercise. Before the experimental procedure all horses were judged by an experienced clinician to be clinically sound during in–hand gait examination and to have no clinical signs of back pain.

III.2.2.2 Data collection

EMG data were collected from the largest epaxial muscle of the equine back, the thoracic and lumbar LD. Surface electrodes were placed at four different sites (T14, T16, T18 and L2) along the right and left LD. The site of the placements have been chosen based on the results of chapter III.1 which showed the most assessable areas of the LD without large overlying musculature between T13 and L3. This electrode placement ensured minimal cross talk of adjacent and overlying muscles. The dorsal spinous processes of T14, T16, T18 and L2 were used as bony landmarks and were identified by manual palpation. Eight bipolar silver/ silver-chloride, self adhesive surface EMG electrodes (10 mm diameter) were placed onto shaved and cleaned (scrubbed) skin patches. The electrodes were arranged bilaterally to the dorsal spinous processes at a distance of 12 cm (T14), 8 cm (T16 and T18) and 4-5 cm (L2) lateral to the midline. A ground electrode was applied to the left tuber coxae. Each EMG signal was

preamplified 5000 times (Biovision, Werheim, Germany) and transmitted through a cable to a multiplexing datalogger unit which was attached to a custom-made harness (Fig. 31).

A uniaxial accelerometer (ADXL 150, Analog Devices, US) was hot-glued to the dorsal hoof wall of the left hind limb (first three horses) and the right hind limb (last three horses). The accelerometer was also connected by a cable to the multiplexing unit at the harness. All cables were secured and taped to the horse to prevent artefacts by cable movements. During data collection it was detected that kinematic measurements were disturbed by cable movement of the accelerometer of the left hindlimb as all infra-red cameras were positioned on the left side of the horses. Therefore the accelerometer was changed to the right hindlimb. During the data collection all collected data was transmitted from the multiplexing unit via cable to a stationary notebook computer (16-bit data acquisition card, 6036E, National Instruments, Austin, Texas) which was set up on a table close by. Data from the EMG electrodes as well as the accelerometer device were recorded at 2000 Hz and captured in a custom written software program (LabView 8.0, National Instrument, Austin, Texas).

Simultaneously to the EMG data collection the triggered collection of three-dimensional kinematic data were collected from the left side of each horse using six cameras from an infrared kinematic motion analysis system (Qualisys, Motion Capturing System, Qualisys AB, Gothenburg, Sweden) at the sampling rate of 200 Hz. The horses were marked with reflective markers. These markers were made from polystyrene hemispheres (Pinflair, Hertford, UK) covered with reflective tape (Scotchlite 8850, EM safety products, Manchester, UK). The reflective markers used in the present study were placed on the lateral and medial hoof wall of the left front and hind limb and using double sided tape (R370, ANCA Industrial Supplies, Halesowen, West Midlands, UK). The kinematic measurements were used to obtain footfall patterns of all four feet.

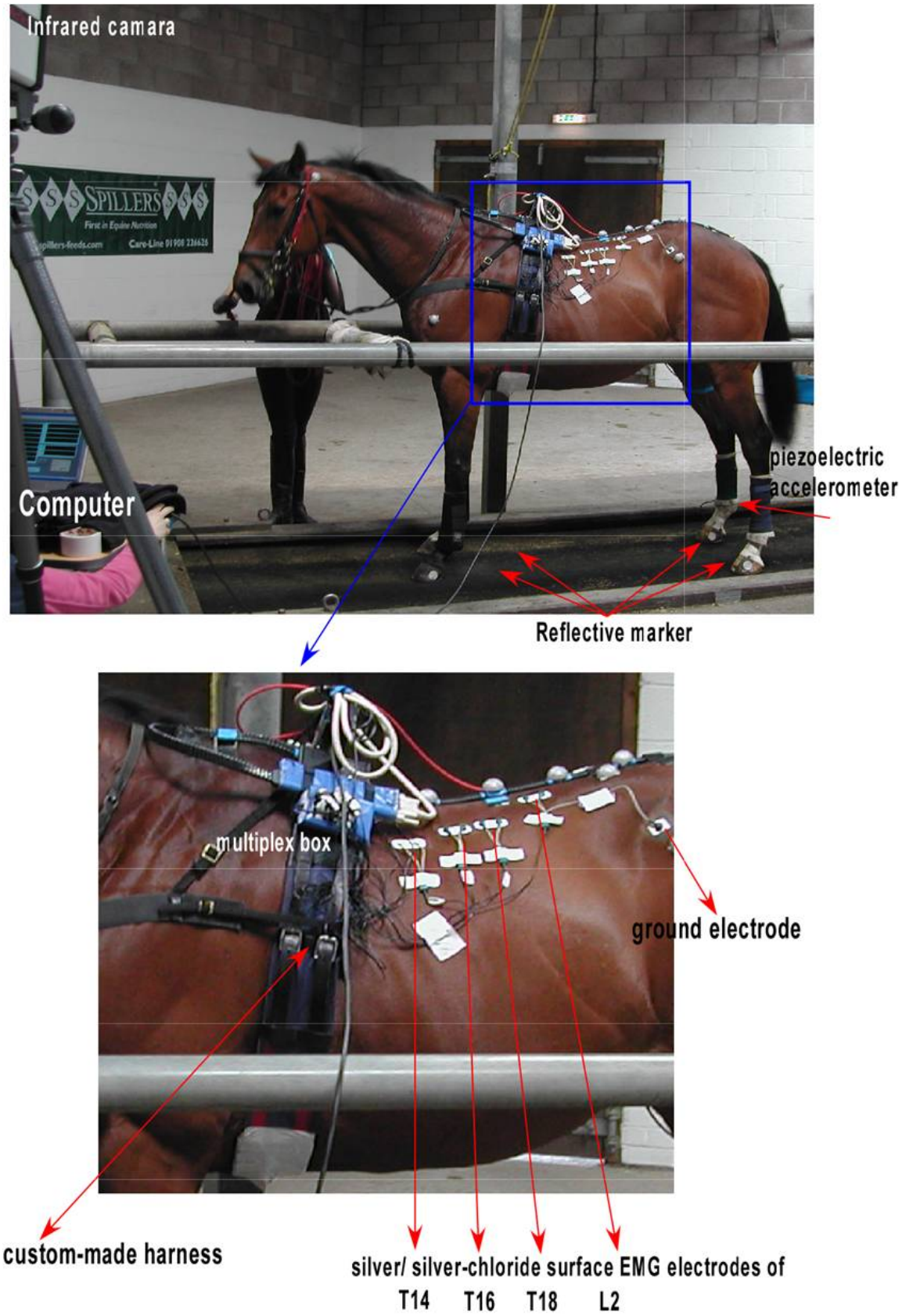

Fig. 31 Experimental set-up: Silver/ silver-chloride surface electrodes were located at T14, T16, T18, L2 and Tuber coxae (ground electrode), all cables connected to the multiplex unit which is attached to the custom-made harness. Reflective markers were glued to the left hoof wall of each foot. An uniaxial accelerometer was hot-glued to the hoof of the right hindlimb.

III.2.2.3 Experimental protocol

Every horse performed a five minute warm-up in walk on the treadmill. Afterwards data were collected at two different sequences of walk and two different sequences of trot with a repetition in reverse order. On a levelled treadmill horses performed a slow walk (1.5 m s^{-1}) and fast walk (1.8 m s^{-1}) followed by slow trot (2.6 m s^{-1}) and fast trot (3.8 m s^{-1}) for respectively five minutes. Accelerometer and EMG data were triggered and were recorded as well as kinematic data for two minutes at the end of each exercise sequence. After the reverse repetition of the different speed levels the horses walked (1.5 m s^{-1}) on a 5% and 10% incline on the treadmill each for the duration of five minutes. Again the exercise program was repeated in reverse order and the last two minutes of each sequence were used for data collection. In each horse EMG was also sampled in a standing position with the feet in square position before and after they walked on/ off the treadmill.

III.2.2.4 Data processing

The EMG signals of the mean ±stdev number of 5831±1475 steps per condition were processed and analysed. EMG signals are often contaminated by the heart muscle electrical activity (ECG) especially when EMG is collected from the trunk. To limit the contamination of EMG an average ECG template was formed from the ECG signals of each standing EMG trace. The ECG template was cross-correlated with the EMG trace of each condition and subtracted at the time of occurrence (Drake and Callaghan 2006). Subsequently the EMG was used to calculate the intensity by wavelet analysis (von Tscharner 2000; Wakeling *et al.* 2002). EMG intensity is a close approximation of the power of the clean EMG trace. Additionally low frequencies (<24Hz) were filtered out of the EMG traces to remove residual ECG and movement artefacts of cables and skin. For each step the total intensity was calculated as the sum of the intensities across wavelet 2-10 (frequency band 24-380 Hz). For each sensor in all conditions the mean intensity was also calculated and interpolated to 100 points per stride cycle which was defined by the foot contact of the left hind limb. All data was normalised to the fastest condition in each horse.

To determine the foot contact of the limbs the signal of the accelerometer of the right/ left hindlimb were visualised on the computer and used to detect initial ground contact for 8835 strides. All data was processed in Mathematica programming environment (Wolfram Research Ltd, Long Hanborough, UK). Although stance and swing phase could only be accurately determined by the accelerometer signals for the respective left or right hindlimb,

stance phase duration for all legs was calculated from collected motion analysis data. For further analysis kinematic was matched to the accelerometer data.

Kinematic data was tracked in Qualysis (Qualisys Track Manager, Motion Capturing System, Qualisys AB, Gothenburg, Sweden) to provide the trajectories of the foot markers. The xyz-coordinates of each marker were exported into Labview 8.0 (National Instrument, Texas) to calculate the following stride parameters: stride time and stance time which was reported as percentage of a 100% stride cycle. For each horse in each condition the four limbs were synchronised to the interpolated EMG intensity.

On and off set time of EMG bursts during one stride cycle were determined by using 50% of the highest amplitude of each normalised trace as a threshold (Fig. 32). This was carried out to avoid the influence of different EMG intensity of each trace.

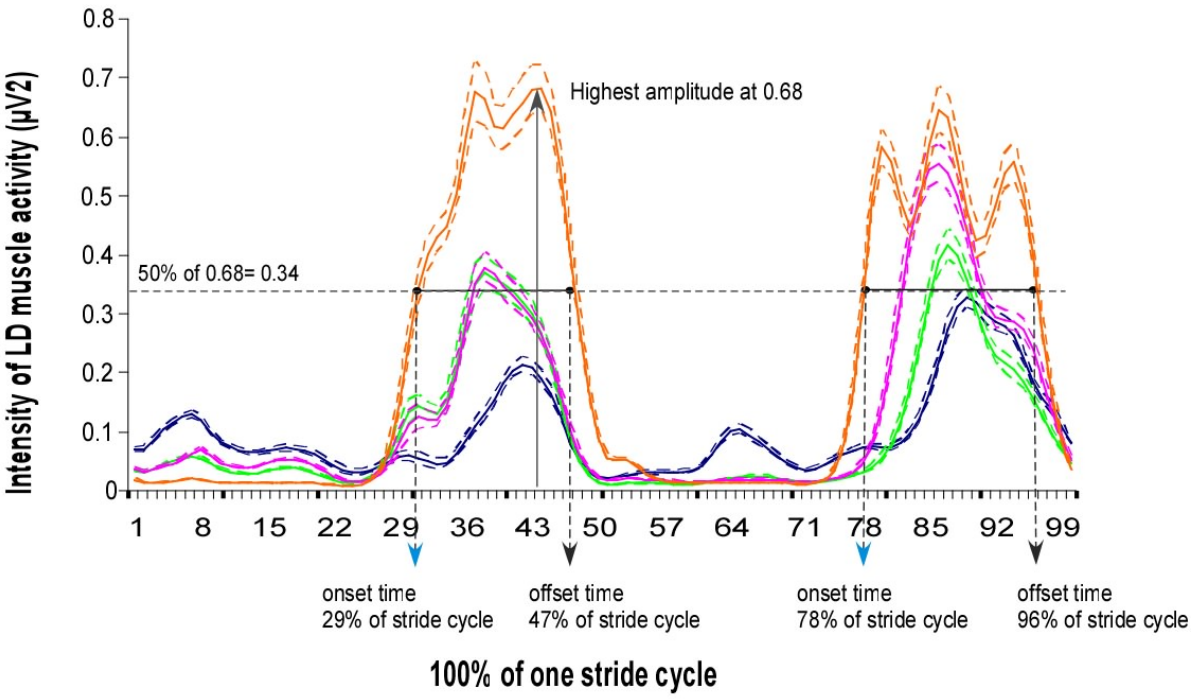

Fig. 32 Calculation of the mean on and offset time (continuous line) with standard error (dotted line) of EMG bursts for different sensor locations (blue =T14, green = T16, pink = T18, orange = L2) in walk on 10% incline. For each EMG trace 50% of the peak EMG intensity was used as threshold to avoid differences of EMG intensity.

III.2.2.5 Data analysis

All data was analysed in SPSS (v.15.0, SPSS Inc., Chicago, Illinois, USA). A univariate linear model used to determine the influence of different conditions (different gaits, speeds and incline) and different locations of EMG sensors (at T14, T16, T18, L2) on the intensity of EMG activity and the number of EMG bursts. For all tests the significant level was set at the level of $p < 0.05$.

III.2.3 Results

III.2.3.1 Stride parameters

The analysis of the accelerometer impact data of 8835 strides of the hindlimb indicating the stride duration in seconds (s) for each condition demonstrated consistent stride durations between horses. Mean ±std values of the stride duration for slow walk 1.08 s ±0.05, fast walk 0.97 s ±0.03, slow trot 0.79 s ±0.04, fast trot 0.68 s ±0.02, walk on 5% incline 1.12 s ±0.03 and walk on 10% incline 1.11 s ±0.03 (Table 24, Fig. 33) showed that the mean stride duration decreased between walk and trot. Within the same gait mean stride duration also decreased with increased speed but on incline stride duration remained unchanged between 5% and 10% of incline.

Table 24 Showing mean values, standard deviation, standard error, minimum and maximum values of stride duration (s) for all horses at all conditions

	Mean	Std. Deviation	StdE	Minimum	Maximum
slow walk	**1.08**	.05	.014	1.01	1.20
fast walk	**0.97**	.03	.009	0.93	1.03
slow trot	**0.79**	.04	.014	0.71	0.89
fast trot	**0.68**	.02	.008	0.63	0.72
walk 5% incline	**1.12**	.03	.010	1.08	1.19
walk 10% incline	**1.11**	.03	.010	1.07	1.20

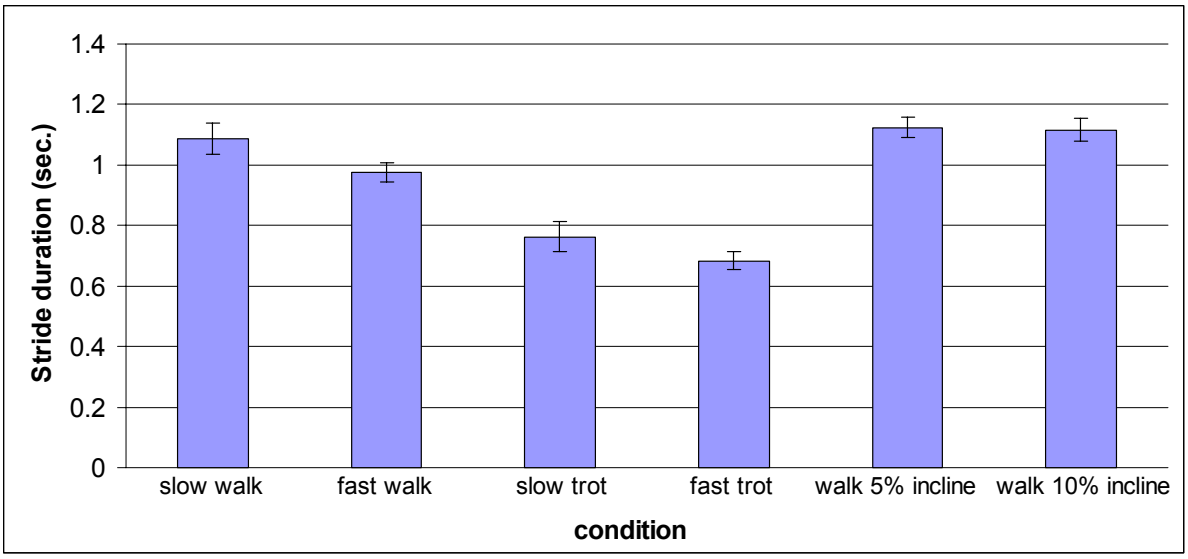

Fig. 33 Mean values (± s.d.) of stride duration (s) for each condition in all horses

Table 25 Shows mean values and standard deviation of the percentage of stance duration (%) per stride cycle in all conditions for the right (RF) and left (LF) forelimb as well as the right (RH) and left (LH) hindlimb of all horses. There is no significant difference of stance duration between front and hind limbs ($p>0.05$) but between slow, fast and walk on incline (5%, 10%) and slow and fast trot ($p<0.05$).

Condition	LH		RH		LF		RF	
	Mean (%)	Stdev	Mean (%)	Stdev	Mean (%)	Stdev	Mean (%)	Stdev
Slow walk	**65**	3.8	**64**	2.6	**61**	6.9	**62**	1.7
Fast walk	**63**	2.1	**60**	0.5	**64**	10.5	**60**	0.5
Slow trot	**50**	6.1	**51**	3.3	**50**	1.2	**51**	2.7
Fast trot	**45**	4.6	**49**	3.5	**46**	1.6	**47**	3.9
Walk incline 5%	**67**	1.1	**65**	0.5	**65**	3.3	**62**	0.8
Walk incline 10%	**67**	3.4	**64**	2.8	**69**	13.7	**61**	1.8

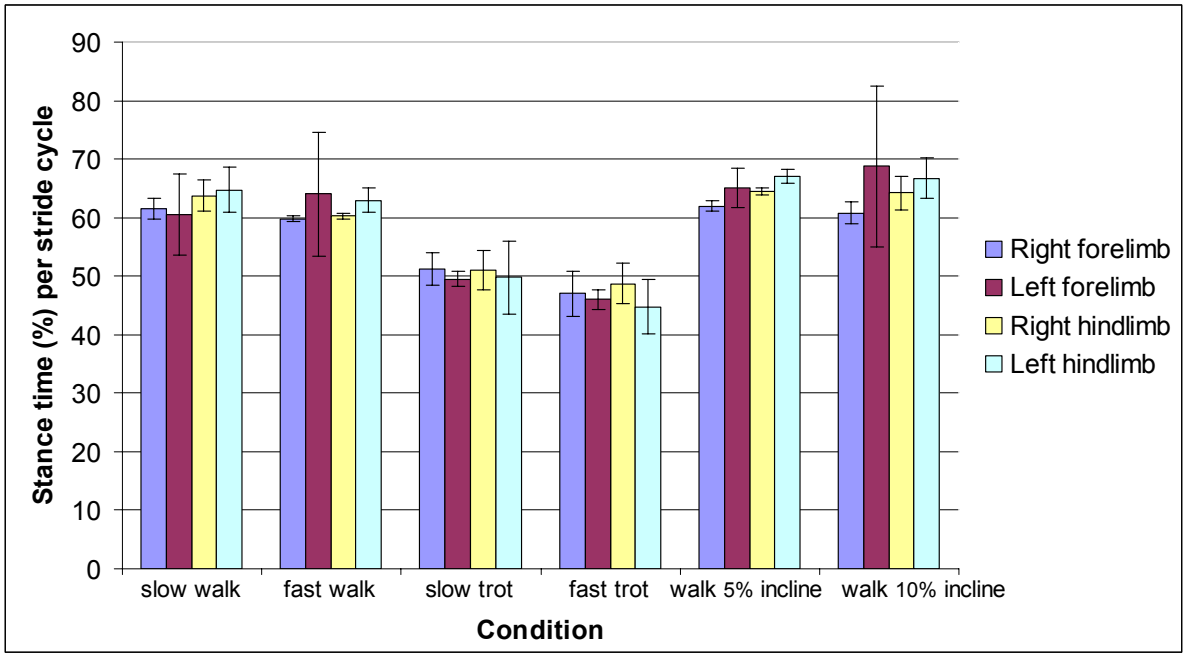

Fig. 34 Mean (± stdev) percentage of stance (%) time per stride cycle in all conditions for the right (blue) and left (red) forelimb and the right (yellow) and left (light blue) hindlimb of all horses.

Table 25 and Fig. 34 showing the mean ±stdev duration of the stance phase of each limb stated as a ratio of a 100% stride cycle. In this study there was no significant difference observed between the percentage of stance duration of front and hind limbs during stride cycles (p=0.8). However between certain conditions a significant difference of the percentages of stance duration could be detected. The duration of the mean ± stdev stance phase for the different conditions was 62.2±1.9 % for slow walk, 61.7±2.0 % for fast walk, 50.3±0.8 % for slow trot, 46.6±1.6 % for fast walk and 64.6±2.0 % and 65.1±3.4 % for 5% and 10% incline in walk. The percentage of stance duration was significantly shorter (p=0.0001) for slow and fast trot than for slow walk, fast walk and walk on incline (5% and 10%).

III.2.3.2 EMG activity pattern

The analysis of the collected EMG data showed that only the EMG electrodes on the right side of the horse recorded reliably muscle activity and therefore only these electrodes were used for further statistical analysis. Due to technical problems such as incomplete signal recordance and noise the EMG measurements of the left LD was not included in the analysis.

The interaction between limb movement and muscle activity of one stride cycle was analysed by relating stride parameters to EMG measurements. During standing only ECG but no muscle activity was recorded along LD in all horses. At walk, trot and walk on incline the majority of stride cycles (42.4%) showed a biphasic EMG activity pattern of LD, interestingly 34.4 % of the measured strides had only one EMG activity burst while 20.9 % had 3 bursts of EMG activity and 4.3 % showed 4 EMG bursts (Fig. 36). Fig. 35 displays an example of the different number of EMG activity bursts between different sensors during one stride cycle of walk on 5% incline in horse 5.

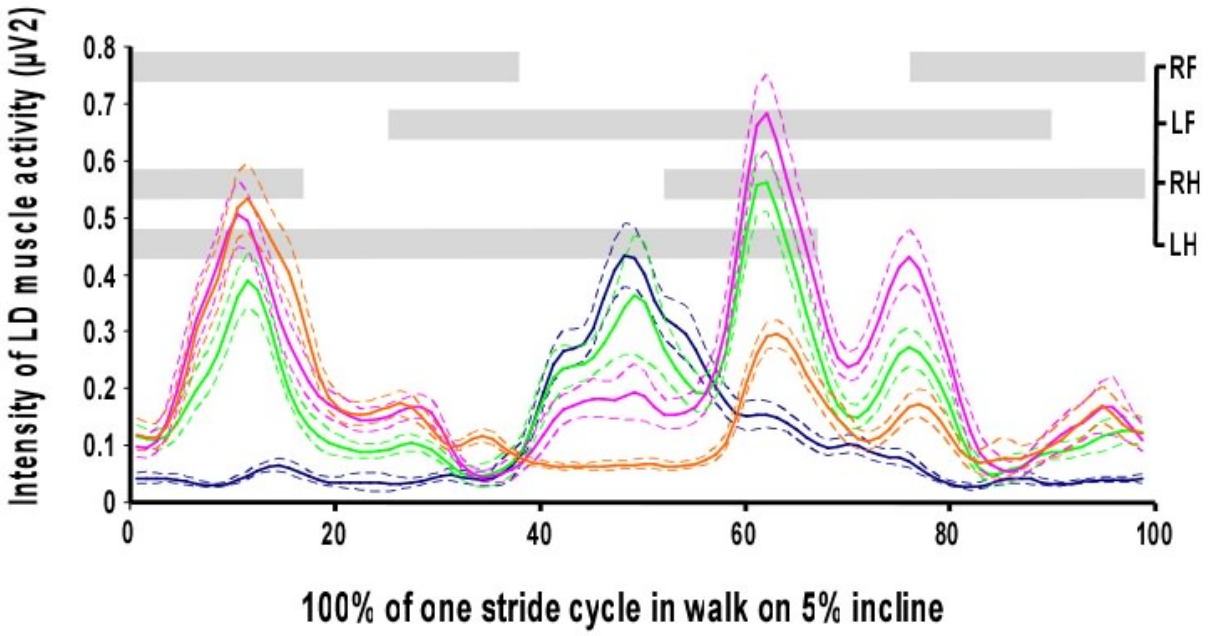

Fig. 35 EMG activity pattern of the right LD during one stride cycle of walk on 5% incline of horse 5. This is an example for three EMG bursts in one stride cycle. Horizontal gray lines display the footfall pattern of all four limbs. Coloured lines display the mean values (continuous line) and standard error (dotted lines) of sensor T14 (blue), T16 (green), T18 (pink) and L2 (orange)

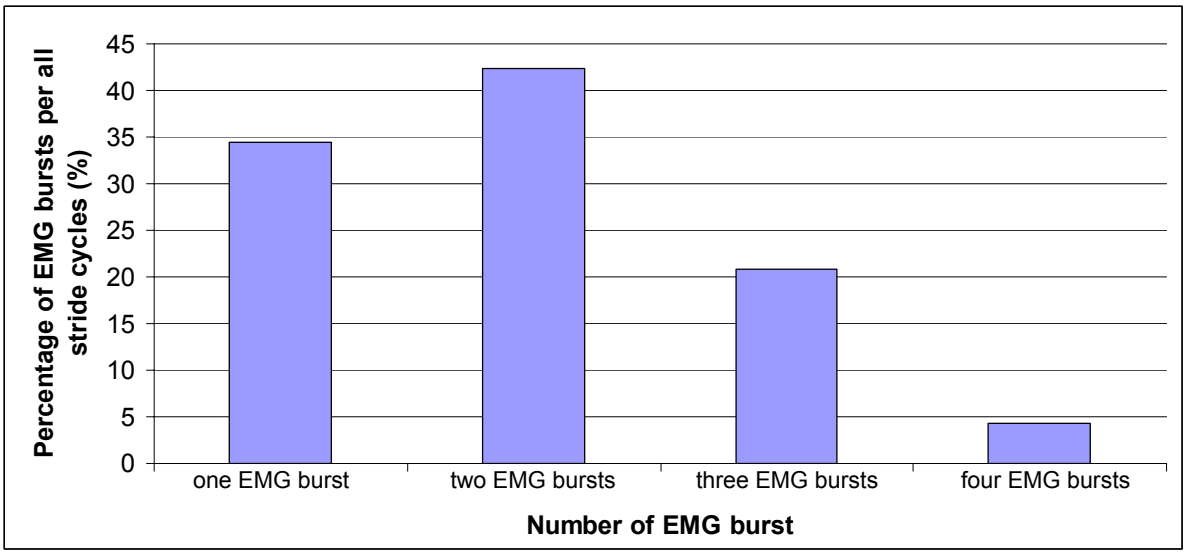

Fig. 36 The proportion of the numbers of EMG bursts per stride cycle in percent (%) for all conditions, sensors and horses

Considering the number of EMG bursts per segment, analysis demonstrated the evidence of significant differences between sensors of T14, T16, T18 and L2 (p=0.0001). A trend of single EMG bursts per stride cycle was observed for the cranial segments of T14 and T16 whereas the increase of biphasic or multiple bursts was more obvious in the caudal segments of T18 and L2. Significant differences were shown between sensor T14 and sensor L2 (p=0.0001) as well as between sensor T16 and sensor L2 (p=0.01) (Table 26)

Table 26 Percentage of the number of EMG bursts per sensor for all stride cycles of all horses during all conditions. A higher number of double EMG bursts per stride cycle were recorded for location T18 and L2 whereas locations of T14 and T16 showed a higher number of single EMG burst grey).

Number of EMG bursts	Sensor			
	T14	**T16**	**T18**	**L2**
1 Burst	**42.4%**	**44.4%**	27.8%	14.7%
2 Bursts	30.3%	38.9%	**50.0%**	**50.0%**
3 Bursts	27.3%	11.1%	16.7%	29.4%
4 Bursts	0%	5.6%	5.6%	5.9%

A significant difference was observed between conditions. Walk on 10% incline showed a significant larger number of EMG bursts (p=0.01). In addition, an obvious but not statistically significant trend of single EMG bursts in slow and fast walk and walk on 5% incline were shown in contrast to a higher percentage of biphasic EMG activity pattern in slow and fast trot (Table 27)

Table 27 Percentage of the number of EMG bursts per stride cycle in all conditions for all horses and sensors. A higher number of single EMG bursts per stride cycle was detected in slow, fast walk and walk on 5% incline, two EMG bursts were recorded in slow and fast trot and three EMG bursts mainly for walk on 10% incline (grey).

Number of EMG bursts	Slow walk	Fast walk	Slow trot	Fast trot	Walk 5% incline	Walk 10% incline
1 Burst	**45.5%**	**45.8%**	8.7%	34.8%	**37.5%**	21.7%
2 Bursts	31.8%	37.5%	**87.0%**	**56.5%**	20.8%	21.7%
3 Bursts	22.7%	16.7%	0	8.7%	33.3%	**43.5%**
4 Bursts	0	0	4.3%	.0%	8.3%	13.0%

Table 28 Mean (± stdev) values of on- and offset times of the different numbers of EMG bursts during 100% percentage of a stride cycle. The majority of EMG bursts of the right LD occurs in the first and the last quarter of the stride cycle.

On- and Offset time of EMG bursts in percentage to stride duration	Mean (%)	Stdev
Onset of burst 1	23.5	13.9
Offset of burst1	35.8	15.2
Onset of burst 2	41.1	17.1
Offset of burst2	50.2	19.2
Onset of burst3	60.0	10.5
Offset of burst3	71.0	12.7
Onset of burst 4	77.7	13.4
Offset of burst 4	95.0	15.8

The number of EMG bursts per stride cycle had an effect on the onset time of EMG bursts (p=0.01) with the consequence that a higher number of EMG bursts results in an earlier onset time. As walk and trot are symmetrical gaits the 100% stride cycles were divided in 50% each in order to relate muscle activity of the right LD to the stride parameters. All stride cycles started with foot-on of the left hind limb. Table 28 shows the distribution of EMG bursts during stride cycles. A higher number of EMG bursts were recorded between 60-95% of the stride cycle (during the second half of the stride cycle) which is related to the muscle activity of the ipsilateral LD. Fewer EMG bursts were recorded during the first half of the stride cycle (between 23-36% of stride cycle). The higher percentage of EMG bursts during the second half of the stride cycle might be due to the fact that the onset time of muscle activity with only one activity burst per stride cycle was significant later in the stride cycle. The onset time of the first burst decreased with increasing number of activity bursts.
The mean onset and offset times of EMG bursts are displayed in Table 28. The location of muscle segments (p=0.6) or different conditions (p=0.3) had no significant effect on onset.

The mean value ±stdev of the total EMG activity duration was calculated to be 29.6±18.41 % per stride cycle. The wide range of duration is related to the varying number of EMG bursts. Correlation of EMG activity duration with the number of EMG bursts showed a significant positive effect (p=0.02).

III.2.3.3 Intensity of muscle activity

The mean ±stdev intensity of muscle activity was 0.0025 μV^2 ±0.0049 for slow walk, 0038 μV^2 ±0154 for fast walk, 0211 μV^2 ±0.0507 for slow trot, 0.023 μV^2 ±0.0516 for fast trot, 0.0034 μV^2 ±0.0056 for walk on 5% incline and 0.0064 μV^2 ±0.0077 for walk on 10% incline (Table 29) Results showed a significant effect on the intensity of muscle activity between different conditions in walk (p=0.0001). Post-hoc comparison indicated that all walking conditions (slow walk, fast walk, walk on 5% and 10% incline) were significantly different (p=0.0001) except fast walk compared with walk on 5% incline (p=0.9). Analysis of the intensity of muscle activity between walk and trot showed a significant difference between gaits and between different speeds (p=0.0001). Post-hoc comparison indicated that slow walk, fast walk, slow trot and fast trot resulted in significant differences of intensity of muscle activity (p= 0.0001).

Table 29 Mean (± stdev) value, minimum and maximum value of the EMG intensity (μV^2) for each condition in all sensors and all horses

	N	Mean (μV^2)	Stdev.	Minimum	Maximum
Slow Walk	5572	.0025	.0049	.0001	.17
Fast Walk	5315	.0038	.0154	.0001	.95
Slow Trot	7077	.0211	.0507	.0002	.50
Fast Trot	8101	.0230	.0516	.0007	1.54
Walk 5% incline	4244	.0034	.0056	.0001	.10
Walk 10% incline	4680	.0064	.0077	.0006	.15

The position of EMG electrodes along LD showed no significant influence on the intensity of muscle activity (p= 1.0) during the different walking conditions although a trend of different intensities could be detected between the different locations (Table 30). During level walk the greatest intensity of muscle activity was shown for T14 and the lowest value for T16 while T18 and L2 recorded very similar intensity of muscle activity. During walk on incline greater intensity of muscle activity was observed over T18 and L2. However the lowest intensity during walk on incline was found over T16. In trot intensity of muscle activity was shown to be increased for sensors at T14 and L2.

The following figures illustrate the intensity of muscle activity between different sensors and in different conditions (Fig. 37).

Table 30 Mean (± stdev) values of the intensity of muscle activity (μV^2) for each condition and each sensor in all horses.

	T14		**T16**		**T18**		**L2**	
	Mean μV^2	Stdev	Mean μV^2	Stdev	Mean μV^2	Stdev	Mean μV^2	Stdev
Slow walk	0.0042	0.0081	0.0014	0.0012	0.0023	0.0023	0.0022	0.0049
Fast walk	0.0082	0.028	0.0019	0.0033	0.0022	0.0017	0.0028	0.0095
Slow trot	0.037	0.083	0.014	0.027	0.0083	0.0089	0.025	0.046
Fast trot	0.035	0.084	0.012	0.0086	0.013	0.01	0.033	0.058
Walk 5% incline	0.0039	0.0052	0.0022	0.0028	0.0034	0.003	0.0044	0.009
Walk 10% incline	0.0059	0.0075	0.0046	0.005	0.009	0.01	0.006	0.006

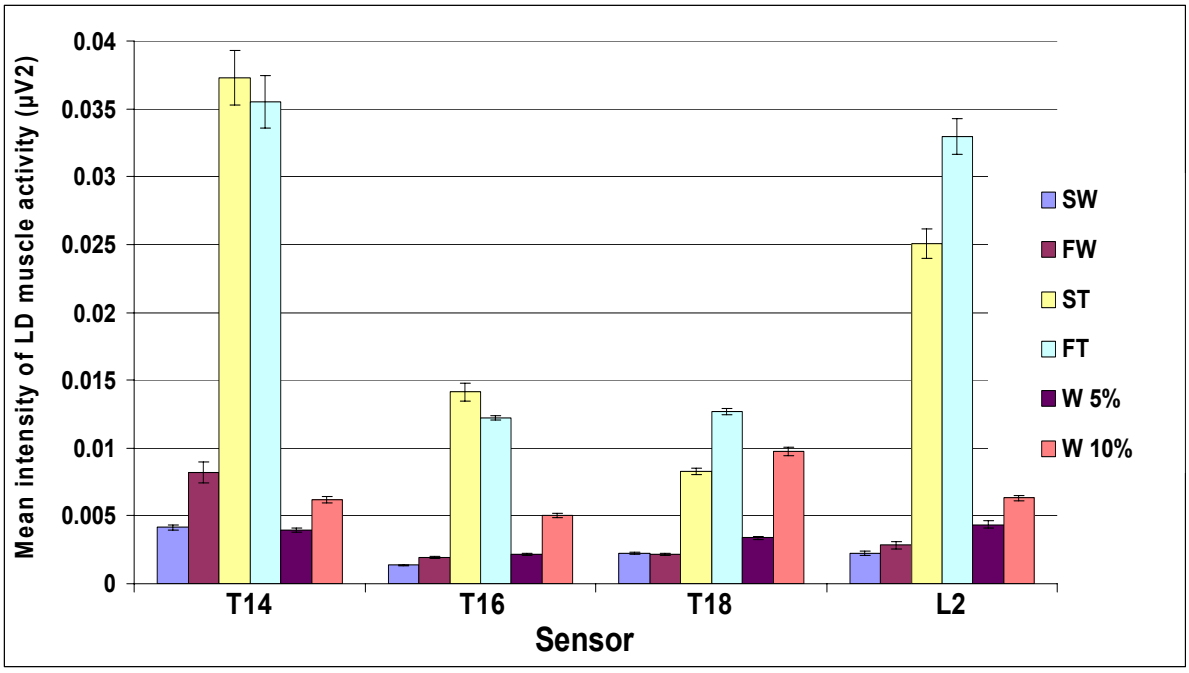

Fig. 37 Mean (± SE) values of muscle intensity (μV^2) of the LD muscle during all conditions (SW= slow walk, FW= fast walk, ST= slow trot, FT= fast trot, W5%= walk on 5% incline, W10%= walk on 10% incline) for all horses. There is an obviously increased muscle intensity of LD activity at T14 and L2.

III.2.4 Discussion and conclusion

The purpose of the presented study was to show the activity pattern along the thoracolumbar LD muscle in different gaits, at different speeds and on different inclines in normal horses. The LD is a segmental muscle and for the first time the interaction of all accessible segments during gait cycles was quantified simultaneously.

III.2.4.1 Muscle activity of thoracolumbar LD during different conditions

In this study EMG activity bursts showed different activity patterns during stride cycles between horses, muscle segments and between gaits, speed and on incline. Although two EMG bursts predominantly occurred in different conditions a significantly higher number of EMG bursts was recorded during walk on 10% incline. In contrast, a trend of single activity bursts per stride cycle was observed in slow, fast walk and walk on 5% incline. These results suggest that different conditions such as faster gaits and movement on increased incline demand more LD activity as well as slow gaits may require less muscle activity. Although

prior studies have documented solely biphasic EMG activity patterns for LD per stride cycle (Licka *et al.* 2004; Robert *et al.* 2001b; Robert *et al.* 2002; Tokuriki *et al.* 1997) a study of another species, the cat, has previously described additional EMG bursts which occurred during walk on incline additionally to EMG burst I and/ or EMG burst II (Wada *et al.* 2006a).
In order to evaluate the interaction between muscle activity and locomotion patterns the EMG activity pattern was related to kinematic measurements. While in this study only kinematic measurements of the feet were recorded thorough kinematic analysis of the back movement by other authors were used to estimate the range of back motion during a stride cycle (Audigie *et al.* 1999; Faber *et al.* 2001a; Faber *et al.* 2001b; Faber *et al.* 2000; Haussler *et al.* 2001; Licka *et al.* 2001a; Licka *et al.* 2001b).
The mean onset time of EMG bursts in the current study corresponded to the second half of the hind limb stance phase which again is related to the phase of back flexion and laterolateral movement (Faber *et al.* 2001a; Faber *et al.* 2000; Haussler *et al.* 2001). In the literature the range of equine back motion was reported to be different between gaits where trot showed a distinct reduction in dorsoventral and laterolateral movement compared to walk. In the present study EMG measurements recorded during different gaits showed a significant increase of the intensity of muscle activity between walk and trot which is conform to other EMG studies (Robert *et al.* 2001b; Robert *et al.* 2002; Tokuriki *et al.* 1997). Due to different muscle activity and different activity pattern of LD the function of this epaxial muscle may differ between gaits due to different dynamic forces acting on the trunk. During walk decelerating forces of the limbs at the beginning of stance phase, vertical force at midstance and accelerating forces during propulsion influence trunk movement at the same time. These forces acting in different directions demand a rather flexible connection between each other. Simultaneous deceleration of a front limb and acceleration of the ipsilateral hind limb may produce larger lateral movement of the vertebral column. As the LD is active during the second half of hind limb stance phase, when the vertebral column moves to the contralateral side, LD might not only restrict back flexion but may also move the back actively towards this direction. In trot kinematic data of horse backs showed a rather rigid structure with a decreased range of motion (Faber *et al.* 2001a; Haussler *et al.* 2001). The diagonal paired limb movements produce forces working simultaneously in the same direction. The back as axis between the diagonal pairs of limbs needs to be rather stiff to move the body forward in an effective and economic way. The increased intensity of LD activity and a higher number of EMG bursts during trot may also support the spine to resist against increased acceleration of the rebouncing visceral mass and the forward and sideway acceleration generated by the

higher push-off force of the contralateral and ipsilateral hind limbs. Significantly higher intensity of muscle activity was measured during walk on 10% incline compared to level walk and walk on 5% incline. On the incline increased forces generated by the hind limbs and transmitted onto the vertebral column may be canalised by a stiffer back in forward, upward direction of the movement.

As hypothesized, differences of EMG activity were not only obvious between gaits also different parts of LD showed significant differences between activity levels along the muscle.

III.2.4.2 Muscle activity of LD between different muscle segments

For the first time the examination of the whole accessible LD was performed during different gaits, speeds and on incline in the horse. Although data was only collected for the right LD and therefore the interpretation of muscle interaction between right and left LD was not possible, analysis of the different segments reflect differences between certain areas.

During trot and walk on incline great intensity of muscle activity was found for the muscle segments of T14 and L2 but during trot the greatest value was observed for T14 and during walk on incline at L2. The high intensity of muscle activity might be due to the relatively close position of these muscle segments to the fore and hind limbs. During faster and more demanding gaits such as trot or walk on incline the impact of the accelerating forces transmitted by the limbs onto the vertebral column during the second half of the stance phase is increased. Higher forces might require higher intensity of epaxial muscle activity in order to support the trunk. In level walk intensity of muscle activity is decreased at L2 and T18 compared to the great value at T14. In all conditions the lowest intensity of muscle activity was recorded at the muscle segment of T16. These results correspond only to some extent with findings of previous studies. In a previous study maximum EMG amplitudes were shown at T12 but decreasing EMG values were recorded for T16 and L2 during trot (Licka *et al.* 2004). Other evaluations of the segmental muscle activity of equine LD are difficult to compare due to different experimental set ups and analysing modalities. Several studies used only one electrode per side (Robert *et al.* 2001b; Robert *et al.* 2002; Tokuriki *et al.* 1997) or electrodes were often placed close to or on top of major muscles (spinalis and middle gluteal muscle) overlying LD (Licka *et al.* 2004; Robert *et al.* 2001b; Robert *et al.* 2002). In the present study placement of surface EMG electrodes was based on previous anatomical dissections (see chapter III.1). Direct access to the LD without overlying other muscles is only possible between T14 and L3. The LD muscle cranial to T14 is covered by the spinalis muscle, the part caudal to L2 partly by the tongue of the middle gluteal muscle. Hence

accurate placement of electrodes is essential to minimize electromyographic cross-talk of overlying and adjacent muscles. However some crosstalk of adjacent muscles could not be entirely excluded. Some crosstalk of the spinalis and middle gluteal muscle might have been recorded and have influenced the EMG trace of LD to a certain degree as EMG electrodes were still placed relatively close to these muscles.

In the present study not only differences of the intensity of muscle activity between LD segments were observed also the number of EMG bursts per stride cycles showed differences among segments. Higher percentages of single EMG bursts were recorded at T14 and T16 whereas the caudal segments of T18 and L2 showed predominantly two and more EMG bursts. The higher percentage of two and more EMG bursts at the caudal part of LD indicated continuous muscle activity during the locomotion of both hind limbs and consequently resulted in an earlier onset time of muscle activity during the stride cycle. Increased LD activity may resist against the impact of accelerating forces of the limbs and support the transmission of propulsive forces onto the trunk. The caudal part of the vertebral column is also more exposed to dynamic forces of the visceral organs due to the lack of the supportive rib cage hence higher muscle activity may also stabilise the trunk.

In this study onset time of EMG bursts were not significantly different between LD segments. This result agrees with a former study of the feline LD (English 1980) which showed synchronous onset of muscle activity along the muscle. But results are contrary to a recent study of the feline LD which found variations between onset of activity times at different levels of LD during level walk and walk on incline (Wada *et al.* 2006a; Wada *et al.* 2006b).

III.2.4.3 Conclusion

This study gives an insight of the muscle activity pattern along the equine LD. Results of this study demonstrate, similar to results of previous studies, that limb movement strongly influences vertebral column movement and therefore is associated with epaxial musculature activity. LD activity increases due to increased speed, faster gait and increased incline influenced by the different accelerating forces of the hind limbs during the second half of stance. An increased muscle activity at the muscle segments close to fore and hind limbs also demonstrate an effect of the transmitted forces through the limbs on to the trunk and interacting epaxial muscle activity. Further research is needed to investigate differences of muscle activity along LD in horses with back pain and lameness.

III.3 Ultrasonographic anatomy of the equine thoracolumbar Longissimus dorsi muscle

III.3.1 Introduction

Disorders of the equine back are thought to cause a variety of unspecific clinical signs, such as poor performance, reluctance to be ridden and secondary hindlimb lameness in some horses. Abnormalities of the vertebral column, spinal ligaments and the sacroiliac joints have been associated with back pain of the horse (Jeffcott and Haussler 2004; Ross and Dyson 2002). It has been suggested that the adjacent epaxial musculature especially of the largest epaxial muscle, the thoracolumbar Longissimus dorsi muscle (LD), plays a role in the pathogenesis of back problems, however little is known at present. Knowledge of the normal muscle structure is essential to evaluate the relationship between paraspinal muscle alterations and back pain in the horse. The visualisation of muscle architecture, muscle size, and relation to adjacent muscle is important to be able to diagnose muscle abnormalities and understand pathological changes. Unlike in humans computed tomography (CT) and magnetic resonance imaging (MRI) are not practical techniques to image the large equine back due to size restrictions, however, ultrasonography is a feasible tool to illustrate the anatomical structure of the epaxial musculature. Due to the non-invasive, portable and low cost properties of this technique it is already widely used in equine practice for a variety of applications. Ultrasonographic examination of the musculoskeletal system has mainly focused on imaging of tendon and ligament abnormalities (Reef 1998). Injuries of muscles are more difficult to detect ultrasonographically apart from cases of severe muscle pathology, such as muscle ruptures or strain, which are easily visualised ultrasonographically as anechoic areas in case of fluid accumulations or hyperechoic areas with thickening of the connective tissue septa within the muscle (Jeffcott and Haussler 2004).

Different tissues are characterised by different echogenicity. The echogenicity describes the amount of ultrasound signals of an ultrasound beam reflected by the tissue, for example, ultrasound images of normal muscle tissue show less echogenic reflections than fat or tendinous structures. The transverse image of normal muscle tissue shows fine echoes scattered throughout the muscle. In the longitudinal view the muscle is characterised by homogeneous, multiple, fine, parallel echoes. This sonographic appearance is due to multiple muscle bundles (fascicles) surrounded by fibroadipose septa (perimysium). Connective tissue fascia and fat overlying the muscle appear as a bright echogenic outer margin (Rantanen and McKinnon 1997).

In humans ultrasound is not only used to distinguish between different types of muscle diseases (Maurits *et al.* 2003; Pillen *et al.* 2003; Zuberi *et al.* 1999) but also to evaluate normal musculature (Binzoni *et al.* 2001; Kawakami *et al.* 2006; Maganaris *et al.* 1998; Rankin *et al.* 2006; Stokes *et al.* 2005).

Ultrasound images of myopathic muscles show an increase in echogenicity whereas neuropathic muscles present areas of increased inhomogeneity due to pathologic disruption of the muscle architecture (Maurits *et al.* 2003; Zuberi *et al.* 1999). To evaluate differences between patients suffering from chronic lower back pain and healthy subjects muscle size was measured ultrasonographically. The localised atrophy of the multifidus muscle in patients with chronic neck or low back pain was observed as significantly decreased cross-section of the muscle compared to healthy, asymptomatic subjects (Hides *et al.* 2008; Kristjansson 2004).

Ultrasonography has also been applied to evaluate the quantitative characterisation of normal skeletal musculature in humans (Kristjansson 2004; Lee *et al.* 2007; Nielsen *et al.* 2000) and has been used to demonstrate that architectural measurements of muscles such as muscle size and muscle thickness, muscle fibre length and pennation angle are related to muscle function (Abe *et al.* 2000a; Kawakami *et al.* 1993; Kawakami *et al.* 1995; Kumagai *et al.* 2000). The architectural measurements of muscles were utilised to demonstrate differences between trained and untrained subjects (Aagard *et al*., 2001; Sipila and Suominen 1991), between gender (Chow *et al.* 2000) and age as well as to show effects of different types of physical training (Abe *et al.* 2000a; Kawakami *et al.* 1995; Kearns *et al.* 2000; Kumagai *et al.* 2000).

Several studies have shown that exercise influences muscle thickness, muscle size, pennation angle and fibre length. Significant increase of pennation angle and muscle fascicle length was reported for different muscles following a four to sixteen weeks of resistance training (Aagard *et al*., 2001; Kawakami *et al.* 1995; Seynnes *et al.* 2007). The effect of training was observed as an increase in muscle thickness and cross-sectional area (Brancaccio *et al.* 2007; Kiesel *et al.* 2007). Following resistance training different muscles such as triceps brachii, gastrocnemius and quadriceps femoris muscles showed an increased pennation angle and increased cross-section area of the muscle (Kawakami *et al.* 2006; Kawakami *et al.* 1995; Seynnes *et al.* 2007; Suetta *et al.* 2008). Differences of muscle architecture were also found in muscles of different types of athletes (Abe *et al.* 2000b; Kanehisa *et al.* 2003; Kumagai *et al.* 2000). In sprinters, for example, longer muscle fascicles and smaller pennation angles were observed compared to long distance runners. Other studies demonstrated significant differences in fibre length, pennation angle, muscle thickness and muscle size of limb muscles

(Chow *et al.* 2000) as well as the multifidus muscle (Hides *et al.* 2008) between gender although another study showed that gender had no effect on neck muscle size after it was corrected for body mass (Rankin *et al.* 2005).
Furthermore, several studies demonstrated that muscle architecture of certain human limb muscles are significantly altered with age (Binzoni *et al.* 2001; Kubo *et al.* 2003a; Narici *et al.* 2003). Decreased muscle size and muscle thickness are thought to be due to a decrease in size of muscle fibres and the disappearance of muscle fibres altogether (Maurits *et al.* 2003). Other age-related muscle alterations were visible as an increase of echogenicity which corresponds to the age-related replacement of contractile muscle tissue by other tissue such as fat and collagen (Maurits *et al.* 2003; Sipila and Suominen 1991).

Based on the knowledge of the role of echogenicity and architectural measurements from human research the ability of ultrasonography to image soft tissue structures may provide valuable information of the equine back musculature. Measurements of muscle thickness, pennation angle, fibre length and echogenicity characterise the capacity of LD to generate force, document muscle atrophy or hypertrophy and assess the ratio between muscle and connective tissue along this muscle (Bleakney and Maffulli 2002; Kawakami *et al.* 2000; Kearns *et al.* 2001; Strobel *et al.* 2005). As the paraspinal stiffness is important for the spinal stability ultrasonographic examination of the LD muscle structure is helpful to characterise this muscle and therefore prevent damage to musculoskeletal structures caused by the lack of muscle strength. In conjunction with radiographic images of the vertebral column muscle ultrasound of LD can document the relationship between pathological changes of the vertebral column and muscle alterations.
Back problems in horses are often accompanied by the wastage of the epaxial musculature (Jeffcott and Haussler 2004). Decrease of muscle thickness and alterations of architectural parameters indicate the disuse of the muscle following for example trauma, lameness or due to underlying pain, bad fitted saddle, and form of training. Studies in disused muscles of humans showed the replacement of muscle tissue by fat and connective tissue which influenced the echogenicity (Strobel *et al.* 2005). Although the degree of fat and connective tissue replacement, changes of muscle thickness, muscle fibre length and pennation angle in the horse is unknown these parameters are useful to assess the degree of muscle involvement and to monitor the results of treatment and training.

The aim of the present study was to illustrate the ultrasonographic anatomy of the equine LD. The objectives of the studies were to compare longitudinal and transverse cross-sectional ultrasound images with matching gross anatomical sections of the equine LD.

III.3.2 Material and Methods

In the present study a 6 year old Thoroughbred mare was used, which was euthanised for reasons unrelated to this study. The dorsal spinous processes of the tenth thoracic vertebra (T10) and the last lumbar vertebra (L6) were identified in the live horse. Between these two landmarks a rectangular area extending 25 cm lateral from the midline was clipped and scrubbed with chlorhexidine (hibiscrub®, ICI, UK). Ultrasound sites were marked at a distance of 5 cm, 10 cm, 15 cm and 20 cm from the midline lateral to T10, T12, T14, T16, T18 and L2 in 5 cm, 10 cm and 15 cm distance caudal to T18 using Tipp-Ex (BIC, Germany) (Fig. 38). Ultrasound images were taken between T10 and L3 as it is impossible to scan parts of LD due to the overlying muscle masses such as the muscles of the shoulder gridle and the middle gluteal muscle. This grid was later used as indicator for the ultrasound sites and as an orientation for sectioning of the frozen back with a band saw. The horse was standing square on all four feet during the ultrasound examination. Ultrasound images were performed using a real-time B mode ultrasound scanner (VingMed system 5, GE, Milwaukee, Wisconsin, USA) with a 7.5 MHz linear transducer. All images were recorded on a digital video recorder (DCR-PC 110E, Sony Cooperation). Longitudinal and transverse ultrasonographic images were acquired at each location. Afterwards the horse was euthanized. After euthanasia the cadaver was positioned in right lateral recumbency. Longitudinal and transverse ultrasound images were collected at the same locations as in the live horse. After the ultrasound examination was completed the neck, shoulder and pelvic girdle as well as the ventral part of the trunk were removed. The isolated equine back was frozen at -20°C for 48 hours. Sagittal and transverse sections were made with a band saw at the level of the previously marked sites. The right side of the equine back was cut in five sagittal slices. The left side was sectioned into ten transverse slices (Fig. 39). The thickness of the sagittal slices were 4.3 - 4.7 cm wide while the thickness of the transverse slices varied between 5.5 cm and 8 cm. Photographs of each slice were taken with a digital camera (Nikon D 70, Nikon Corporation, Japan).

Ultrasound images of the live horse and the cadaver were compared to evaluate visibility of anatomical structures and image quality between the two conditions. Longitudinal and transverse ultrasound images of the equine LD were compared to the corresponding sections of the frozen equine back. The relationship between anatomical structures and muscle

architecture was determined and described to provide a better interpretation of the internal structure and fibre orientation.

Fig. 38 Setup for the ultrasonographic examination of the equine cadaver (left). Markings for longitudinal and transverse ultrasound images at different sites along the equine back and in the distances of 5, 10, 15 and 20 cm to the midline (right).

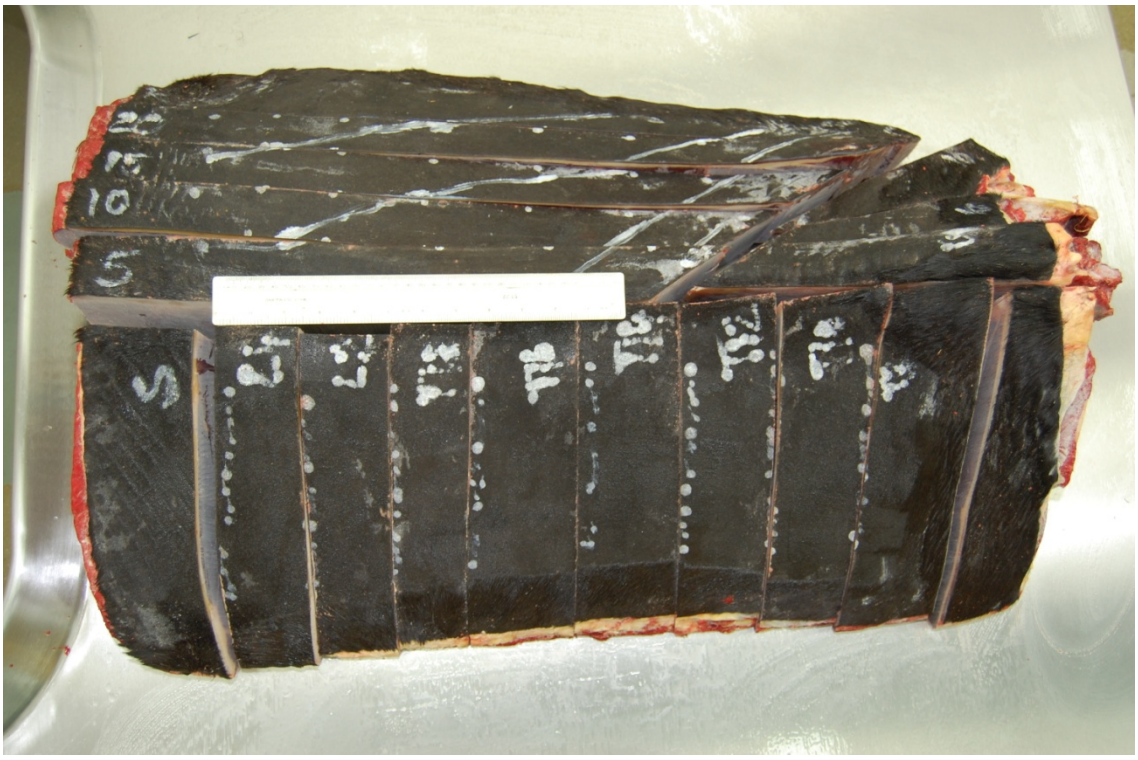

Fig. 39 Transverse and longitudinal sections of the frozen equine back orientated on the markings used for the previous ultrasound examination.

III.3.3 Results

The LD is the largest epaxial muscle and is located bilateral to the dorsal spinous processes, dorsal to the ribs and the transverse spinous processes of the thoracolumbar vertebral column. LD runs parallel to the vertebral column and its major part is accompanied by the multifidus muscle at the medial aspect and the iliocostal muscle at the lateral aspect (Fig. 49-Fig. 53). Large parts of LD are covered by adjacent musculature of the shoulder girdle (cranial) and the middle gluteal muscle (caudal) (Fig. 41-Fig. 50 and Fig. 53-Fig. 55). Only the muscle area between T14 and T18 lies superficially under the superficial thoracolumbar fascia and the skin (Fig. 40).

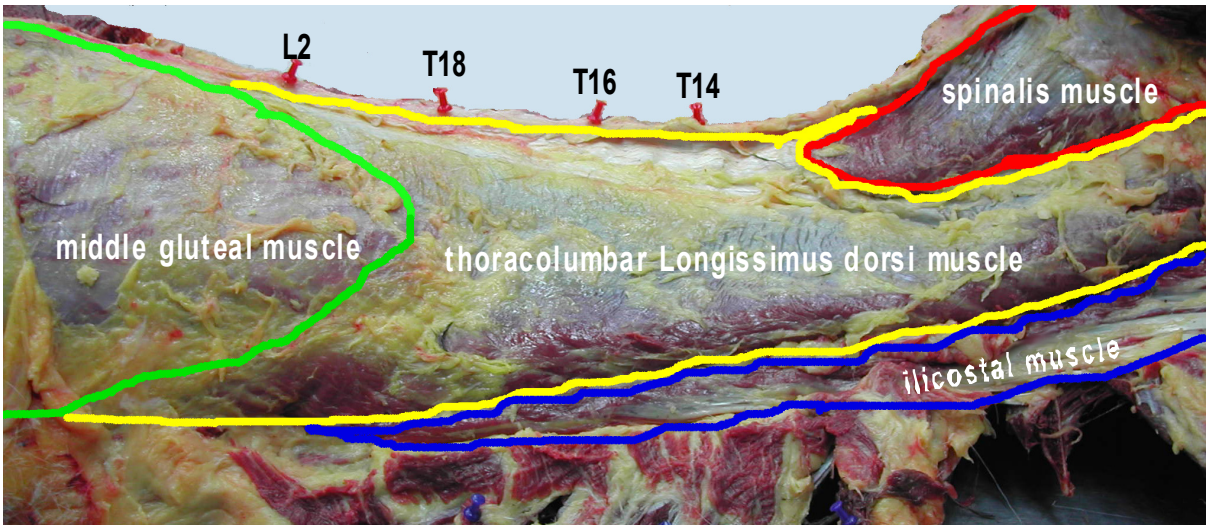

Fig. 40 Showing LD in relation to adjacent muscles. Spinalis muscle (SP) is overlying the cranial part of LD, the tongue of the middle gluteal muscle (GM) covers the caudal part of LD. The ilicostal (IC) muscle margins LD laterally.

The cranial part of the imaged LD (T10-T14) is covered by the latissimus dorsi, serratus ventralis and the thoracic spinalis muscle. The latissimus dorsi muscle ends in the strong superficial thoracolumbar fascia. The serratus ventralis muscle reduces its dimension in ventral direction, only the spinalis muscle is overlying LD and is visible on ultrasound images, caudal to T10. At the level of T10 the dimension of the spinalis muscle extends between the midline and 10cm ventral to the midline. The muscle is demarcated from LD by the distinctive deep layer of the spinocostotransversal fascia which increases in its thickness in caudal direction. The dimension of the spinalis muscle gradually decreases as far as T13 and T14 where the muscle ends (Fig. 41 and Fig. 50). On the longitudinal ultrasound images the spinal muscle is presented dorsal to LD. It is separated from LD by the distinct

hyperechoic spinocostotransversal fascia. Muscle fibre arrangement is clearly visible due to the hyperechoic muscle septa. The muscle fibres of the spinal muscle are orientated in craniodorsal to caudoventral direction, in contrast to the muscle fibre orientation of LD which runs in cranioventral to caudodorsal direction (Fig. 41).

In the caudal part between T18 and the pelvis LD is covered by the gluteal tongue. The triangular gluteal tongue is the cranial muscle part of the middle gluteal muscle which fills in a recession of LD and is demarcated from this muscle by the deep layer of the thoracolumbar fascia. The apex of the gluteal tongue reaches cranial as far as T18 (Fig. 44 and Fig. 53) where it inserts between 10 cm and 15 cm away from the midline onto the superficial thoracolumbar fascia. On ultrasound images the middle gluteal muscle is demarcated by the hyperechoic thoracolumbar fascia. Similar to LD muscle fibre orientation the muscle fibres of the middle gluteal muscle continue in a cranioventral to caudodorsal direction with a slightly smaller pennation angle towards the thoracolumbar fascia (Fig. 44).

Parallel to this overlying muscle a distinct internal fascia arises from the superficial thoracolumbar fascia subdividing LD caudal to T17. This internal fascia could be visualised in the sagittal (Fig. 42 and Fig. 44) and transverse sections of the frozen back as well as on the ultrasound images as a hyperechoic line. This fascia becomes stronger during the course of the caudal LD. It runs from dorsolateral in a ventromedial direction in a distance of approximately 10 cm lateral to the midline (Fig. 53- Fig. 55).

The muscle fibre orientation can be partly observed in the sagittal slices of the frozen cadaver as well as in the longitudinal ultrasound images in form of hyperechoic muscle septa (Fig. 41-Fig. 48). Muscle fibre orientation changes in a dorsal to ventral direction from a large pennation angle inserting onto the aponeurosis (dorsal) to smaller pennation angle (ventral). No distinct change was observed in the cranial to caudal direction. In the dorsal sections, 5 cm and 10 cm away from the midline, muscle fibres appear to have a larger insertion angle into the superficial thoracolumbar fascia. As LD reduces its depth further ventral (15 cm and 20 cm away from the midline) muscle fibres seem to decrease their pennation angle and insert in a more horizontal direction to the rib cage. This is visible on the ultrasound images of Fig. 47 and Fig. 48. Muscle fibre septa run as hyperechoic line almost parallel to the transverse cross-section of the rib which represents the hyperechoic image of bone.

The following pictures (Fig. 41-Fig. 55) display the sagittal and transverse frozen cuts and corresponding ultrasound images of the epaxial musculature.

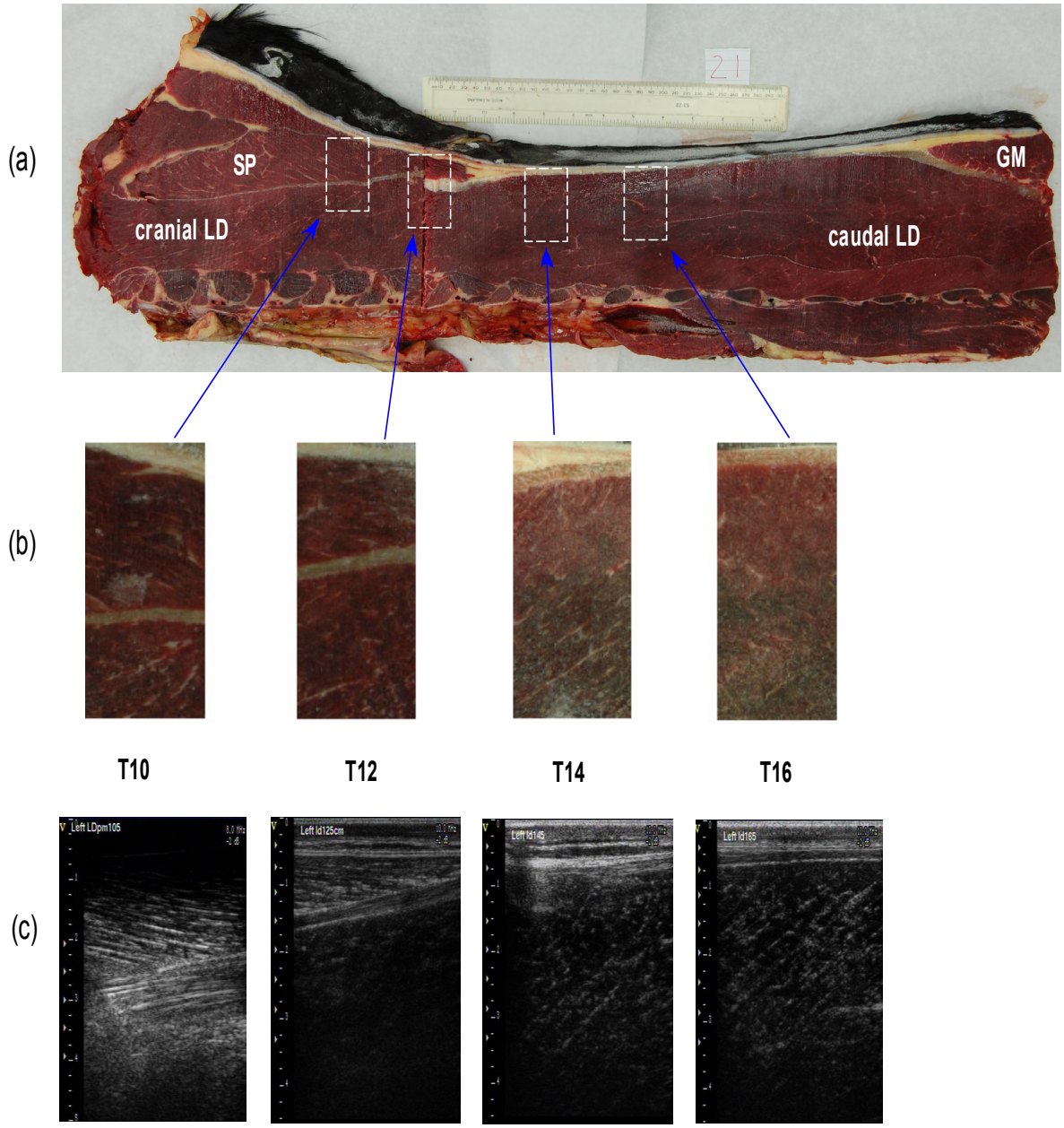

Fig. 41 (a) Sagittal section of the equine back 5 cm lateral to the midline, (b) details of the anatomic reference images corresponding to ultrasound images shown in (c) between T10- T16.

Images of T10 and T12 show the spinalis muscle (SP) overlying LD. Both muscles are demarcated by a strong aponeurosis from each other. The muscle fibres of SP are orientated in craniodorsal to caudoventral direction whereas muscle fibres of LD run in a cranioventral to caudodorsal direction. The strong superficial thoracolumbar fascia and the skin define the dorsal border of the images.

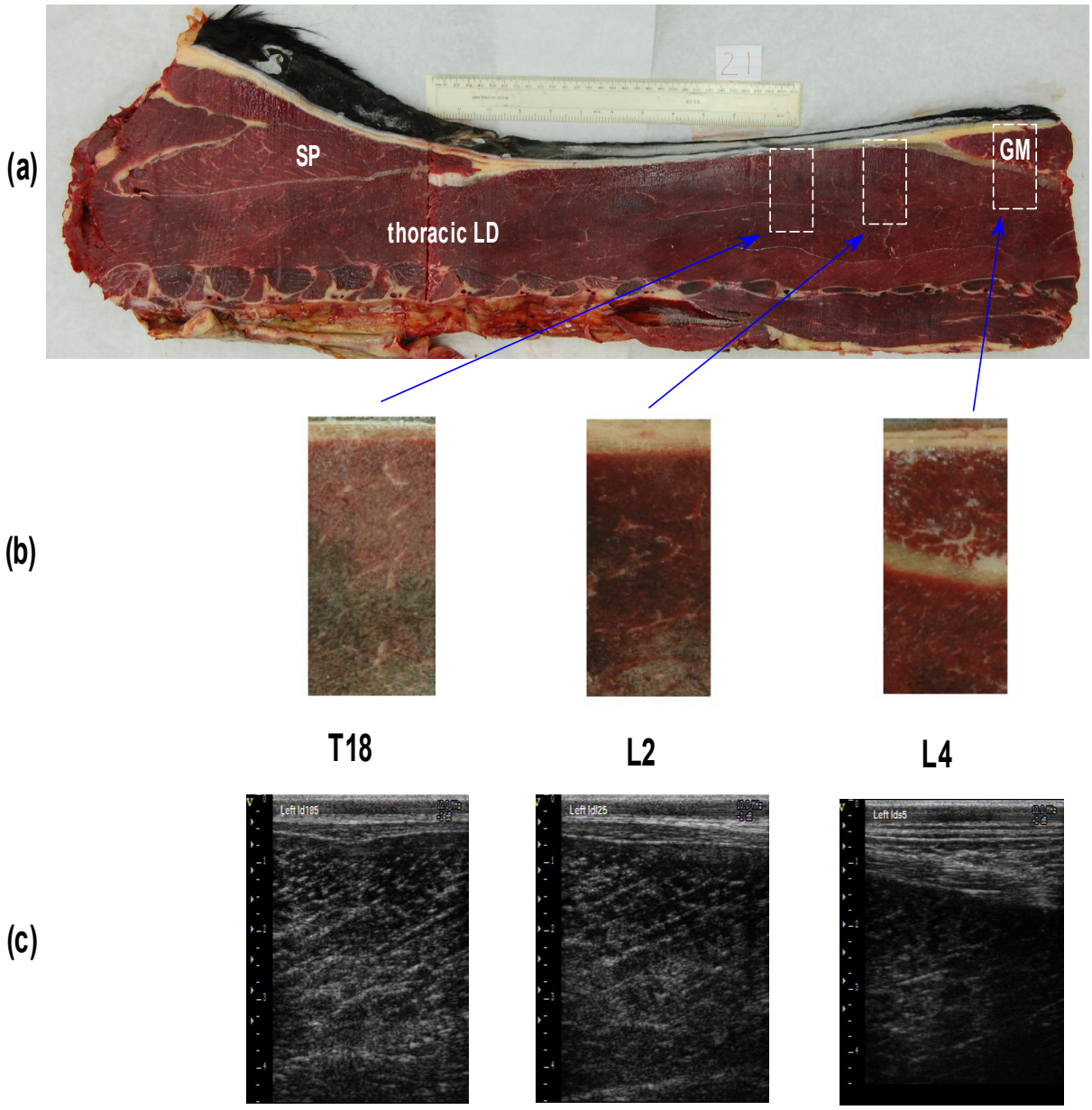

Fig. 42 (a) Sagittal section of the equine back 5 cm lateral to the midline, (b) details of the anatomic reference images between T18- L4 corresponding to ultrasound images shown in (c).
The image of L4 shows dorsal the overlying gluteal tongue which is demarcated by the prominent deep layer of the thoracolumbar fascia from LD. The muscle fibres of LD run in a cranioventral to caudodorsal direction. The strong superficial thoracolumbar fascia, subcutaneous fat and skin define the dorsal boundary of LD.

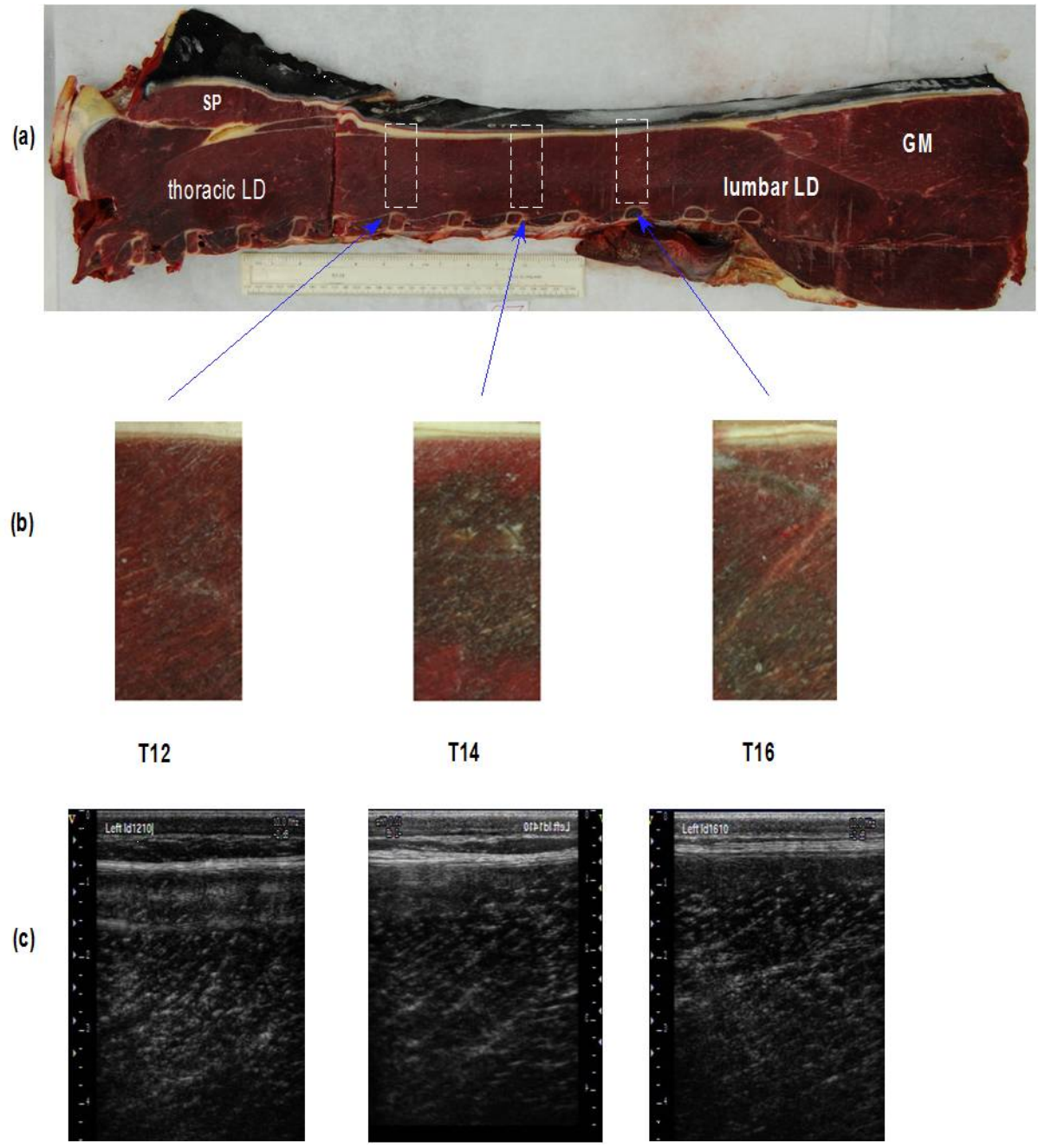

Fig. 43 (a) Sagittal section of the equine back 10 cm lateral to the midline, (b) details of the anatomic reference images corresponding to ultrasound images shown in (c) between T12-T16.

Images of T12, T14 and T16 show LD. Muscle fibres are orientated in a cranioventral to caudodorsal direction. The strong superficial thoracolumbar fascia and the skin define the dorsal border of the images.

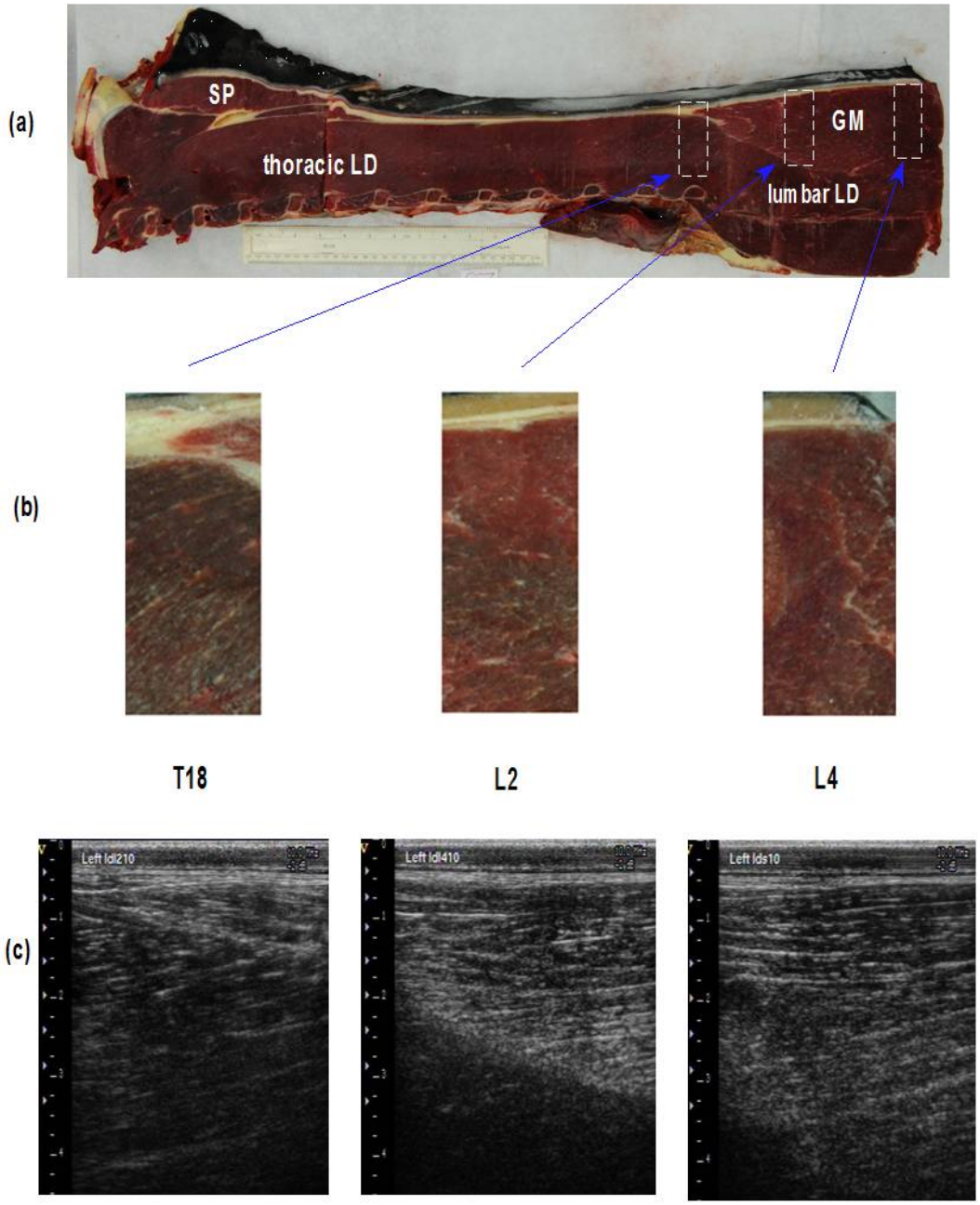

Fig. 44 (a) Sagittal section of the equine back 10 cm lateral to the midline, (b) details of the anatomic reference images corresponding to ultrasound images shown in (c) between T18- L4.

Images of T18 and L2 show the gluteal tongue of the middle gluteal muscle (GM) overlying LD. Both muscles are demarcated from each other by the strong deep thoracolumbar fascia which is visible in the gross anatomic picture and the ultrasound images at the level of T18 and L2. The image at L4 shows only gluteal musculature. The muscle fibres of LD are orientated in a cranioventral to caudodorsal direction. The gluteal muscle fibres are orientated in a similar direction as LD but with a slightly smaller pennation angle. The strong superficial thoracolumbar fascia and the skin define the dorsal border of the images.

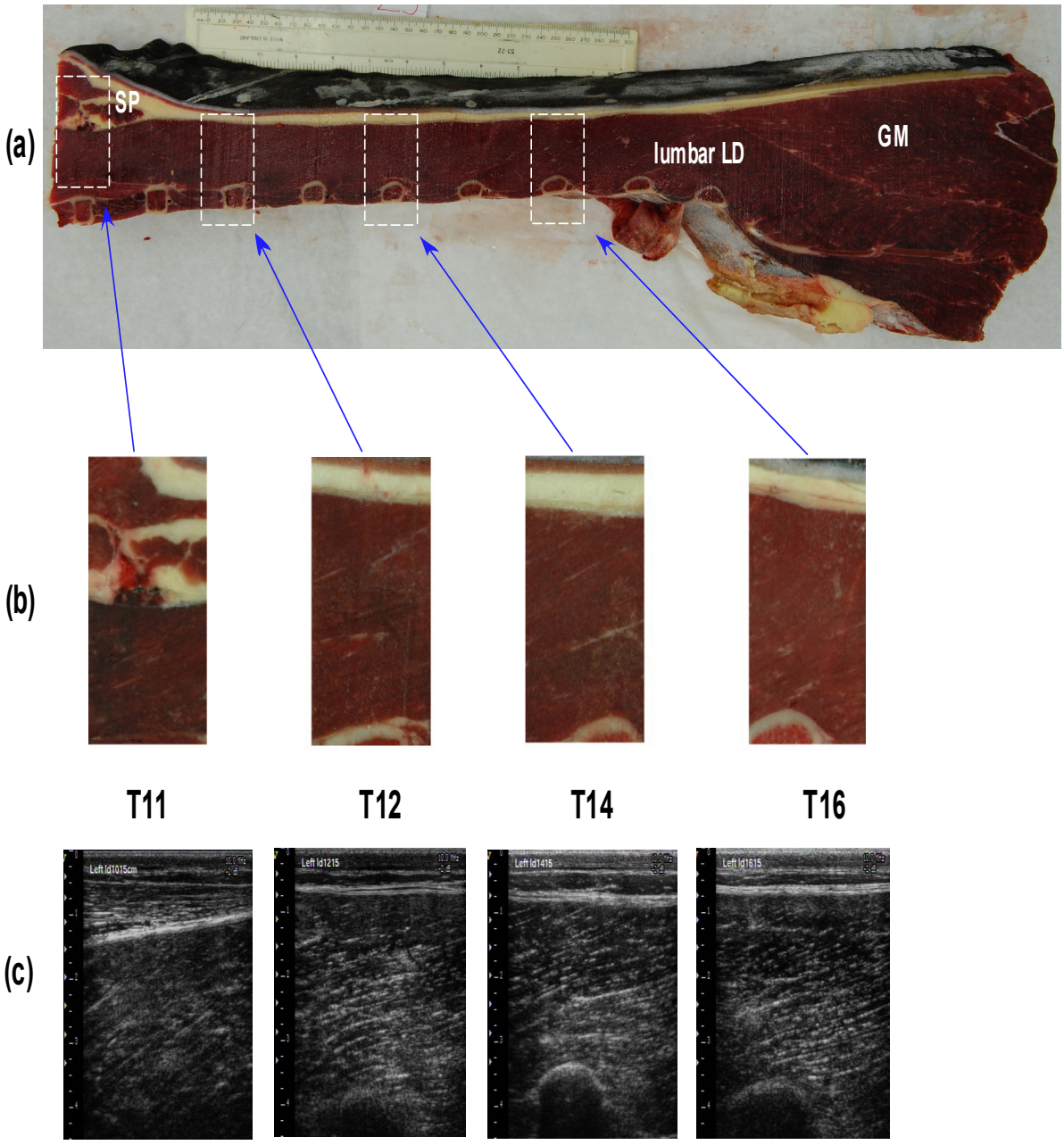

Fig. 45 (a) Sagittal section of the equine back 15 cm lateral to the midline, (b) details of the anatomic reference images corresponding to ultrasound images shown in (c) between T11- T16.
The image at T11 shows the spinalis muscle (SP) overlying LD. Both muscles are demarcated by the strong deep spinocostotransversal fascia from each other. The images of T12, T14 and T16 show the transverse cut of the corresponding ribs (ventral). Muscle fibres of LD run in a cranioventral to caudodorsal direction. The strong superficial thoracolumbar fascia and the skin define the dorsal border of the images.

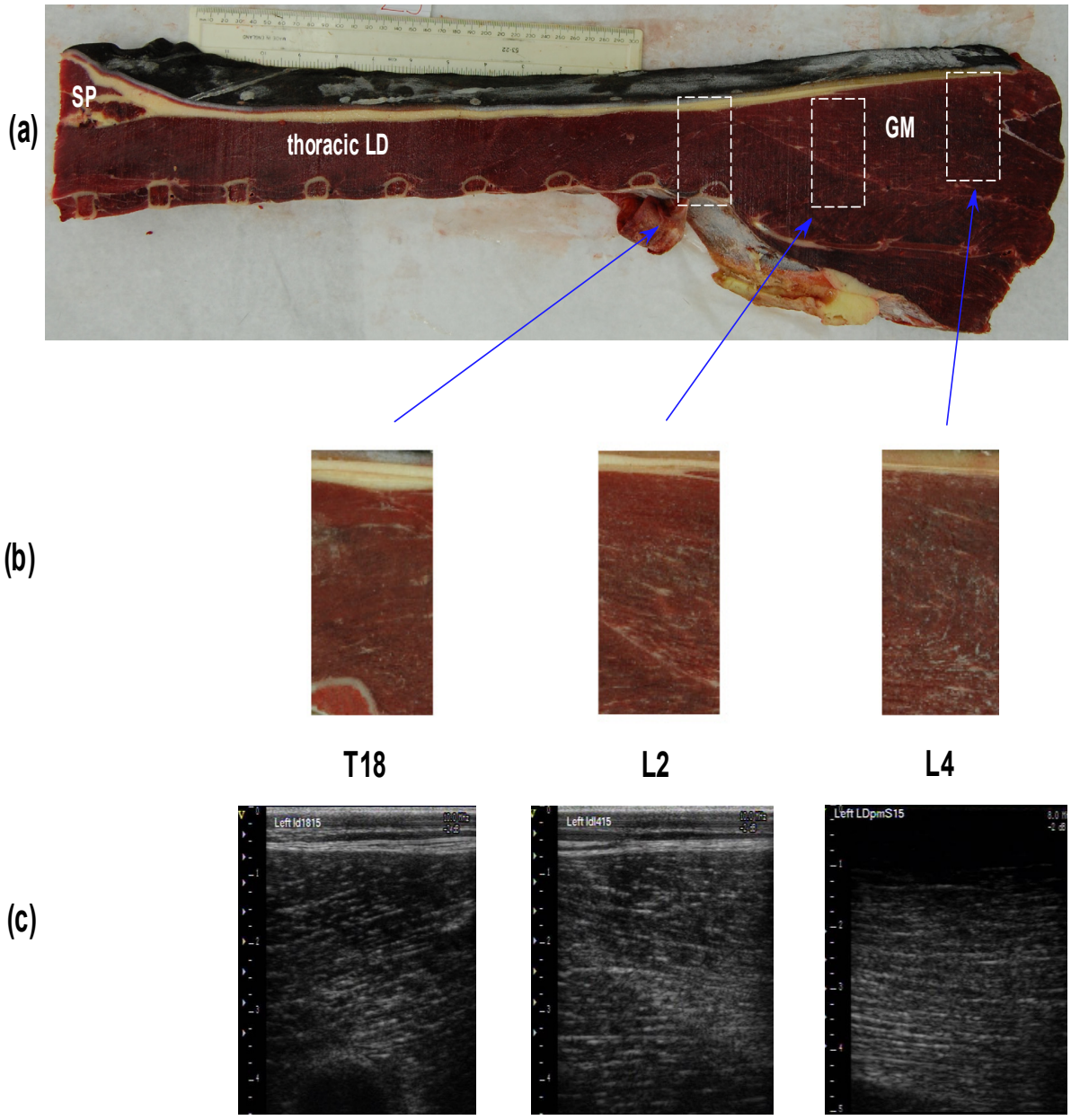

Fig. 46 (a) Sagittal section of the equine back 15 cm lateral to the midline, (b) details of the anatomic reference images corresponding to ultrasound images shown in (c) between T18- L4.
Images of L2 and L4 show the gluteal tongue of the middle gluteal muscle (GM) overlying LD. Both muscles are demarcated from each other by the deep thoracolumbar fascia. The muscle fibres of LD run in a cranioventral to caudodorsal direction. Muscle fibres of GM are orientated more parallel to the skin. The strong superficial thoracolumbar fascia and the skin define the dorsal border of the images.

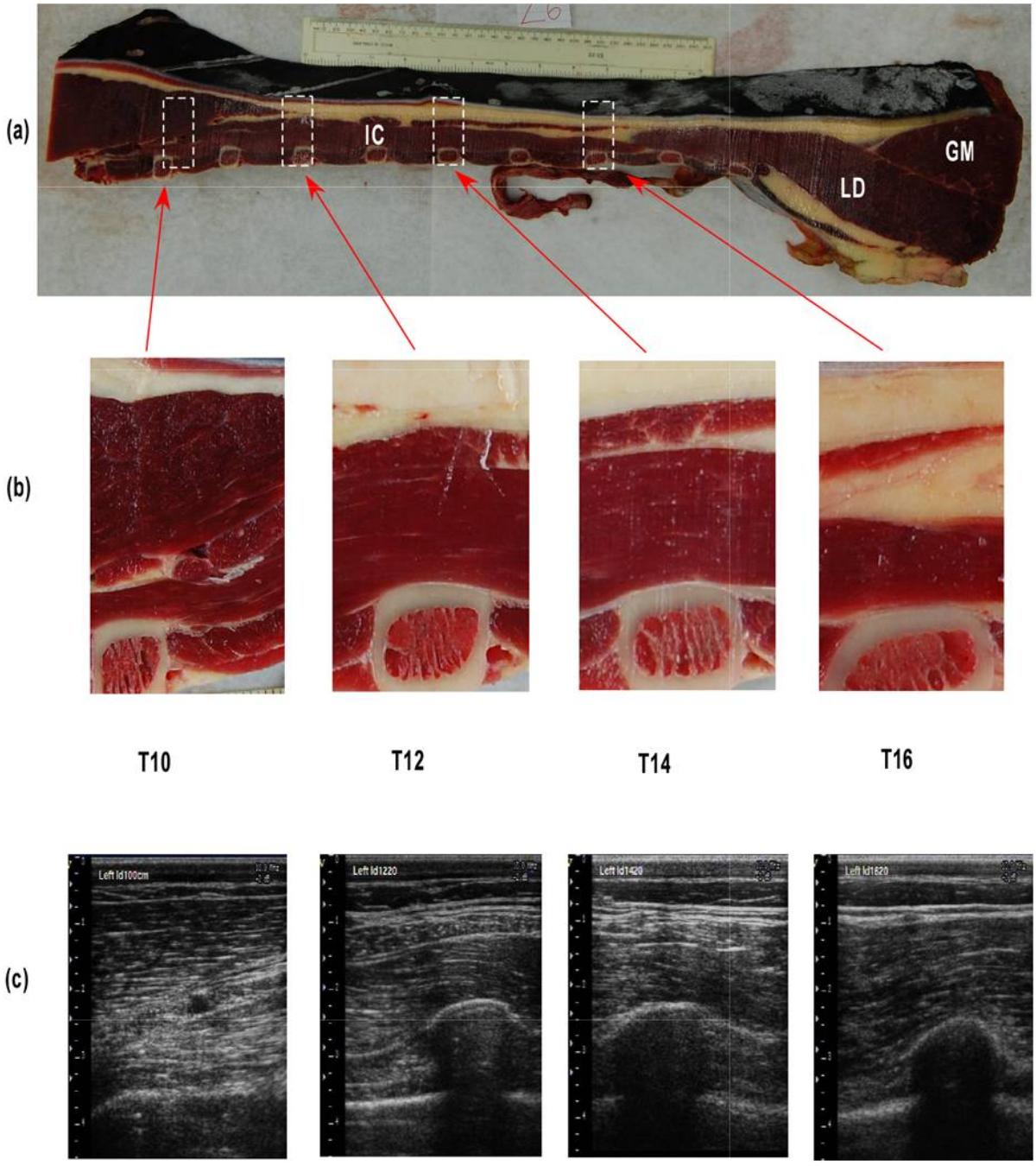

Fig. 47 (a) Sagittal section of the equine back 20 cm lateral to the midline, (b) details of the anatomic reference images corresponding to ultrasound images shown in (c) between T10- T16.

Images at T12, T14 and T16 show the sagittal section of the iliocostal muscle (IC). Muscle fibres of IC are orientated relatively parallel to the skin. The ribs are clearly visible on the ventral border of the images. The strong superficial thoracolumbar fascia and the skin define the dorsal border of the images.

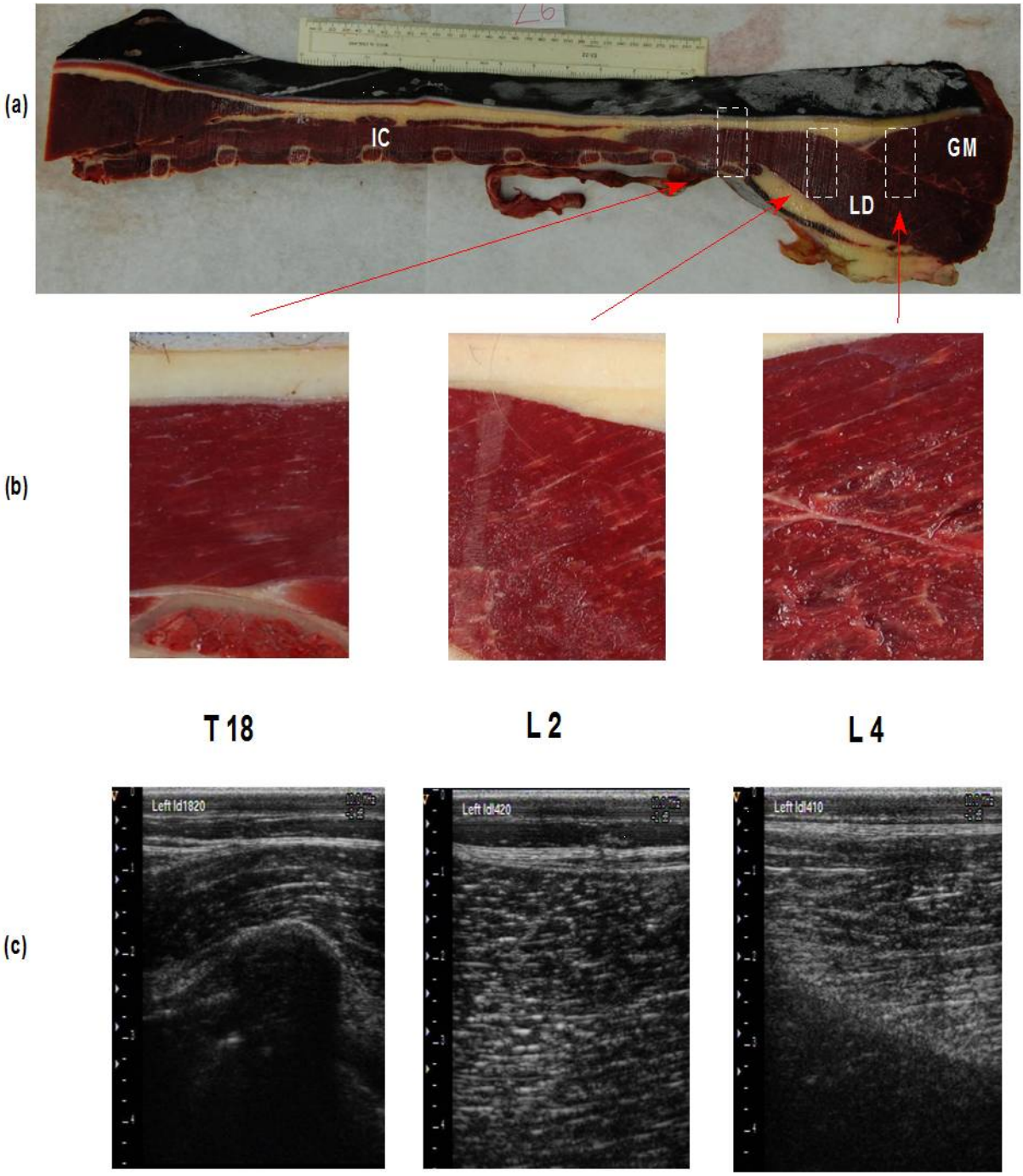

Fig. 48 (a) Sagittal section of the equine back 20 cm lateral to the midline, (b) details of the anatomic reference images corresponding to ultrasound images shown in (c) between T18-L4.

Images at T18 and L2 show the LD muscle. At T18 muscle fibres orientate relatively parallel to the skin whereas muscle fibres imaged at L2 and L4 insert in a steeper pennation angle onto the deep thoracolumbar fascia. At L4 middle gluteal muscle overlies LD. The strong superficial thoracolumbar fascia, fat and the skin define the dorsal border of the images.

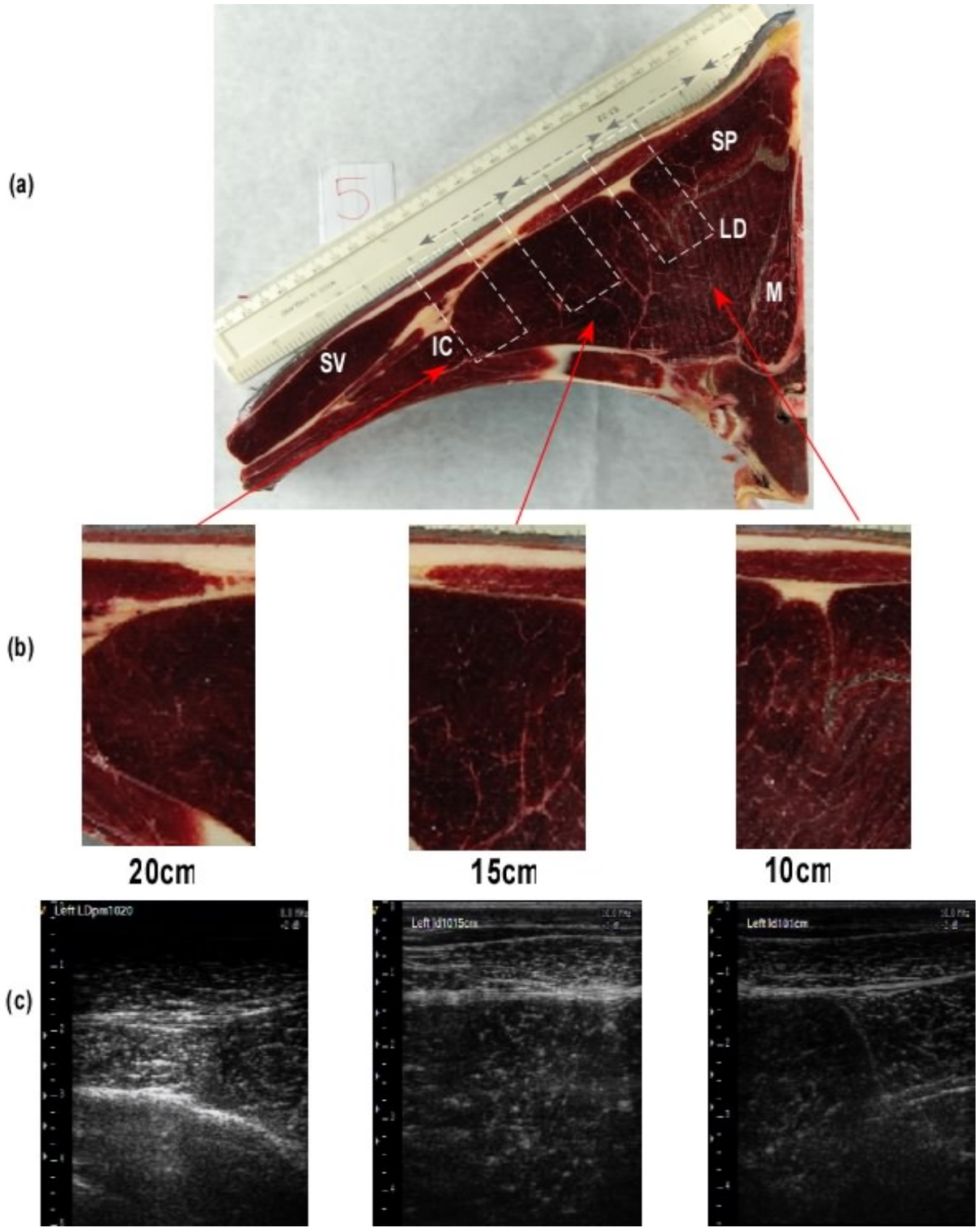

Fig. 49 (a) Transverse section of the equine back at the level of T10, (b) details of the anatomic reference images corresponding to ultrasound images shown in (c). The image 10 cm lateral to the midline shows the prominent strong deep spinocostotransversal fascia demarcating the spinalis muscle (SP) from LD, at 15 cm lateral to the midline LD is covered by the latissimus dorsi muscle (LT), LD shows distinct marbling. The image of LD 20 cm lateral to the midline shows its ventral extension and the adjacent ilicostal muscle (IC) demarcated by the thoracolumbar fascia. The superficial thoracolumbar fascia and skin define the dorsal boundary of the images. Multifidus (M) and serratus ventralis (SV) muscle are located medial and ventral to LD.

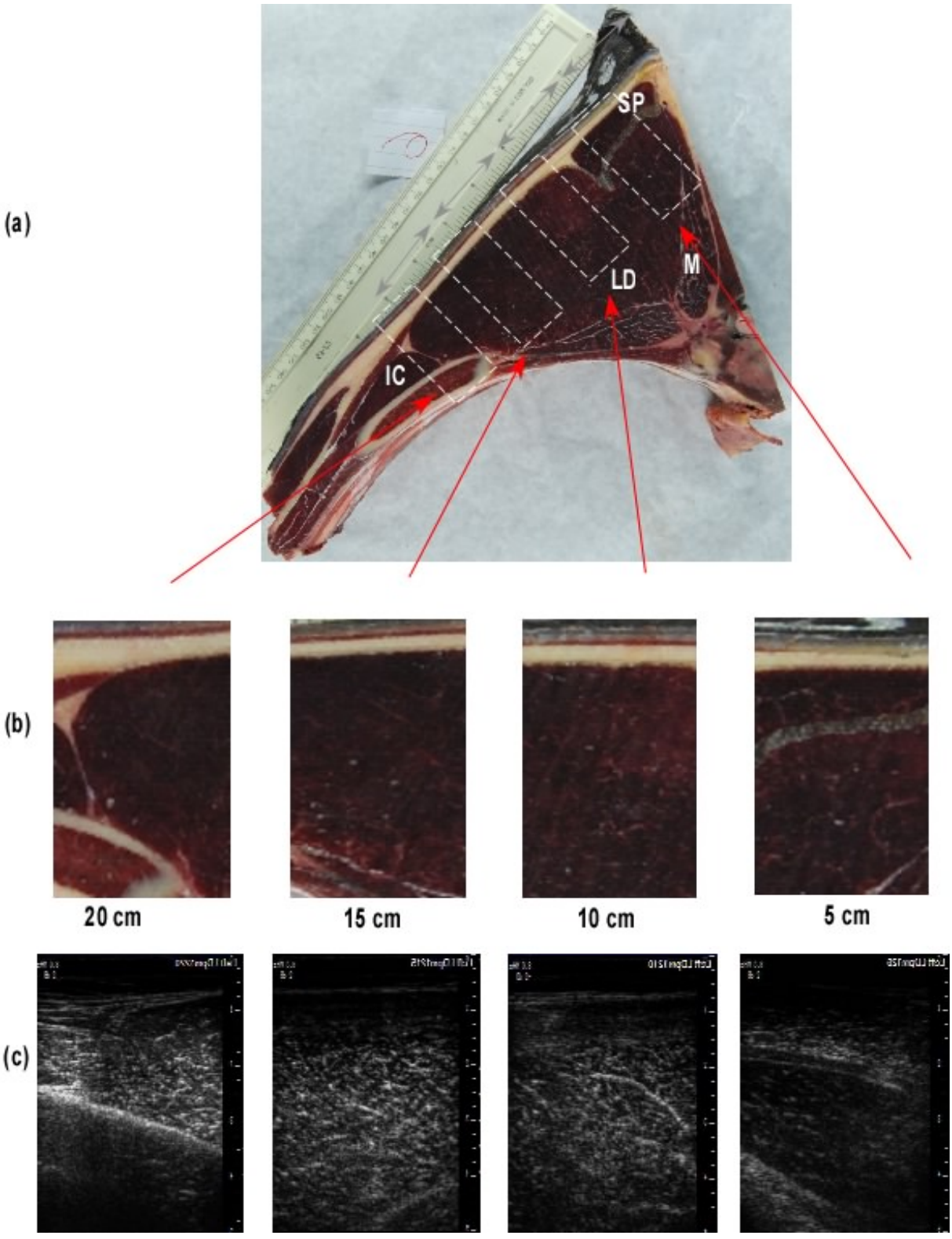

Fig. 50 (a) Transverse section of the equine back at the level of T12. (b) details of the anatomic reference images corresponding to ultrasound images shown in (c). The image 5 cm lateral to the midline shows the prominent strong spinocostotransversal fascia demarcating spinalis muscle (SP) from LD, images 10 cm and 15 cm lateral to the midline show the cross-section of LD, the image 20 cm lateral to the midline shows the distinct demarcation between LD and IC and the cross-section of the 12th rib confining IC. The superficial thoracolumbar fascia and skin define the dorsal boundary of the images. The multifidus muscle (M) is located medial to LD.

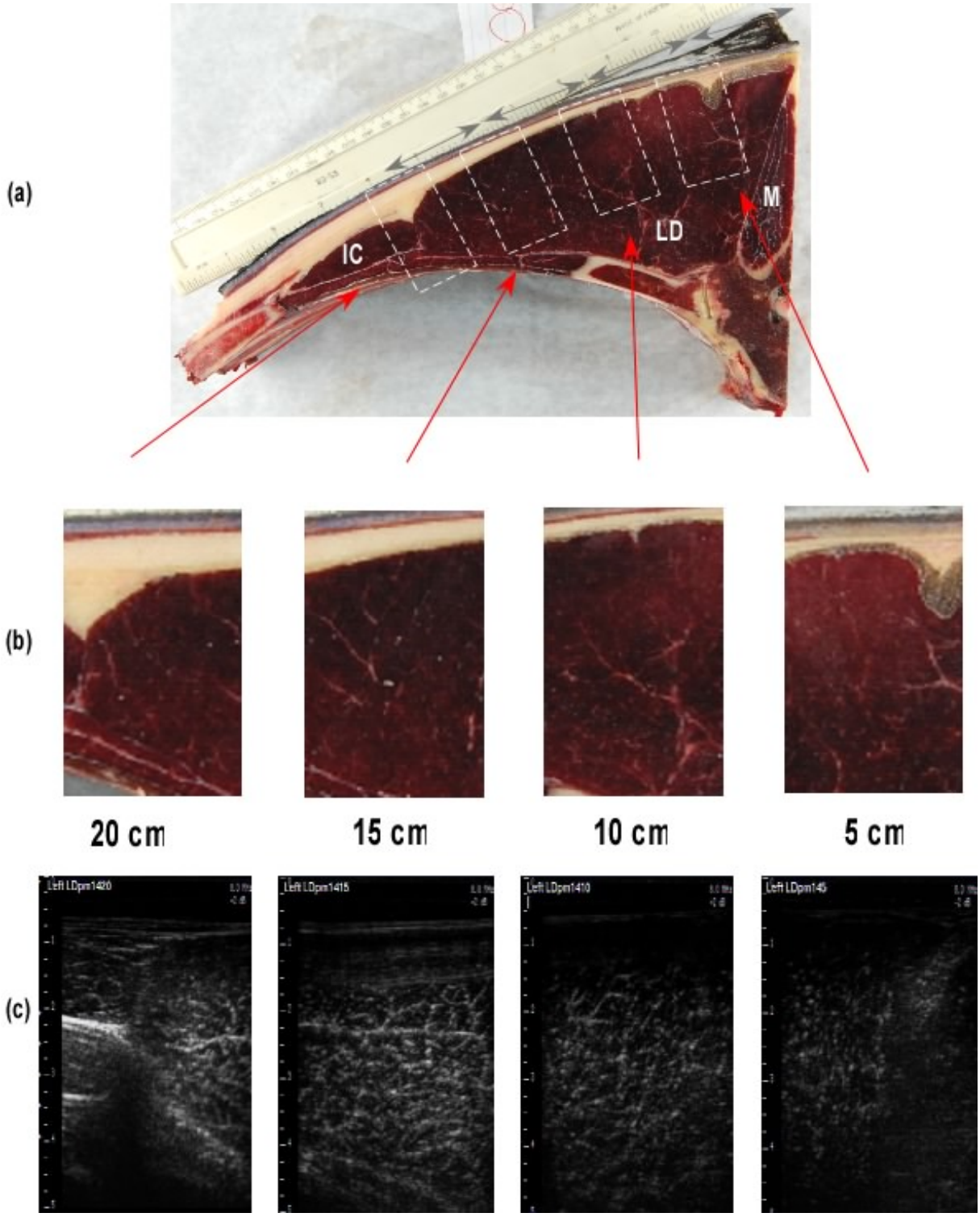

Fig. 51 (a) Transverse section of the equine back at the level of T14, (b) details of the anatomic reference images corresponding to ultrasound images shown in (c). The image 5 cm lateral to the midline shows a residual strong fascia, at 10 cm and 15 cm lateral to the midline the marbled transverse cross-section of LD is visible, the image at 20 cm lateral to the midline shows the ventral extension of LD and the adjacent IC, the rib is visualised as a hyperechoic line. The superficial thoracolumbar fascia and skin define the dorsal boundary of the images. The multifidus muscle (M) is located medial to LD.

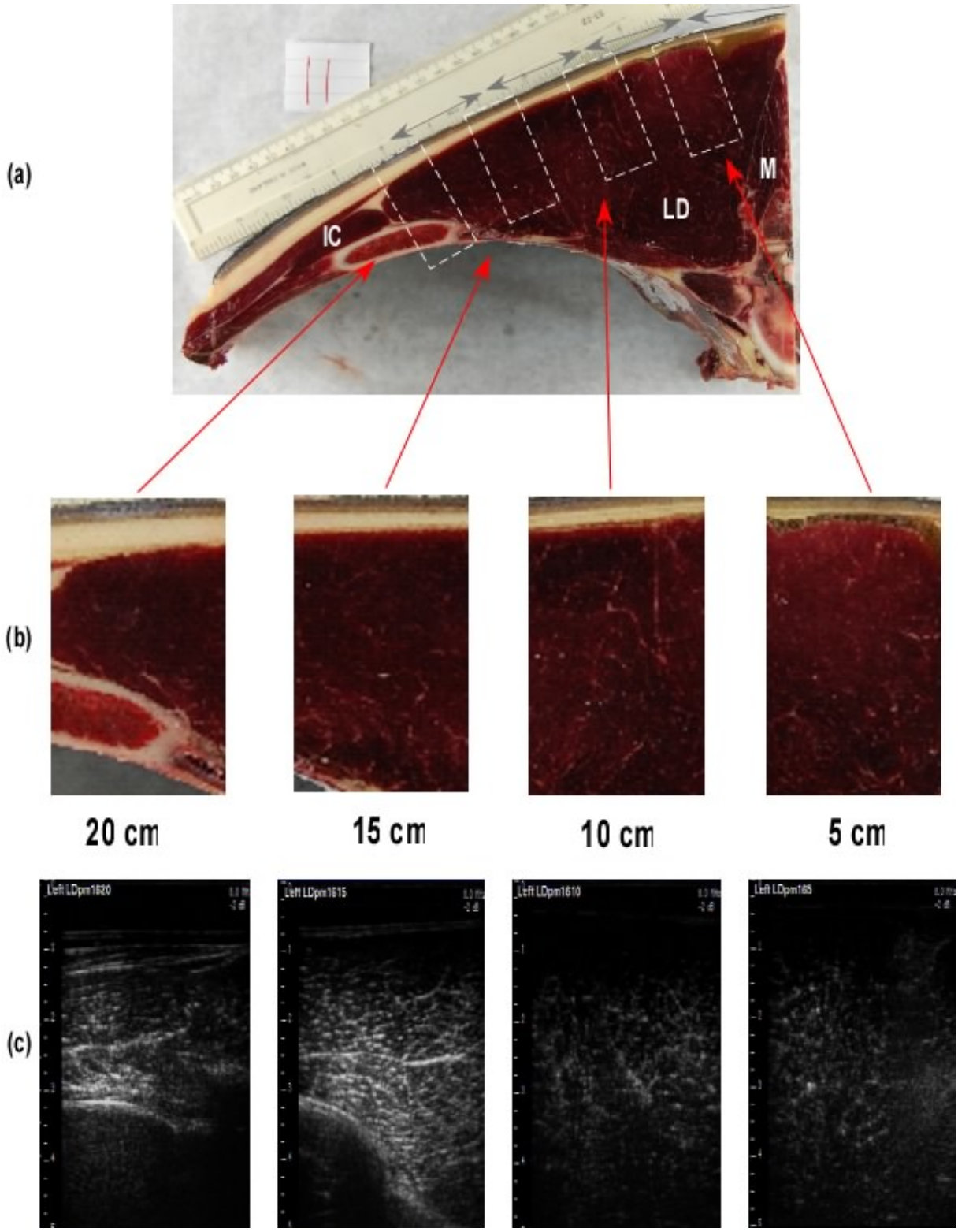

Fig. 52 (a) Transverse section of the equine back at the level of T16, (b) details of the anatomic reference images corresponding to ultrasound images shown in (c). Images at 5 cm and 10 cm lateral to the midline show the marbled LD, images 15 cm and 20 cm lateral to the midline, the 16th rib borders the ventral aspect of LD as a hyperechoic line. The superficial thoracolumbar fascia and skin define the dorsal boundary of the images. The multifidus muscle (M) is located medial to LD.

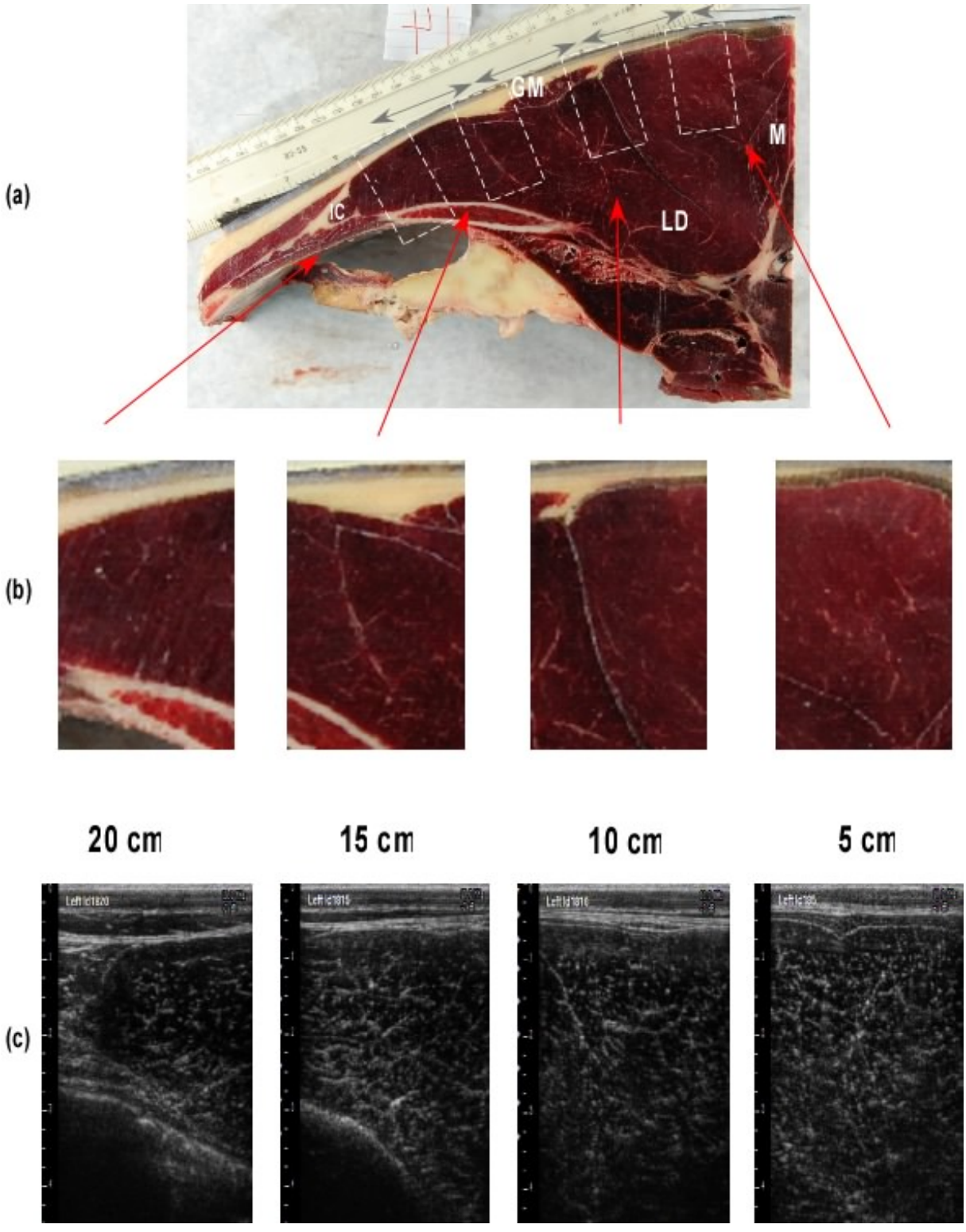

Fig. 53 (a) Transverse section of the equine back at the level of T18, (b) details of the anatomic reference images corresponding to ultrasound images shown in (c). The image 5 cm lateral from the midline shows LD covered by the strong superficial thoracolumbar fascia. 10 cm lateral to the midline LD is covered by the cranial extension of the gluteal tongue. Both muscles are demarcated by the deep layer of the superficial thoracolumbar fascia from which a thick aponeurosis runs in ventromedial direction. Images 15 cm and 20 cm lateral to the midline show LD and the corresponding rib as a hyperechoic line, at the distance of 20 cm lateral to the midline the caudal IC is separated from LD by a thin fascia. The multifidus muscle is located medial to LD.

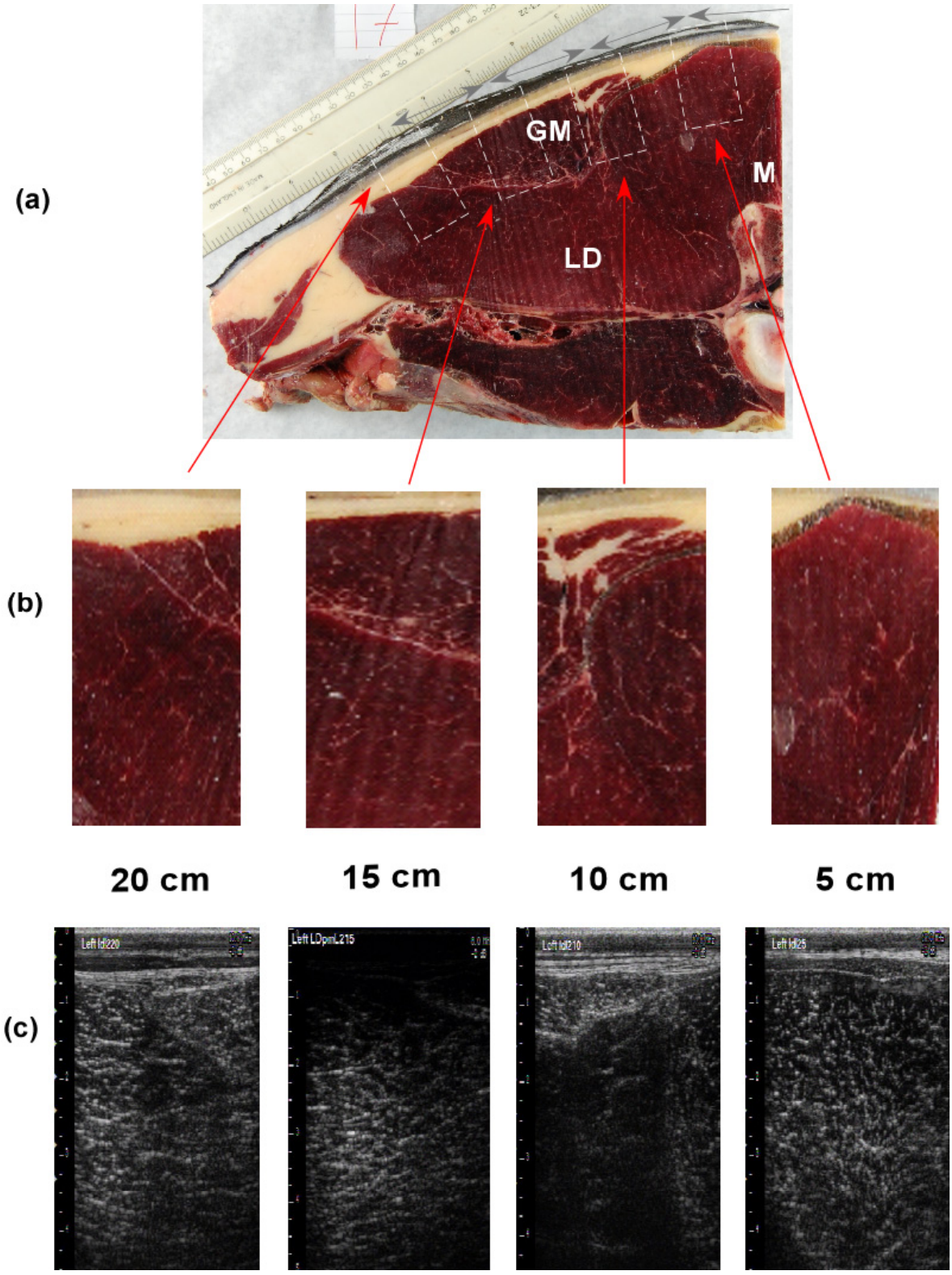

Fig. 54 (a) Transverse section of the equine back at the level of L2, (b) details of the anatomic reference images corresponding to ultrasound images shown in (c). Images taken at 5 cm and 10 cm lateral to the midline show the strong deep layer of the superficial thoracolumbar fascia covering LD and demarcating LD from the gluteal tongue (GM), 15 cm lateral to the midline the gluteal tongue takes up the majority of the image, 20 cm lateral to the midline the image shows LD and the ventral extension of the gluteal tongue. The superficial thoracolumbar fascia, fat and skin define the dorsal boundary of the images. The multifidus muscle (M) is located medial to LD.

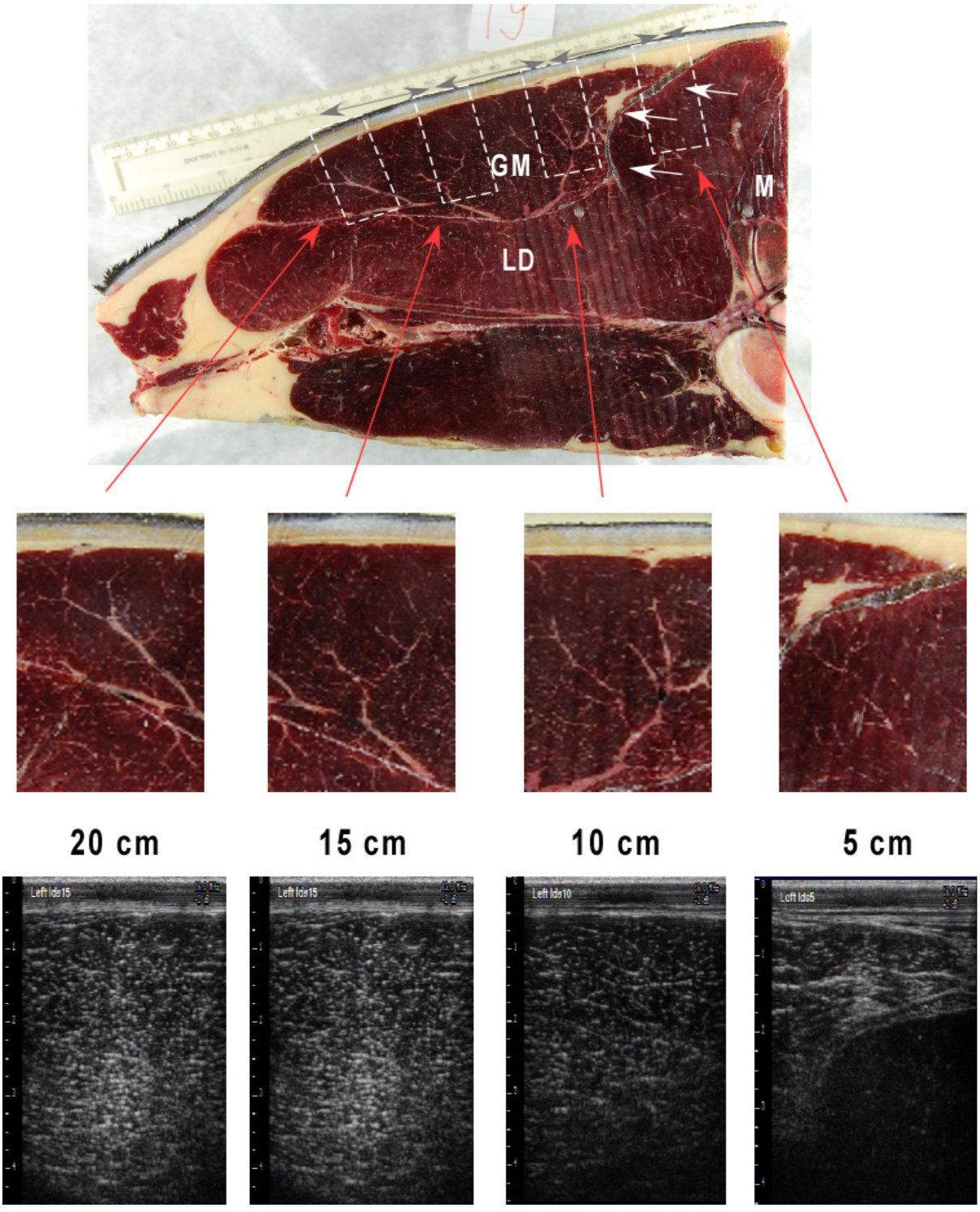

Fig. 55 (a) Transverse section of the equine back at the level of L4, (b) details of the anatomic reference images corresponding to ultrasound images shown in (c). The image 5 cm lateral to the midline shows the strong deep layer of the superficial thoracolumbar fascia overlying LD and demarcating LD from the middle gluteal muscle (GM). Images at 10 cm, 15 cm and 20 cm display the middle gluteal muscle. The superficial thoracolumbar fascia, fat and skin define the dorsal boundary of the images. In the transverse cross-section of the whole frozen slice the multifidus muscle (M) is located medial to LD and the internal fascia (white arrows) released from the deep layer of the thoracolumbar fascia is visible running in dorsolateral to ventromedial direction.

III.3.4 Discussion and Conclusion

The aim of this study was to develop an ultrasound guide of the equine LD. The lack of familiarity with the normal cross-sectional anatomy of the equine epaxial musculature is a major factor limiting the interpretation of ultrasound images. Therefore the frozen slices of the equine back facilitated an accurate interpretation of the anatomical structures on ultrasound images. Longitudinal and transverse ultrasound images were correlated to the corresponding cross-sections of the frozen cadaver which showed a consistent match of ultrasonographic features with the frozen anatomical structures.

In the present study the topographic anatomy of overlying and adjacent muscles to LD were visualised to document the relationship between the different muscles in certain regions. The knowledge of the exact location of LD and the relationship between adjacent muscles and LD is important for the clinical examination of the equine back. Muscle alterations, such as swelling, muscle hypertrophy or atrophy, muscle spasm, muscle pain, observed by visual inspection and palpation need to be related to the correct muscle structure to allow the adequate treatment and training. The comparison of ultrasound pictures and frozen slices showed that parts of LD are covered by the spinalis muscle and serratus ventralis muscle (cranial) and also the tongue of the middle gluteal muscle (caudal). Parallel to LD the iliocostal muscle runs along its lateral border. Therefore muscle atrophy along the withers, for example, may not include LD alone but also the spinalis muscle and therefore may have different clinical significance.
It is also important to indicate the strong superficial thoracolumbar fascia which surrounds LD and demarcates it from adjacent muscles. The superficial thoracolumbar fascia releases a distinct, additional, internal fascia caudal to T17 which divides LD in a medial and lateral part. This was visible on ultrasound images as well as in the cross-section of the corresponding cadaver slices. Due to the internal fascia the effective line of pull of the muscle fibres is altered. The visualisation of the LD muscle structure and the characteristics of the fascia are important to document normal muscle structure which then can be used to compare normal LD structure to LDs of horses with back problems.

Ultrasound images and dissections of LD showed that muscle volume changes through the course of LD. The dimension of the cross-section of the medial part of LD next to the dorsal spinous processes is large and decreases in lateral direction. The full muscle thickness of LD was only visible with ultrasound in its whole depth in a distance of >10 cm away from the

midline as the medial muscle region was too thick to image in full depth. The pennation angle decreases in a mediolateral direction. Although the muscle fibre length was not visible in its full extent the decreasing pennation angle might be associated with decreasing muscle thickness at a constant muscle fibre length. Changes of fibre orientation and muscle thickness result in changes of muscle properties. The total PCSA increases in proportion to the pennation angle of the muscle fascicles and volume (Aagard *et al.*, 2001; Alexander and Vernon 1975; Rutherford and Jones 1992). This means that the PCSA is decreased in the lateral LD not only because of the decreased pennation angle but also because of reduced muscle thickness. As the force generating capacity is proportional to PSCA it can be presumed that the muscle force is less in the lateral LD compared to the medial LD (Payne *et al.* 2004).

Not only the gross anatomical structure but also the basic internal muscle structure of LD allows conclusions on the biomechanical function of this muscle. Detailed information of muscle thickness, muscle fibre length and pennation angle characterise the functional capacity of the muscle which can be used to compare normal LD structure to LDs of horses with back problems. In humans parameters of the internal muscle structure including muscle fibre orientation, muscle and fat thickness, echogenity and ratio of tendinous structures compared to muscle tissue have been shown to be important to interpret muscle quantity (Aagard and al 2001; Binzoni *et al.* 2001; Kawakami *et al.* 2006; Kubo *et al.* 2003a; Maganaris *et al.* 1998; Maurits *et al.* 2003; Narici *et al.* 2003; Nielsen *et al.* 2000; Strobel *et al.* 2005).

Changes of the muscle structure of the equine LD play an important role to diagnose primary and secondary back problems in the horse. Measurements of pennation angle and muscle thickness are helpful to monitor changes in muscle quantity influenced by factors such as type of training, age, bad fitted saddles, back pain and lameness.

In humans, bed rest and muscle inactivity had a negative effect on muscle thickness and pennation angle (Abe *et al.* 1997). As horses with back problems often show an atrophy of LD parameters such as muscle thickness and pennation angle might be helpful to evaluate the degree of muscle atrophy. These parameters could also be used to monitor the effect of treatment and training as in humans, pennation angle and muscle thickness was shown to increase with training resulting in an increase of maximal force-generating capacity (Aagard *et al.* 2001; Seynnes *et al.* 2007).

It also might be important to valid the influence of age on LD after studies have documented that muscle thickness is influenced by age (Kubo *et al.* 2003a, b). Age-related muscle atrophy

was observed in certain muscles of humans. For example, muscle thickness of elderly men and woman was decreased compared to younger men (Reimers *et al.* 1998).

Other ultrasound studies in human musculature have demonstrated that ultrasound is able to depict changes of the muscle composition. The replacement of muscle tissue by fat resulted in an increased echogenicity and a decrease of the muscle bulk (Reimers *et al.* 1993; Sofka *et al.* 2004; Strobel *et al.* 2005). Substantial fatty atrophy was also characterised by the loss of the visibility of tendons and the loss of the typical pennate muscle pattern (Khoury *et al.* 2008; Strobel *et al.* 2005). Similar results were documented in a study comparing trained and untrained men. Increased intramuscular echogenicity with decreased echoes reflected from connective tissue septa and the bone were visible in untrained men compared to trained athletes. These changes were thought to be due to the increase of intramuscular connective tissue and fat in proportion to muscle tissue. An age-related increase of echogenicity of the ultrasound images was detected in muscles of older men compared to middle aged men. In this study increased echogenicity was reported to be the result of centripetalisation and internalisation of fat into the muscle (Sipila and Suominen 1991). Therefore the replacement of muscle tissue by fat in LD of horses with muscle atrophy due to back problems and age could be evaluated by the echogenicity measurements of ultrasound images. According to studies in humans, the atrophy and disuse of the equine LD is visible on the ultrasound image as higher echogenicity and effaced muscle fibre pattern (Khoury *et al.* 2008; Sipila and Suominen 1991)

In conclusion, ultrasound is a readily available and practical technique to image soft tissue structures of the equine back. The present study provides anatomical information on the equine LD, which will assist both clinical and research purposes. As the examined LD came from a horse with no history of clinical signs of back problems, ultrasound images and frozen cadaver slices could not be related to any obvious changes of muscle structure and images do not give any conclusion on horses with back problems. But the present description provides a reference for the ultrasonographic evaluation of the equine LD and may support the interpretation of pathological conditions of the equine back. It was demonstrated that ultrasound is relatively easy to perform with standard ultrasound equipment. Hypo- and hyperechoic areas, fibre pattern and pennation angle as well as muscle depth and fat thickness can be visualised and measured. Although ultrasound has been demonstrated to be useful to monitor muscle quantity in humans the role of ultrasound measurements as parameters to

characterise the equine LD needs to be further evaluated. Differences between breed, age and gender and in particular differences between horses with and without back pain need accurate validation to install ultrasound as a precise technique to distinguish between normal and pathological conditions.

III.4 Quantitative Ultrasonography of the equine thoracolumbar Longissimus dorsi muscle: repeatability of muscle thickness and pennation angle measurements

III.4.1 Introduction

Ultrasonography as a diagnostic technique has been widely used to evaluate soft tissue structures in the horse (Reef 1998). Although ultrasound is mainly applied to image tendons, ligaments and joints it has also been employed to determine the internal structure of muscles and differentiate between soft, solid, vascular and cystic lesions (Rantanen and McKinnon 1997). Transverse images of muscle show the connective tissue surrounding the muscle fascicles as fine, disorganized hyperechoic echoes scattered throughout the hypoechoic muscle tissue. In the longitudinal view it is characterized by fine, homogeneous, multiple and parallel hyperechoic lines within the hyperechoic muscle (see chapter III.3). This sonographic appearance is due to multiple muscle bundles (fascicles) surrounded by fibroadipose septa (perimysium). Internal and overlying connective tissue, fascia and fat appear as a bright echogenic structures compared to the less echogenic muscle tissue (Rantanen and McKinnon 1997). Ultrasonograpic examination of the equine back muscles has been described in the literature mainly in association with pathological findings such as muscle fibre tearing or haemorrhage (Reef 1998; Ross and Dyson 2002). In chapter III.3 the normal ultrasonographic anatomy is described in detail.

In humans ultrasonography is not only performed to characterise muscle lesions or diagnose neuromuscular disorders (Zuberi *et al.* 1999), it is also used as a non-invasive tool for the evaluation of muscle function by quantifying muscle architecture. Architectural measurements such as pennation angle, muscle fibre length and muscle volume are important characteristics of whole muscle function (Fukunaga *et al.* 1997; Gans 1982; Gans and Bock 1965; Otten 1988). Muscle fibre length describes the number of sarcomeres in series which is related to shortening velocity and the range over which force can be generated. Pennation angle defines the angle in which muscle fibres insert to the corresponding tendon or aponeurosis. Increased pennation angle in a given muscle cross-section area and muscle volume results in decreased muscle fibre length. Thus, shortening velocity and range of excursion is reduced but the number of contractile muscle fibres placed in parallel is increased which in turn increases maximum force generation (Maganaris *et al.* 1998). As it is often difficult to image the whole muscle volume or cross-sectional area by ultrasound images, muscle thickness can be used as an indirect measurement to help determine muscle function

(Klimstra *et al.* 2007; Maganaris and Baltzopoulos 1999). Previous studies have determined the correlation between architectural measurements and muscle thickness using ultrasound and verified these results by magnetic resonance imaging (MRI) or computed tomographic (CT) measurements/ images (Dupont *et al.* 2001). A significant correlation between both muscle fibre length and pennation angle and muscle thickness was observed (Abe *et al.* 1998; Kawakami *et al.* 1993; Kearns *et al.* 2000) and it was suggested that pennation angle is a function of the relative state of muscle enlargement (Kearns *et al.* 2000).

The equine thoracolumbar Longissimus dorsi muscle (LD) is one of the largest muscles of the horse. The muscle is thought to be involved in the clinical signs of back pain, poor performance, reluctance to riding and in back pain secondary to hind limb lameness (Jeffcott and Haussler 2004; Ross and Dyson 2002). To date there is no documentation of LD changes in normal horses or horses suffering from back pain, it would be useful however to have a technique that would allow the evaluation of muscle structure reliably in the live horse. In humans, it is well documented that back pain is associated with changes in the volume of back muscles (Hides *et al.* 1994). Affected muscle groups undergo hypertrophy in the acute stage and atrophy with an increase of fatty tissue in chronic cases (Kamaz *et al.* 2007). In these studies many of the paraspinal muscle evaluations have been performed by MRI (Hides *et al.* 1995) and CT-scans (Danneels *et al.* 2000) which are not feasible techniques for the large equine body. However, comparison of MRI, CT and ultrasound scans have justified the use of ultrasound as a method for the detection of changes throughout large muscles in response, for example, to disuse, training or muscle degeneration (Reeves *et al.* 2004; Walton *et al.* 1997). Ultrasonographic measurements showed to be highly reliable and valid involving muscle architecture and muscle thickness of humans (Baumgartner *et al.* 1998; Reeves *et al.* 2004; Reimers *et al.* 1998; Sanada *et al.* 2006). Therefore it seems to be a promising method to image the equine LD. It provides non-invasive visualization of muscle changes without any exposure to ionizing radiation. Furthermore, ultrasound has the advantage to be a most practical and cost-effective method to determine skeletal muscle.

Ultrasound studies in humans of different skeletal muscles, for example multifidus, erector spinae and quadriceps muscle, have tried to establish normal values of muscle thickness and architectural parameters to standardize real-time ultrasound examinations and use them as a database for normal values (Blazevich *et al.* 2006; Kristjansson 2004; Reimers *et al.* 1996; Scholten *et al.* 2003). Therefore measurements have been tested for inter- and intraobserver

reliability to prove ultrasound is an accurate and precise method. The results indicated that ultrasound provides reliable data for muscle thickness and muscle architectural measurements (Blazevich *et al.* 2006; Kristjansson 2004; Watanabe *et al.* 2004). Curently no data is available on the reliability of ultrasound in the assessment of muscle morphology in the horse, however ultrasound was proven to be a repeatable technique for the measurement of the volume of tendon lesions in the horse and muscle volume in the dog (Weller *et al*., 2007; Ferrari *et al.* 2006).

The aim of this study was to determine the practicability and reliability of ultrasonography to determine muscle architecture of the LD in the live horse.

The objectives of the study were to

- determine inter- and intraobserver repeatability for measuring LD depth and pennation angle using ultrasonography
- determine the practicability of using ultrasonography to measure LD depth and pennation angle in live horses

III.4.2 Material and Methods

III.4.2.1 Subjects

Ten Welsh mountain ponies (section A, all mares, owned by the Royal Veterinary College) weighing 227 kg to 525 kg (mean ±stdev 396 ± 104 kg) were used in this experiment. Their height ranged from 112 cm to 152 cm (mean ±std 134 ±14 cm) and their age ranged from four years to 11 years (mean ±stdev 7±4 years). Previous to the experimental procedure all horses were judged to be clinically sound during in–hand gait examination and to have no clinical signs of back pain by an experienced equine clinician.

III.4.2.2 Data collection

Ultrasonographic images were collected from the left and right thoracic and lumbar LD at the level of the 16th rib, 10 cm lateral to the midline. For the procedure all ponies were confined in stocks and stand square. Rib 16 was identified by palpation and a 6 cm x 4 cm skin patch was clipped 10 cm lateral to the midline of the back. The skin patch was cleaned with water and spirit to remove dirt. Ultrasound gel was applied to the ultrasound transducer and to the scanning area to optimise acoustic coupling. Two observers acquired twenty B-mode images each of the right and left LD from each pony, using a 7.5 MHz linear transducer with a laptop

based ultrasound machine (Echo Blaster 128 EXT-1Z, UAB Telemed, Vilnius, Lithuania). Gain and power settings were kept constant for each acquisition: gain 82, power 82 (these settings were selected based on pilot data). Images were acquired into a 512x512 matrix and the images were saved as "tagged image file format" (TIFF) files for further processing.
A total of 800 ultrasound images were obtained by two different examiners in 10 horses. Based on image quality, mainly definition of muscle fibre and aponeurosis visibility, 440 images were selected. Measurements of muscle thickness and pennation angle were performed in the JAVA image processing program Image J (Author: Wayne Rasband, Research Service Brach, National Institute of Mental Health, Bethesda, Maryland, USA). The muscle thickness was measured from the aponeurosis-muscle interface to the muscle-bone interface with electronic callipers by one operator in 440 images. The repeatability of using the electronic calipers was assessed by a standardised 2.0 cm measurement taken from the scale displayed in each ultrasound image. Pennation angle were calculated by identifying and tracking muscle fascicles and relate them to their corresponding aponeurosis with the help of the electronic goniometer of Image J.

III.4.2.3 Data analysis

Muscle depth measurements resulting from the repeated ultrasonographic images of the two examiners were used to assess the variation in muscle depth and pennation angle between measurements of the right and left LD, between horses and to determine the intra- and inter observer repeatability.
Mean and standard deviation were calculated for the different horses, observers and right and left LD. The distribution of the data was assessed graphically and tested for normality using a Kolmogorov-Smirnov test. An independent samples t-test, paired samples t-test and ANOVA (with a Bonferroni post-hoc test) were carried out to test the differences between examiners, right and left LD and the ten horses respectively. In this study, the statistical significance level was set at $p < 0.05$. The inter-observer agreement was expressed as the 95% limits of agreement of the differences between observers and calculated as the mean difference ± 1.96 x standard deviation of the differences (Bland and Altman 1986). This was performed after the assumptions that the differences were normally distributed and that the differences were independent from the size of the measurement were satisfied.
Intra-observer repeatability was determined by calculating the repeatability coefficient by multiplying the standard deviation of the differences by 2.77 (British Standards Instituion,

1975). Variation in measurements was also expressed as ratio between standard deviation and mean (coefficient of variation, CoV).

The relationship between age, weight and heights of the horses and muscle thickness or pennation angle was assessed by calculating the Pearson's correlation coefficient.

All data was processed in Excel (Microsoft Office 2003, Microsoft Cooperation, USA) and SPSS 14.0 (SPSS Inc. Chicago, Illinois, USA).

III.4.3 Results

III.4.3.1 Variation in muscle thickness measurements

Muscle thickness measurements of the ten horses ranged from 2.2 cm to 5.3 cm resulting in a mean±stdev value of 3.0 ±0.6 cm. There was a significant difference between horses (p= 0.0001) which reflected the influence of age, size and composition on LD muscle thickness. No significant difference was detected between right and left LD of each horse (p= 0.5).

Calculation of the mean ±std muscle thickness values for operator 1 and operator 2 showed 3.6 ±0.8 cm (operator 1) and 3.4 ±0.8 cm (operator 2). There was no significant inter-operator difference (p= 0.1). The variation of the measurements in the ten horses expressed as coefficient of variation (CoV) ranged between 1.5-11.6 % for operator 1 and between 1.5-11.3% for operator 2.

III.4.3.1.1 Intra-operator repeatability for muscle thickness measurements

Variation in measurement due to identifying endpoints with electronic callipers by the same operator was shown to be small as standardised measurements of the image scale for all 440 selected scans resulted in a mean ±stdev value of 2.0±0.06 cm with a CoV of 0.3%.

The standard deviation of the difference between repeated muscle thickness measurements of the ten horses for each operator ranged from 0.05-0.3 cm (operator 1) and from 0.05 cm to 0.4 cm (operator 2). This resulted in a repeatability coefficient (2.77 x stdev) of 0.40 cm for operator 1 and in a repeatability coefficient of 0.42 cm for operator 2.

III.4.3.1.2 Inter-operator agreement for muscle thickness measurements

The mean ±std difference of muscle thickness measurements between operator 1 and operator 2 was 0.09 ±0.2 cm. Therefore the 95% limits of agreement were calculated to be between 0.3 cm and 0.5 cm. The width of the 95% limits of agreement was 0.8 cm.

Mean muscle thickness, standard deviation and minimum and maximum values for each operator, right and left LD in each horse are displayed in Table 31-Table 34.

Table 31 Mean value, standard deviation and minimum and maximum values of the muscle thickness measurements of the right LD in all horses taken by operator 1 in cm.

Horse	N	Mean (cm)	Stdev. (cm)	Minimum (cm)	Maximum (cm)
1	11	3.1	0.16	2.9	3.5
2	11	3.2	0.16	2.9	3.5
3	11	2.4	0.16	2.2	2.7
4	11	2.7	0.29	1.9	2.9
5	11	3.1	0.09	2.9	3.2
6	11	4.4	0.10	4.3	4.7
7	11	2.0	0.21	1.9	2.5
8	11	3.1	0.19	2.7	3.4
9	11	3.6	0.05	3.5	3.7
10	11	3.5	0.07	3.4	3.6

Table 32 Mean value, standard deviation and minimum and maximum values of the muscle thickness measurements of the left LD in all horses taken by operator 1 in cm.

Horse	N	Mean (cm)	Stdev. (cm)	Minimum (cm)	Maximum (cm)
1	11	3.2	0.12	3.0	3.4
2	11	3.1	0.18	2.7	3.4
3	11	2.1	0.08	2.0	2.3
4	11	3.1	0.15	2.8	3.4
5	11	3.5	0.09	3.3	3.7
6	11	3.4	0.12	3.2	3.6
7	11	2.0	0.24	1.7	2.4
8	11	1.9	0.10	1.8	2.1
9	11	3.6	0.14	3.4	3.9
10	11	3.9	0.08	3.7	4.0

Table 33 Mean value, standard deviation and minimum and maximum values of the muscle thickness measurements of the right LD in all horses taken by operator 2 in cm.

Horse	N	Mean (cm)	Stdev. (cm)	Minimum (cm)	Maximum (cm)
1	11	2.8	0.14	2.7	3.1
2	11	3.1	0.12	3.0	3.3
3	11	2.7	0.11	2.6	2.9
4	11	2.4	0.13	2.2	2.6
5	11	3.0	0.07	2.9	3.1
6	11	4.0	0.42	3.2	4.3
7	11	1.9	0.07	1.8	2.0
8	11	2.6	0.12	2.3	2.8
9	11	3.4	0.39	2.6	3.7
10	11	3.5	0.10	3.4	3.7

Table 34 Mean value, standard deviation and minimum and maximum values of the muscle thickness measurements of the left LD in all horses taken by operator 2 in cm.

Horse	N	Mean (cm)	Stdev. (cm)	Minimum (cm)	Maximum (cm)
1	11	3.3	0.12	3.1	3.5
2	11	3.2	0.14	3.1	3.5
3	11	2.4	0.11	2.2	2.6
4	11	3.2	0.17	2.9	3.5
5	11	3.3	0.05	3.2	3.4
6	11	3.2	0.10	3.0	3.3
7	11	1.8	0.15	1.5	2.0
8	11	1.8	0.12	1.6	2.0
9	11	3.7	0.17	3.5	4.0
10	11	3.6	0.10	3.4	3.7

III.4.3.2 Variation in pennation angle

The pennation angle measurements of the ten horses showed a range between 8° to 30° and a mean±stdev value of 17 ±5°. There was a significant difference between the different horses (p= 0.0001) which reflected the influence of age, size and composition on LD muscle quality. No significant difference was detected between right and left LD of each horse (p= 0.1).

III.4.3.2.1 Intra-operator agreement for pennation angle

The repeatability coefficient was 8° for operator 1 and 7° for operator 2. Mean pennation angle of LD, standard deviation and minimum and maximum values for each operator, right and left LD in each horse are displayed in Table 35-Table 38.

III.4.3.2.2 Inter-operator repeatability for pennation angle

The calculations of the mean ±std pennation angle values for examiner 1 and examiner 2 showed 18 ±4° (operator 1) and 18 ±3° (operator 2). There was no significant inter-operator difference detected (p= 0.1). The variation of the measurements in the ten horses were shown as coefficient of variation (CoV) and ranged between 8.5-89.8% for operator 1 and between 4.5-46.9% for examiner 2. The mean ±std difference of pennation angle measurements between operator 1 and operator 2 was -0.7° ±4°. Therefore the 95% limits of agreement were calculated to be between -8° and 6°. The width of the 95% limits of agreement was 14°.

Table 35 Mean value, standard deviation, minimum and maximum of the pennation angle of the right LD in all horses taken by operator 1 in (°).

Horse	N	Mean (°)	Stdev. (°)	Minimum (°)	Maximum (°)
1	11	15	1.92	12	19
2	11	16	3.17	12	20
3	11	19	2.70	14	24
4	11	19	3.34	14	25
5	11	18	3.66	11	24
6	11	22	2.71	17	27
7	11	15	2.57	11	22
8	11	20	2.35	17	24
9	11	11	1.13	10	12
10	11	20	2.77	13	24

Table 36 Mean value, standard deviation, minimum and maximum of the pennation angle of the left LD in all horses taken by operator 1 in (°).

Horse	N	Mean (°)	Stdev. (°)	Minimum (°)	Maximum (°)
1	11	16	2.45	12	19
2	11	15	3.03	10	20
3	11	20	2.27	16	24
4	11	21	2.75	16	25
5	11	17	2.88	11	21
6	11	21	3.15	17	27
7	11	16	2.50	11	22
8	11	20	2.47	17	24
9	11	12	1.39	10	13
10	11	20	2.82	13	24

Table 37 Mean value, standard deviation, minimum and maximum of the pennation angle of the right LD in all horses taken by operator 2 in (°).

Horse	N	Mean (°)	Stdev. (°)	Minimum (°)	Maximum (°)
1	11	15	2.27	12	19
2	11	14	2.37	10	17
3	11	18	2.13	14	23
4	11	19	3.47	14	25
5	11	18	3.18	11	24
6	11	22	3.17	17	27
7	11	15	2.45	11	22
8	11	21	2.04	18	24
9	11	13	0.65	12	13
10	11	20	2.71	13	23

Table 38 Mean value, standard deviation, minimum and maximum of the pennation angle of the left LD in all horses taken by operator 2 in (°).

Horse	N	Mean (°)	Stdev. (°)	Minimum (°)	Maximum (°)
1	11	16	2.01	14	19
2	11	15	3.03	10	20
3	11	19	2.56	14	24
4	11	20	3.87	14	25
5	11	19	2.92	12	24
6	11	20	2.65	17	25
7	11	16	0.97	14	17
8	11	20	2.15	17	23
9	11	12	1.39	10	13
10	11	21	2.04	18	24

III.4.4 Discussion and Conclusion

In humans, numerous studies demonstrated that ultrasound images are helpful in quantifying muscle tissue by measuring muscle depth, muscle fibre pennation angle, muscle fibre length and echogenicity (Aagard and al 2001; Binzoni *et al.* 2001; Kawakami *et al.* 2006; Kubo *et al.* 2003a; Maganaris *et al.* 1998; Maurits *et al.* 2003; Narici *et al.* 2003; Nielsen *et al.* 2000; Strobel *et al.* 2005). Ultrasound measurements of the human multifidus and abdominal muscle thickness have been described in the literature (Kiesel *et al.* 2007) but there was no such ultrasound study of the equine LD to the author's knowledge.

In the presented study 800 ultrasound images of LD of ten ponies were obtained by two examiners to test inter- and intraoperator repeatability of LD muscle thickness and pennation angle measurements. Image quality was very variable and therefore only 440 images were selected for further processing. The quality of the images was influenced by different factors. Due to the standardised imaging modality (standardised gain) the image quality was not adjusted for individual images. Image quality was also influenced by the resolution of the ultrasound machine. Muscle fibre architecture of LD and fascicle layers were not always well-defined in all of the ultrasound images. Nevertheless the distance between subcutaneous tissue and the rib, functioning as a landmark for the vertebral level and as reference for the ventral circumference of LD, was visible as hyperechoic line in the selected images. On some images it was difficult to detect the dorsal circumference of the rib without putting pressure on the ultrasound transducer. As varying pressure would have altered and falsified muscle thickness measurements the obtained images showed only indistinct muscle structure and a small rib

section in some cases. Fat tissue has been demonstrated to influence the quality of ultrasound images of skeletal muscles and increase muscle echogenicity in humans (Haberkorn *et al.* 1993; Lee *et al.* 2006; Reimers *et al.* 1993). Additionally, the lack of visual defined muscle structure has been described previously in humans and was suspected as a diagnostic sign of muscle atrophy (Kristjansson 2004). As the examined horses were untrained and overweight they had varying layer of subcutaneous fat as well as intramuscular fat and connective tissue which might have influenced image quality. The difference between image quality of trained and untrained LD as well as between different ultrasound machines is demonstrated in Fig. 56. The architecture of muscle fascicles of a trained thoroughbred horse imaged with an advanced high-tech ultrasound machine is more clearly defined and hence more easily visualised ultrasonographically compared to untrained ponies imaged with a middle of the range ultrasound machine.

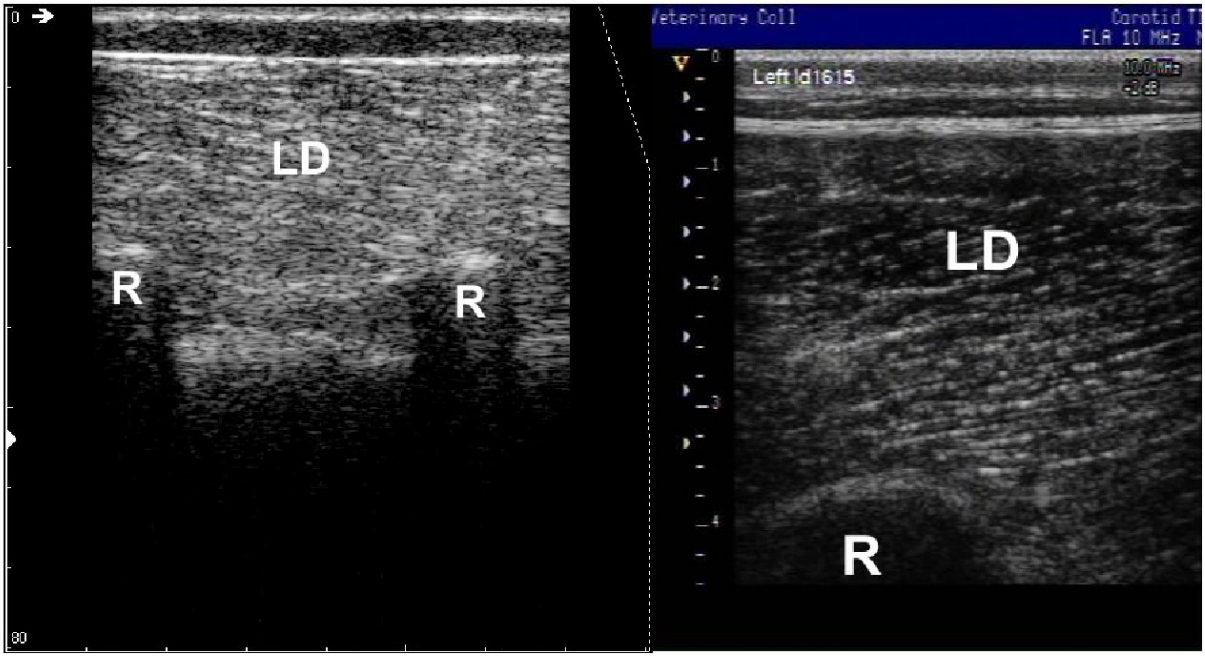

Fig. 56 Ultrasound image of LD of a trained thoroughbred imaged by a high quality ultrasound mashine (right) in comparison with an ultrasound image of LD of an untrained pony imaged by a ultrasound mashine of less quality

Analysed muscle parameters showed that muscle thickness and pennation angle were not significant different between right and left LD which would be expected in horses without any back pathology and/or lameness. But muscle thickness and pennation angle measurements were significant different between horses. The significant difference between horses can be related to multiple factors such as training condition of the horse, age, different height and

weight. Although the influence of weight, age and training condition was described in the literature in humans (Seynnes *et al.*, 2007; Sipila and Suominen, 1996) there was no correlation between age, weight and heights of the horses and muscle thickness or pennation angle.

LD muscle thickness imaged by two different examiners was proven to be a repeatable parameter. The results correspond to human ultrasound studies where intra- and interobserver reliability was tested for different skeletal muscles. Results demonstrated a high repeatability for intra-observer and inter-observer measurements (Hides *et al.* 2007; Wallwork *et al.* 2007) although one study found a lack of agreement between experienced and novice observers. In conclusion it was suggested that inexperienced observers perform ultrasound training before using ultrasound measurements to quantify muscle tissue (Hides *et al.* 2007). In the present study limits of agreement were found to range from -0.3 cm to 0.5 cm (Bland and Altman 2007). These upper and lower limits seem to be satisfying in regards to a study of the cross-section area of the equine multifidus where the lower and upper limit of agreement ranged from -1.35 cm^2 to 1.54 cm^2 and were found to be acceptable (Tabor and McGowan 2002).

The average repeatability coefficient for both examiners was 0.4 cm which seems to be acceptable in comparison with the mean± stdev muscle thickness value. However, ultrasound studies of human muscle parameters showed a 10-31% increase of muscle thickness after training or 2-6% decrease after 20 days of bed rest depending on the measured muscle group (Abe et al 1997, Abe et al 2000) as there are no comparable studies available in the equine LD or equine musculature it is difficult to predict the amount of muscle thickness changes of LD due to disuse or training. With regards to the reported percentages of human muscle changes following disuse and training the repeatability coefficient of 0.4 cm in the present study suggests that only muscle changes larger then >13% would give reliable evidence of LD changes.

In contrast to LD muscle thickness LD pennation angle showed low repeatability in this study. The width of 95% limits of agreement (14°) is not acceptable for using this parameter as a measurement to document muscle atrophy or monitor training or treatment effects. Repeatability of measuring pennation angle was affected by the ability of the operator to identify muscle fibres but also influenced by the fact that pennation angle changes with muscle contraction.

In conclusion, ultrasonography is a non-invasive, safe and relatively cheap technique to visualise skeletal muscle. In this study ultrasonography was proven to be a repeatable

technique to evaluate muscle thickness in the equine LD. To be able to evaluate relatively small muscle thickness changes and pennation angle of the equine LD ultrasonography needs to be reassessed in comparison with other techniques for example dissection and/ or computed tomography.

IV. Discussion and Conclusion

The equine back is part of the axis of the equine body and provides the connection between fore- and hindlimbs. Back pain has been frequently reported to effect the horse but misleading clinical signs and unspecific symptoms make its diagnosis and treatment a challange. The aetioapathogenesis of back pain is poorly understood and the role of the paraspinal muscles, influencing and causing back pain, is unclear.
This thesis aimed at enhancing the understanding of the functional capacity of the thoracolumbar LD by examining the muscle architecture of LD and its muscle activity at different levels along this muscle. This knowledge provides a basis for further research into horses with back problems. Additionally, ultrasonography was evaluated by imaging LD muscle structure and measuring muscle parameters such as muscle thickness in order to install this diagnostic technique as valuable method to examine LD for pathological changes and quantify the muscle.

Muscle architectural parameters were shown to be useful in estimating the functional capacity of muscles. Muscle fascicle length, pennation angle and physiological cross-section area characterise muscle structure and determine muscle function. From these architectural parameters the preference of the muscle for either generating force or high velocity contraction over a wide range of excursion can be predicted (Wickiewicz *et al.* 1983). In chapter III.1 architectural measurements of the equine LD revealed the complex structure of this muscle. Muscle parameters show longer muscle fascicles and smaller pennation angle in the cranial part of LD demonstrating that the muscle can perform contractions at higher contraction velocity and over a wider range of excursion. These findings are supported by kinematic experiments which show a higher range of motion at the cranial thoracic vertebral column (Gomez Alvarez 2007). In contrast, architectural parameters of the caudal LD show shorter muscle fascicle length and larger pennation angle. Additionally an internal fascia divides LD in a lateral and a medial part increasing the attachment for muscle fibres and hence the physiological cross-section area of the muscle. The muscle structure of the caudal LD suggests a large capacity to generate force. Again, kinematic measurements of the caudal

equine back support this finding. Except for the lumbosacral junction decreased range of motion was observed for the lumbar vertebral column and implicates strong muscle contraction to restrict back flexion and stabilise the spine. This suggests that LD muscle function in the lumbar area supports the lumbar vertebral spine against dynamic forces of the abdominal contents especially as there is no support of ribs and rib cage. Furthermore the strong lumbar LD provides a base for the attaching cranial part of the middle gluteal muscle and transmits propulsive forces developed by the hindlimb and the hindlimb muscles to the vertebral column.

Measurements of muscle activity of LD (Chapter III.2) supported the functional complexity of the muscle structure. In Chapter III.2 EMG measurements of LD were recorded in the second half of the stance phase of each hindlimb during flexion of the back. Higher intensity of muscle activity was measured at T14 and L2. This finding might be related to the larger range of motion in the cranial thoracic spine and the higher force generation of the lumbar LD. Potential cross-talk of adjacent muscle may have influenced the intensity of LD activity at these segments. In spite of the high muscle intensity at T14 and L2 the muscle activity pattern showed differences between these two segments. A higher percentage of only single or two EMG bursts was demonstrated for T14 and T16 while a higher percentage of two to four EMG bursts were measured mainly at L2. The pattern of two EMG bursts is associated to the second half of the stance phase of each hindlimb. Therefore the lumbar muscle segment showed a higher muscle activity and contracted not only during the ipsilateral but also during the collateral stance phase of the hindlimbs. The effect of gait and incline was demonstrated by the significantly increased intensity of muscle activity on incline of 10% as well as increased intensity of muscle activity between walk and trot. The number of recorded EMG bursts was higher in walk on incline compared to level walk. Increased LD activity on incline has been reported previously for the cat and horses (Robert *et al.* 2001b; Wada *et al.* 2006a). The study in cats walking up an incline suggested that LD actively contributes not only to restrict dorsal flexion but also limit lateral bending which was higher during walk on incline by active muscle contraction (Wada *et al.* 2006a). Although horses have a stiffer vertebral column compared to cats, the propulsive and vertical forces of the hindlimb increase on incline (Dutto *et al.* 2004; Parsons *et al.* 2008). This requires increased stiffness of the vertebral column to transmit the propulsion up the incline against gravity onto the whole body without losing propulsive forces by lateral bending of the body axis.

The difference of LD activity between gaits is related to increased muscle activity and therefore force generation of LD which increases the stiffness of the vertebral column and

spinal stability. Kinematic studies have shown that back motion is significantly decreased in trot compared to walk which depends on higher muscle forces and therefore increased spinal stiffness.

The results of the presented study can provide a base for further research and thorough examination of horses with back pain. In humans back problems were related to unexpected loads or spinal instability which can lead to inflammation, local pain and altered motion which activate mechanoreceptors in ligaments and joint capsules, muscle spindles in the paraspinal musculature and skin receptors (Denegar *et al.* 2006). The afferent signals are processed in the CNS which responds through the activation of appropriate muscles to avoid pain and damage to musculoskeletal structures (Denegar *et al.* 2006). The origin of primary back pain in horses was also reported to be due to mechanical, chemical or other damaging factors affecting nociceptive receptors of soft tissue, vertebral bone or articulations of the equine back (Jeffcott and Haussler 2004).

In human patients with low back pain altered EMG activity of the back muscles was detected during trunk motion and gait (van Dieën, 2003). Increased EMG activity was recorded during the swing phase where the lumbar muscles are normally silent. Another study of patients with chronic back pain showed decreased EMG activity during trunk motion suggesting avoidance behaviour and disuse (Thomas, 2008). Experimentally induced back pain and slight lameness in horses were shown to effect back kinematics significantly (Gomez Alvarez 2007). Increased extension and compensatory lateral movement in horses with unilateral back pain suggest an increase in back muscle activity. Increased flexion and extension and a lateral bending away from the lame forelimb was detected in horses with induced forelimb lameness. Also horses with increased hindlimb lameness showed a slight increase of back motion but a decreased range of motion of the lumbosacral segment and the pelvis (Gomez Alvarez 2007). Consequently LD muscle activation would be expected to change with back pain and lameness. Increased LD activity may support increased lateral bending and extension to avoid unexpected painful movements. Based on the presented EMG measurements the influence of back pain on the activity of muscle segments along the equine LD could be examined.

Changes of LD structure due to back problems, training or treatment are more difficult to document in live horses as architectural measurements of the equine LD can obviously be not accomplished by dissections in live horses. In chapter III.3 and III.4 of the present thesis ultrasound was evaluated as a method to visualise and measure LD and its architectural parameters in live horses. For the examination of the paraspinal soft tissue structures ultrasonography seems to be the method of choice as it is non-invasive, low-cost intensive and

practicable to use. The gross LD structure documented in longitudinal and transverse ultrasound images corresponded to the frozen muscle slices of the same muscle section. Therefore ultrasound allows visualisation of the overall muscle structure, subcutaneous fat amount and the relationship between LD and adjacent muscles such as spinalis, ilicostal and the cranial part of the middle gluteal muscle. The proportion of fat and connective tissue is visible as hyperechoic marbling (Wood *et al.* 1999). In future it would be interesting to show the ratio of intramuscular fat and connective tissue to LD muscle tissue in horses with back problems since studies in humans have demonstrated an increase of intramuscular fat with disuse. Other muscle parameters measured on ultrasound images such as muscle thickness, pennation angle and muscle fibre length were shown to quantify musculature in humans.
Chapter III.4 showed the repeatability of LD muscle thickness measurements in the horse. Muscle thickness is closely associated with muscle volume (Miyatani *et al.* 2004) and therefore could be a helpful parameter to document equine back muscle dysfunction leading, for example, to muscle atrophy or hypertrophy. In humans, quantifying muscle tissue by ultrasound has been already used to show changes of musculature due to disuse and back or neck pain as well as muscle changes following training (Abe *et al.* 1997; Hides *et al.* 2008; Kawakami *et al.* 1995; Suetta *et al.* 2008). Therefore measurements of LD muscle thickness could be helpful to monitor back treatment and training effects by ultrasound in horses. In present study muscle thickness measurements were found to be repeatable but pennation angle measurements on ultrasound images were not. The reason for this might be due to the quality of ultrasound images where in some cases muscle fascicle insertion and orientation were difficult to follow and the variability of pennation angle with contraction status of the muscle. Ultrasound image quality between different horses was influenced by the standardised imaging set up (standardised depth and gain) which could not be adjusted to the different physical conditions of the individual horse. Additionally subcutaneous fat thickness of the untrained horses might have influenced the image quality as increased thickness of fat layers were shown to effect image brightness and sharpness in humans (Haberkorn *et al.* 1993) However, ultrasound was shown to be a useful and practical technique to examine back muscle structure but further studies are necessary to document the influence of age and gender as well as to document the effect of back problems on changes of LD muscle parameters.

In conclusion the presented thesis provides anatomical as well as functional information about the equine LD and also includes data about the use of ultrasound in the assessement of the LD in live horses. This will aid in determining the role of LD disorders in the development of

back problems in the horse, the pathogenesis of which is is not well understood at the moment, one of the reasons why the diagnosis and treatment of back problems presents the equine practitioner with a huge challenge.

V. References

Aagard, P *et al*., (2001) A mechanism for increased contractile strength of human pennate muscle in response to strength training: changes in muscle architecture. *The Journal of Physiology*, 613-623.

Abe, T., Brechue, W.F., Fujita, S. and Brown, J.B. (1998) Gender differences in FFM accumulation and architectural characteristics of muscle. *Med Sci Sports Exerc* **30**, 1066-1070.

Abe, T., DeHoyos, D.V., Pollock, M.L. and Garzarella, L. (2000a) Time course for strength and muscle thickness changes following upper and lower body resistance training in men and women. *Eur J Appl Physiol* **81**, 174-180.

Abe, T., Kawakami, Y., Suzuki, Y., Gunji, A. and Fukunaga, T. (1997) Effects of 20 days bed rest on muscle morphology. *J Gravit Physiol* **4**, S10-14.

Abe, T., Kumagai, K. and Brechue, W.F. (2000b) Fascicle length of leg muscles is greater in sprinters than distance runners. *Med Sci Sports Exerc* **32**, 1125-1129.

Alexander, M.J. (1985) Biomechanical aspects of lumbar spine injuries in athletes: a review. *Can J Appl Sport Sci* **10**, 1-20.

Alexander, R. (2003) *Principles of animal locomotion*, Princeton University, Princeton, New Jersey.

Alexander, R., Dimery, N. and Ker, R. (1985) Elastic structures in the back and their role in galloping in some mammals. *Journal of Zoology*, 467-482.

Alexander, R. and Vernon, A. (1975) The dimensions of knee and ankle muscles and the forces they exert. *Journal of Human Movement Studies* **1**, 115-123.

Alexander, R.M. (1991) Energy-saving mechanisms in walking and running. *J Exp Biol* **160**, 55-69.

Audigie, F., Pourcelot, P., Degueurce, C., Denoix, J.M. and Geiger, D. (1999) Kinematics of the equine back: flexion-extension movements in sound trotting horses. *Equine Vet J Suppl* **30**, 210-213.

Back, W. and Clayton, H. (2001) *Equine Locomotion*, Saunders.

Baumgartner, R.N., Koehler, K.M., Gallagher, D., Romero, L., Heymsfield, S.B., Ross, R.R., Garry, P.J. and Lindeman, R.D. (1998) Epidemiology of sarcopenia among the elderly in New Mexico. *Am J Epidemiol* **147**, 755-763.

Biewener, A.A. (2003) *Animal Locomotion*, Oxford University Press Inc., New York.

Biewener, A.A. and Roberts, T.J. (2000) Muscle and tendon contributions to force, work, and elastic energy savings: a comparative perspective. *Exerc Sport Sci Rev* **28**, 99-107.

Binzoni, T., Bianchi, S., Hanquinet, S., Kaelin, A., Sayegh, Y., Dumont, M. and Jequier, S. (2001) Human gastrocnemius medialis pennation angle as a function of age: from newborn to the elderly. *J Physiol Anthropol Appl Human Sci* **20**, 293-298.

Bland, J.M. and Altman, D.G. (1986) Statistical methods for assessing agreement between two methods of clinical measurement. *Lancet* **1**, 307-310.

Bland, J.M. and Altman, D.G. (2007) Agreement between methods of measurement with multiple observations per individual. *J Biopharm Stat* **17**, 571-582.

Blazevich, A.J., Gill, N.D. and Zhou, S. (2006) Intra- and intermuscular variation in human quadriceps femoris architecture assessed in vivo. *J Anat* **209**, 289-310.

Bleakney, R. and Maffulli, N. (2002) Ultrasound changes to intramuscular architecture of the quadriceps following intramedullary nailing. *J Sports Med Phys Fitness* **42**, 120-125.

Bogduk, N. (1980) A reappraisal of the anatomy of the human lumbar erector spinae. *J Anat* **131**, 525-540.

Bojadsen, T.W., Silva, E.S., Rodrigues, A.J. and Amadio, A.C. (2000) Comparative study of Mm. Multifidi in lumbar and thoracic spine. *J Electromyogr Kinesiol* **10**, 143-149.

Boszczyk, B.M., Boszczyk, A.A. and Putz, R. (2001) Comparative and functional anatomy of the mammalian lumbar spine. *Anat Rec* **264**, 157-168.

Brancaccio, P., Limongelli, F.M., D'Aponte, A., Narici, M. and Maffulli, N. (2007) Changes in skeletal muscle architecture following a cycloergometer test to exhaustion in athletes. *J Sci Med Sport*.

British Standards Institution (1975) *Precision of test methods 1: Guide for the determination and reproducibility for a standard test method (BS 597, Part 1,* London, BSI.

Brown, N.A., Kawcak, C.E., McIlwraith, C.W. and Pandy, M.G. (2003a) Architectural properties of distal forelimb muscles in horses, Equus caballus. *J Morphol* **258**, 106-114.

Brown, N.A., Pandy, M.G., Kawcak, C.E. and McIlwraith, C.W. (2003b) Force- and moment-generating capacities of muscles in the distal forelimb of the horse. *J Anat* **203**, 101-113.

Caldwell, J.S., McNair, P.J. and Williams, M. (2003) The effects of repetitive motion on lumbar flexion and erector spinae muscle activity in rowers. *Clin Biomech (Bristol, Avon)* **18**, 704-711.

Carlson, H. (1978) Morphology and contraction properties of cat lumbar back muscles. *Acta Physiol Scand* **103**, 180-197.

Cassiat, G., Pourcelot, P., Tavernier, L., Geiger, D., Denoix, J.M. and Degueurce, D. (2004) Influence of individual competition level on back kinematics of horses jumping a vertical fence. *Equine Vet J* **36**, 748-753.

Chiou, W.K., Wong, M.K. and Lee, Y.H. (1994) Epidemiology of low back pain in Chinese nurses. *Int J Nurs Stud* **31**, 361-368.

Chow, R.S., Medri, M.K., Martin, D.C., Leekam, R.N., Agur, A.M. and McKee, N.H. (2000) Sonographic studies of human soleus and gastrocnemius muscle architecture: gender variability. *Eur J Appl Physiol* **82**, 236-244.

Clayton, H. (1999) The Mysteries of the Back. *Dressage Today*, 28.

Danneels, L.A., Vanderstraeten, G.G., Cambier, D.C., Witvrouw, E.E. and De Cuyper, H.J. (2000) CT imaging of trunk muscles in chronic low back pain patients and healthy control subjects. *Eur Spine J* **9**, 266-272.

Demoulin, C., Crielaard, J.M. and Vanderthommen, M. (2007a) Spinal muscle evaluation in healthy individuals and low-back-pain patients: a literature review. *Joint Bone Spine* **74**, 9-13.

Demoulin, C., Distree, V., Tomasella, M., Crielaard, J.M. and Vanderthommen, M. (2007b) Lumbar functional instability: a critical appraisal of the literature. *Ann Readapt Med Phys* **50**, 677-684, 669-676.

Denegar, C., Saliba, E. and Saliba, S. (2006) *Therapeutic Modalities for Musculoskeletal Injuries*, 2nd Edition edn. p 312.

Denoix, J. (1999a) Lesions of the vertebral column in poor performance horses. In: *Proceedings of the World Equine Veterinary Association symposium*, Paris, France.

Denoix, J.M. (1999b) Spinal biomechanics and functional anatomy. *Vet Clin North Am Equine Pract* **15**, 27-60.

Denoix, J.M. (1999c) Ultrasonographic evaluation of back lesions. *Vet Clin North Am Equine Pract* **15**, 131-159.

Denoix, J.M. (2006) Ultrasonographic examination: Back. In: *Back and Beyond, Orhtopaedic Poor Performance: Hindlimbs and Back*, Newmarket. pp 23-30.

Denoix, J.M. and Pailloux, J. (2001) *Physical therapy and massage for the horse*, Manson Publishing Ltd., London.

Drake, J.D. and Callaghan, J.P. (2006) Elimination of electrocardiogram contamination from electromyogram signals: An evaluation of currently used removal techniques. *J Electromyogr Kinesiol* **16**, 175-187.

Drevemo, S., Dalin, G., Fredricson, I. and Hjerten, G. (1980) Equine locomotion; 1. The analysis of linear and temporal stride characteristics of trotting standardbreds. *Equine Vet J* **12**, 60-65.

Dumas, G.A., Poulin, M.J., Roy, B., Gagnon, M. and Jovanovic, M. (1991) Orientation and moment arms of some trunk muscles. *Spine* **16**, 293-303.

Dupont, A.C., Sauerbrei, E.E., Fenton, P.V., Shragge, P.C., Loeb, G.E. and Richmond, F.J. (2001) Real-time sonography to estimate muscle thickness: comparison with MRI and CT. *J Clin Ultrasound* **29**, 230-236.

Dutto, D.J., Hoyt, D.F., Cogger, E.A. and Wickler, S.J. (2004) Ground reaction forces in horses trotting up an incline and on the level over a range of speeds. *J Exp Biol* **207**, 3507-3514.

English, A. (1980) The functions of the lumbar spine during stepping in the cat. *Journal of Morphology*, 55-66.

Erichsen, C., Eksell, P., Holm, K.R., Lord, P. and Johnston, C. (2004) Relationship between scintigraphic and radiographic evaluations of spinous processes in the thoracolumbar spine in riding horses without clinical signs of back problems. *Equine Vet J* **36**, 458-465.

Ettema, G.J. and Huijing, P.A. (1989) Properties of the tendinous structures and series elastic component of EDL muscle-tendon complex of the rat. *J Biomech* **22**, 1209-1215.

Faber, M., Johnston, C., Schamhardt, H., van Weeren, R., Roepstorff, L. and Barneveld, A. (2001a) Basic three-dimensional kinematics of the vertebral column of horses trotting on a treadmill. *Am J Vet Res* **62**, 757-764.

Faber, M., Johnston, C., Schamhardt, H.C., van Weeren, P.R., Roepstorff, L. and Barneveld, A. (2001b) Three-dimensional kinematics of the equine spine during canter. *Equine Vet J Suppl*, 145-149.

Faber, M., Johnston, C., van Weeren, P.R. and Barneveld, A. (2002) Repeatability of back kinematics in horses during treadmill locomotion. *Equine Vet J* **34**, 235-241.

Faber, M., Schamhardt, H., van Weeren, R., Johnston, C., Roepstorff, L. and Barneveld, A. (2000) Basic three-dimensional kinematics of the vertebral column of horses walking on a treadmill. *Am J Vet Res* **61**, 399-406.

Felder, A., Ward, S.R. and Lieber, R.L. (2005) Sarcomere length measurement permits high resolution normalization of muscle fiber length in architectural studies. *J Exp Biol* **208**, 3275-3279.

Ferrari, M., Weller, R., Pfau, T., Payne, R.C. and Wilson, A.M. (2006) A comparison of three-dimensional ultrasound, two-dimensional ultrasound and dissections for determination of lesion volume in tendons. *Ultrasound Med Biol* **32**, 797-804.

Fuglsang-Frederiksen, A., Scheel, U. and Buchthal, F. (1976) Diagnostic yield of analysis of the pattern of electrical activity and of individual motor unit potentials in myopathy. *J Neurol Neurosurg Psychiatry* **39**, 742-750.

Fukunaga, T., Kawakami, Y., Kuno, S., Funato, K. and Fukashiro, S. (1997) Muscle architecture and function in humans. *J Biomech* **30**, 457-463.

Gambaryan, P. (1974) *How Mammals Run: Anatomical Adaptation*, Wiley, New York.

Gans, C. (1982) Fiber architecture and muscle function. *Exerc Sci Sport Sci Revs* **10**, 160-207.

Gans, C. and Bock, W.J. (1965) The functional significance of muscle architecture--a theoretical analysis. *Ergeb Anat Entwicklungsgesch* **38**, 115-142.

Gills, C. (1999) Spinal ligament pathology. *Vet Clin North Am Equine Pract* **15**, 97-102.

Gomez Alvarez, C.B. (2007) *The biomechanical interaction between vertebral column and limbs in the horse: A kinematical study*, University of Utrecht, Utrecht.

Gordon, A.M., Huxley, A.F. and Julian, F.J. (1966) Tension development in highly stretched vertebrate muscle fibres. *J Physiol* **184**, 143-169.

Haberkorn, U., Layer, G., Rudat, V., Zuna, I., Lorenz, A. and van Kaick, G. (1993) Ultrasound image properties influenced by abdominal wall thickness and composition. *J Clin Ultrasound* **21**, 423-429.

Haussler, K.K. (1999) Anatomy of the thoracolumbar vertebral region. *Vet Clin North Am Equine Pract* **15**, 13-26, v.

Haussler, K.K., Bertram, J.E., Gellman, K. and Hermanson, J.W. (2001) Segmental in vivo vertebral kinematics at the walk, trot and canter: a preliminary study. *Equine Vet J Suppl*, 160-164.

Henson, F. (2005) How to: Use diagnostic imaging to work up the back case. In: *BEVA Congress*, Harrogate. p 139.

Herzog, W. (2000) *Skeletal Muscle Mechanisms*, John Wiley & Sons, New York.

Hides, J., Gilmore, C., Stanton, W. and Bohlscheid, E. (2008) Multifidus size and symmetry among chronic LBP and healthy asymptomatic subjects. *Man Ther* **13**, 43-49.

Hides, J.A., Miokovic, T., Belavy, D.L., Stanton, W.R. and Richardson, C.A. (2007) Ultrasound imaging assessment of abdominal muscle function during drawing-in of the abdominal wall: an intrarater reliability study. *J Orthop Sports Phys Ther* **37**, 480-486.

Hides, J.A., Richardson, C.A. and Jull, G.A. (1995) Magnetic resonance imaging and ultrasonography of the lumbar multifidus muscle. Comparison of two different modalities. *Spine* **20**, 54-58.

Hides, J.A., Stokes, M.J., Saide, M., Jull, G.A. and Cooper, D.H. (1994) Evidence of lumbar multifidus muscle wasting ipsilateral to symptoms in patients with acute/subacute low back pain. *Spine* **19**, 165-172.

Hildebrand, M. (1959) Motions of the running cheetah and horse. *Journal of Mammalogy* **40**, 481-495.

Hildebrand, M. (1974) *Analysis of vertebrate structure*, John Wiley and Sons, New York.

Holm, K.R., Wennerstrand, J., Lagerquist, U., Eksell, R. and Johnston, C. (2006) Effect of local analgesia on movement of the equine back. *Equine Vet J* **38**, 65-69.

Hunter, G. (2000) *Muscle physiology, In: NSCA´s essentials of strength training and conditioning*, 2nd edition edn., TB Baechle and RW Earle.

Huxley, A.F. (1957) Muscle structure and theories of contraction. *Prog Biophys Biophys Chem* **7**, 255-318.

Jeffcott, L.B. (1979) The Fourth Sir Frederick Hobday Memorial Lecture. Back problems in the horse--a look at past, present and future progress. *Equine Vet J* **11**, 129-136.

Jeffcott, L.B. (1980) Disorders of the thoracolumbar spine of the horse--a survey of 443 cases. *Equine Vet J* **12**, 197-210.

Jeffcott, L.B. and Dalin, G. (1980) Natural rigidity of the horse's backbone. *Equine Vet J* **12**, 101-108.

Jeffcott, L.B., Dalin, G., Drevemo, S., Fredricson, I., Bjorne, K. and Bergquist, A. (1982) Effect of induced back pain on gait and performance of trotting horses. *Equine Vet J* **14**, 129-133.

Jeffcott, L.B., Dalin, G., Ekman, S. and Olsson, S.E. (1985) Sacroiliac lesions as a cause of chronic poor performance in competitive horses. *Equine Vet J* **17**, 111-118.

Jeffcott, L.B. and Haussler, K.K. (2004) *Back and pelvis; In: Equine Sports Medicine and Surgery,* Saunders.

Johnston, C., Holm, K.R., Erichsen, C., Eksell, P. and Drevemo, S. (2004) Kinematic evaluation of the back in fully functioning riding horses. *Equine Vet J* **36**, 495-498.

Johnston, C., Holmt, K., Faber, M., Erichsen, C., Eksell, P. and Drevemo, S. (2002) Effect of conformational aspects on the movement of the equine back. *Equine Vet J Suppl*, 314-318.

Kamaz, M., Kiresi, D., Oguz, H., Emlik, D. and Levendoglu, F. (2007) CT measurement of trunk muscle areas in patients with chronic low back pain. *Diagn Interv Radiol* **13**, 144-148.

Kandel, E., Schwartz, J. and Jessell, T. (2000) Principles of neural science, McGraw-Hill Professional. p 1568.

Kanehisa, H., Muraoka, Y., Kawakami, Y. and Fukunaga, T. (2003) Fascicle arrangements of vastus lateralis and gastrocnemius muscles in highly trained soccer players and swimmers of both genders. *Int J Sports Med* **24**, 90-95.

Kawakami, Y., Abe, T. and Fukunaga, T. (1993) Muscle-fiber pennation angles are greater in hypertrophied than in normal muscles. *J Appl Physiol* **74**, 2740-2744.

Kawakami, Y., Abe, T., Kanehisa, H. and Fukunaga, T. (2006) Human skeletal muscle size and architecture: variability and interdependence. *Am J Hum Biol* **18**, 845-848.

Kawakami, Y., Abe, T., Kuno, S.Y. and Fukunaga, T. (1995) Training-induced changes in muscle architecture and specific tension. *Eur J Appl Physiol Occup Physiol* **72**, 37-43.

Kawakami, Y., Muraoka, Y., Kubo, K., Suzuki, Y. and Fukunaga, T. (2000) Changes in muscle size and architecture following 20 days of bed rest. *J Gravit Physiol* **7**, 53-59.

Kearns, C.F., Abe, T. and Brechue, W.F. (2000) Muscle enlargement in sumo wrestlers includes increased muscle fascicle length. *Eur J Appl Physiol* **83**, 289-296.

Kearns, C.F., Isokawa, M. and Abe, T. (2001) Architectural characteristics of dominant leg muscles in junior soccer players. *Eur J Appl Physiol* **85**, 240-243.

Khoury, V., Cardinal, E. and Brassard, P. (2008) Atrophy and fatty infiltration of the supraspinatus muscle: sonography versus MRI. *AJR Am J Roentgenol* **190**, 1105-1111.

Kiesel, K.B., Underwood, F.B., Mattacola, C.G., Nitz, A.J. and Malone, T.R. (2007) A comparison of select trunk muscle thickness change between subjects with low back pain classified in the treatment-based classification system and asymptomatic controls. *J Orthop Sports Phys Ther* **37**, 596-607.

Kimura, J. (2001) *Electrodiagnosis in Diseases of Nerve and Muscle: Principles and Practice*, Oxford University Press. p 1024.

Kitamura, K., Tokunaga, M., Iwane, A.H. and Yanagida, T. (1999) A single myosin head moves along an actin filament with regular steps of 5.3 nanometres. *Nature* **397**, 129-134.

Klimstra, M., Dowling, J., Durkin, J.L. and MacDonald, M. (2007) The effect of ultrasound probe orientation on muscle architecture measurement. *J Electromyogr Kinesiol* **17**, 504-514.

Koob, T. and Long, J. (2000) The Vertebrate Body Axis: Evolution and Mechanical Function. *American Zoologist* **40**, 1-18.

Kristjansson, E. (2004) Reliability of ultrasonography for the cervical multifidus muscle in asymptomatic and symptomatic subjects. *Man Ther* **9**, 83-88.

Kubo, K., Kanehisa, H., Azuma, K., Ishizu, M., Kuno, S.Y., Okada, M. and Fukunaga, T. (2003a) Muscle architectural characteristics in women aged 20-79 years. *Med Sci Sports Exerc* **35**, 39-44.

Kubo, K., Kanehisa, H., Azuma, K., Ishizu, M., Kuno, S.Y., Okada, M. and Fukunaga, T. (2003b) Muscle architectural characteristics in young and elderly men and women. *Int J Sports Med* **24**, 125-130.

Kumagai, K., Abe, T., Brechue, W.F., Ryushi, T., Takano, S. and Mizuno, M. (2000) Sprint performance is related to muscle fascicle length in male 100-m sprinters. *J Appl Physiol* **88**, 811-816.

Labeit, S. and Kolmerer, B. (1995) Titins: giant proteins in charge of muscle ultrastructure and elasticity. *Science* **270**, 293-296.

Lee, J.P., Tseng, W.Y., Shau, Y.W., Wang, C.L., Wang, H.K. and Wang, S.F. (2007) Measurement of segmental cervical multifidus contraction by ultrasonography in asymptomatic adults. *Man Ther* **12**, 286-294.

Lee, S.W., Chan, C.K., Lam, T.S., Lam, C., Lau, N.C., Lau, R.W. and Chan, S.T. (2006) Relationship between low back pain and lumbar multifidus size at different postures. *Spine* **31**, 2258-2262.

Licka, T., Frey, A. and Peham, C. (2009) Electromyographic activity of the longissimus dorsi muscles in horses when walking on a treadmill. *Vet J* **180 (1)**, 71-76.

Licka, T. and Peham, C. (1998) An objective method for evaluating the flexibility of the back of standing horses. *Equine Vet J* **30**, 412-415.

Licka, T., Peham, C. and Zohmann, E. (2001a) Range of back movement at trot in horses without back pain. *Equine Vet J Suppl*, 150-153.

Licka, T.F., Peham, C. and Frey, A. (2004) Electromyographic activity of the longissimus dorsi muscles in horses during trotting on a treadmill. *Am J Vet Res* **65**, 155-158.

Licka, T.F., Peham, C. and Zohmann, E. (2001b) Treadmill study of the range of back movement at the walk in horses without back pain. *Am J Vet Res* **62**, 1173-1179.

Lieber, R.L. (2002) *Skeletal Muscle Structure, Function and Plasticity*, Lippincott Williams & Wilkins. p 369.

Lieber, R.L. and Blevins, F.T. (1989) Skeletal muscle architecture of the rabbit hindlimb: functional implications of muscle design. *J Morphol* **199**, 93-101.

Lu, W.W., Hu, Y., Luk, K.D., Cheung, K.M. and Leong, J.C. (2002) Paraspinal muscle activities of patients with scoliosis after spine fusion: an electromyographic study. *Spine* **27**, 1180-1185.

Lupton, J.I. (1876) *Mayhew´s illustrated horse management*, Allen, London.

Maganaris, C.N. and Baltzopoulos, V. (1999) Predictability of in vivo changes in pennation angle of human tibialis anterior muscle from rest to maximum isometric dorsiflexion. *Eur J Appl Physiol Occup Physiol* **79**, 294-297.

Maganaris, C.N., Baltzopoulos, V. and Sargeant, A.J. (1998) In vivo measurements of the triceps surae complex architecture in man: implications for muscle function. *J Physiol* **512 (Pt 2)**, 603-614.

Magid, A. and Law, D.J. (1985) Myofibrils bear most of the resting tension in frog skeletal muscle. *Science* **230**, 1280-1282.

Maurits, N.M., Bollen, A.E., Windhausen, A., De Jager, A.E. and Van Der Hoeven, J.H. (2003) Muscle ultrasound analysis: normal values and differentiation between myopathies and neuropathies. *Ultrasound Med Biol* **29**, 215-225.

McLaughlin, R.M., Jr., Gaughan, E.M., Roush, J.K. and Skaggs, C.L. (1996) Effects of subject velocity on ground reaction force measurements and stance times in clinically normal horses at the walk and trot. *Am J Vet Res* **57**, 7-11.

Medler, S. (2002) Comparative trends in shortening velocity and force production in skeletal muscles. *Am J Physiol Regul Integr Comp Physiol* **283**, R368-378.

Mendez, J. and Keys, A. (1960) Density and composition of mammalian muscle. *Metabolism* **9**, 184-188.

Miyatani, M., Kanehisa, H., Ito, M., Kawakami, Y. and Fukunaga, T. (2004) The accuracy of volume estimates using ultrasound muscle thickness measurements in different muscle groups. *Eur J Appl Physiol* **91**, 264-272.

Moorhouse, K. (2005) *Role of Intrinsic and Reflexive Dynamics in the Control of Spinal Stability*, State University Virginia, Blacksburg, Virginia.

Narici, M. (1999) Human skeletal muscle architecture studied in vivo by non-invasive imaging techniqiue: functional significance and application. *Journal of Electromyography and Kinesiology* **9**, 97-103.

Narici, M.V., Maganaris, C.N., Reeves, N.D. and Capodaglio, P. (2003) Effect of aging on human muscle architecture. *J Appl Physiol* **95**, 2229-2234.

Nickel, R., Schummer, A. and Seiferle E.. (1984) *Lehrbuch der Anatomie der Haustiere*, Verlag Paul Parey.

Nielsen, P.K., Jensen, B.R., Darvann, T., Jorgensen, K. and Bakke, M. (2000) Quantitative ultrasound image analysis of the supraspinatus muscle. *Clin Biomech (Bristol, Avon)* **15 Suppl 1**, S13-16.

Nordin, M. and Hirsch-Frankel, V. (2001) *Basic Biomechanics of the Musculoskeletal System*, Lippincott Williams & Wilkins. p 467.

O´Reilly, J., Summers, A. and Ritter, D. (2000) The Evolution of the Functional Role of Trunk Muscles During Locomotion in Adult Amphibians. *American Zoologist*, 123-135.

Otten, E. (1988) Concepts and models of functional architecture in skeletal muscle. *Exerc Sport Sci Rev* **16**, 89-137.

Pabst, D. (2000) To Bend a dolphin: convergence of Force Transmission Designs in Cetaceans and Scombrid Fishes. *American Zoologist* **40**.

Panjabi, M.M. (2003) Clinical Spinal Instabilitz and Low Back Pain.. *J Electromyogr Kinesiol* ***13,371-379***.

Panjabi, M.M. (1992a) The stabilizing system of the spine. Part I. Function, dysfunction, adaptation, and enhancement. *J Spinal Disord* **5**, 383-389; discussion 397.

Panjabi, M.M. (1992b) The stabilizing system of the spine. Part II. Neutral zone and instability hypothesis. *J Spinal Disord* **5**, 390-396; discussion 397.

Parsons, K.J., Pfau, T. and Wilson, A.M. (2008) High-speed gallop locomotion in the thoroughbred racehorse. I. The effect of incline on stride parameters. *J Exp Biol* **211**, 935-944.

Payne, R.C., Crompton, R.H., Isler, K., Savage, R., Vereecke, E.E., Gunther, M.M., Thorpe, S.K. and D'Aout, K. (2006) Morphological analysis of the hindlimb in apes and humans. I. Muscle architecture. *J Anat* **208**, 709-724.

Payne, R.C., Hutchinson, J.R., Robilliard, J.J., Smith, N.C. and Wilson, A.M. (2005) Functional specialisation of pelvic limb anatomy in horses (Equus caballus). *J Anat* **206**, 557-574.

Payne, R.C., Veenman, P. and Wilson, A.M. (2004) The role of the extrinsic thoracic limb muscles in equine locomotion. *J Anat* **205**, 479-490.

Peham, C., Frey, A., Licka, T. and Scheidl, M. (2001) Evaluation of the EMG activity of the long back muscle during induced back movements at stance. *Equine Vet J Suppl*, 165-168.

Peham, C. and Schobesberger, H. (2006) A novel method to estimate the stiffness of the equine back. *J Biomech* **39**, 2845-2849.

Pillen, S., Scholten, R.R., Zwarts, M.J. and Verrips, A. (2003) Quantitative skeletal muscle ultrasonography in children with suspected neuromuscular disease. *Muscle Nerve* **27**, 699-705.

Pourcelot, P., Audigie, F., Degueurce, C., Denoix, J.M. and Geiger, D. (1998) Kinematics of the equine back: a method to study the thoracolumbar flexion-extension movements at the trot. *Vet Res* **29**, 519-525.

Prentice, W. and Voight, M. (2001) *Techniques in Musculoskeletal Rehabilitation*, McGraw-Hill Professional. p 780.

Quiroz-Rothe, E., Novales, M., Aguilera-Tejero, E. and Rivero, J.L. (2002) Polysaccharide storage myopathy in the M. longissimus lumborum of showjumpers and dressage horses with back pain. *Equine Vet J* **34**, 171-176.

Rankin, G., Stokes, M. and Newham, D.J. (2005) Size and shape of the posterior neck muscles measured by ultrasound imaging: normal values in males and females of different ages. *Man Ther* **10**, 108-115.

Rankin, G., Stokes, M. and Newham, D.J. (2006) Abdominal muscle size and symmetry in normal subjects. *Muscle Nerve* **34**, 320-326.

Rantanen, N.W. and McKinnon, A.O. (1997) *Equine Diagnostic Ultrasonography*, Blackwell Publishing.

Rassier, D.E., MacIntosh, B.R. and Herzog, W. (1999) Length dependence of active force production in skeletal muscle. *J Appl Physiol* **86**, 1445-1457.

Reef, V. (1998) *Equine Diagnostic Ultrasound*, Saunders.

Reeves, N.D., Maganaris, C.N. and Narici, M.V. (2004) Ultrasonographic assessment of human skeletal muscle size. *Eur J Appl Physiol* **91**, 116-118.

Reimers, C.D., Harder, T. and Saxe, H. (1998) Age-related muscle atrophy does not affect all muscles and can partly be compensated by physical activity: an ultrasound study. *J Neurol Sci* **159**, 60-66.

Reimers, C.D., Schlotter, B., Eicke, B.M. and Witt, T.N. (1996) Calf enlargement in neuromuscular diseases: a quantitative ultrasound study in 350 patients and review of the literature. *J Neurol Sci* **143**, 46-56.

Reimers, K., Reimers, C.D., Wagner, S., Paetzke, I. and Pongratz, D.E. (1993) Skeletal muscle sonography: a correlative study of echogenicity and morphology. *J Ultrasound Med* **12**, 73-77.

Rewcastle, S. (1983) Fundamental adaptations in hte lacertilian hind limb: A partial analysis of the sprawling limb posture and gait. *Copeia*, 476-487.

Rhodin, M., Johnston, C., Holm, K.R., Wennerstrand, J. and Drevemo, S. (2005) The influence of head and neck position on kinematics of the back in riding horses at the walk and trot. *Equine Vet J* **37**, 7-11.

Ritter, D. (1995) Epaxial muscle function during locomotion in a lizard (Varanus salvator) and the proposal of a key innovation in the vertebrate axial musculoskeletal system. *J Exp Biol* **198**, 2477-2490.

Ritter, D.A., Nassar, P.N., Fife, M. and Carrier, D.R. (2001) Epaxial muscle function in trotting dogs. *J Exp Biol* **204**, 3053-3064.

Robert, C., Audigié, F., Valette, J.P., Pourcelot, P. and Denoix, J.M. (2001a) Effects of treadmill speed on the mechanics of the back in the trotting saddlehorse. *Equine Vet J Suppl*, 154-159.

Robert, C., Valette, J.P., Degueurce, C. and Denoix, J.M. (1999) Correlation between surface electromyography and kinematics of the hindlimb of horses at trot on a treadmill. *Cells Tissues Organs* **165**, 113-122.

Robert, C., Valette, J.P. and Denoix, J.M. (2001b) The effects of treadmill inclination and speed on the activity of three trunk muscles in the trotting horse. *Equine Vet J* **33**, 466-472.

Robert, C., Valette, J.P., Pourcelot, P., Audigié, F. and Denoix, J.M. (2002) Effects of trotting speed on muscle activity and kinematics in saddlehorses. *Equine Vet J Suppl*, 295-301.

Rockwell, E., Evans, F. and Pheasant, H. (1938) The comparative morphology of the vertebral spinal column. *Journal of Morphology*.

Rooney, J. (1982) The Horse Back: Biomechanics of Lameness. *Equine Practice* **4**, 17-27.

Ross, M. and Dyson, S. (2002) *Diagnosis and Management of Lameness in the horse*, Saunders.

Rutherford, O.M. and Jones, D.A. (1992) Measurement of fibre pennation using ultrasound in the human quadriceps in vivo. *Eur J Appl Physiol Occup Physiol* **65**, 433-437.

Sacks, R.D. and Roy, R.R. (1982) Architecture of the hind limb muscles of cats: functional significance. *J Morphol* **173**, 185-195.

Sanada, K., Kearns, C.F., Midorikawa, T. and Abe, T. (2006) Prediction and validation of total and regional skeletal muscle mass by ultrasound in Japanese adults. *Eur J Appl Physiol* **96**, 24-31.

Schlacher, C., Peham, C., Licka, T. and Schobesberger, H. (2004) Determination of the stiffness of the equine spine. *Equine Vet J* **36**, 699-702.

Scholten, R.R., Pillen, S., Verrips, A. and Zwarts, M.J. (2003) Quantitative ultrasonography of skeletal muscles in children: normal values. *Muscle Nerve* **27**, 693-698.

Seidman, J. and Seidman, C. (2001) The genetic basis for cardiomyopathy: from mutation identification to mechanistic paradigms. *Cell* **104**, 5557-5567.

Seynnes, O.R., de Boer, M. and Narici, M.V. (2007) Early skeletal muscle hypertrophy and architectural changes in response to high-intensity resistance training. *J Appl Physiol* **102**, 368-373.

Sharir, A., Milgram, J. and Shahar, R. (2006) Structural and functional anatomy of the neck musculature of the dog (Canis familiaris). *J Anat* **208**, 331-351.

Sipila, S. and Suominen, H. (1991) Ultrasound imaging of the quadriceps muscle in elderly athletes and untrained men. *Muscle Nerve* **14**, 527-533.

Smith, N.C., Wilson, A.M., Jespers, K.J. and Payne, R.C. (2006) Muscle architecture and functional anatomy of the pelvic limb of the ostrich (Struthio camelus). *J Anat* **209**, 765-779.

Sofka, C.M., Haddad, Z.K. and Adler, R.S. (2004) Detection of muscle atrophy on routine sonography of the shoulder. *J Ultrasound Med* **23**, 1031-1034.

Stokes, M., Rankin, G. and Newham, D.J. (2005) Ultrasound imaging of lumbar multifidus muscle: normal reference ranges for measurements and practical guidance on the technique. *Man Ther* **10**, 116-126.

Strobel, K., Hodler, J., Meyer, D.C., Pfirrmann, C.W., Pirkl, C. and Zanetti, M. (2005) Fatty atrophy of supraspinatus and infraspinatus muscles: accuracy of US. *Radiology* **237**, 584-589.

Stubbs, N.C., Hodges, P.W., Jeffcott, L.B., Cowin, G., Hodgson, D.R. and McGowan, C.M. (2006) Functional anatomy of the caudal thoracolumbar and lumbosacral spine in the horse. *Equine Vet J Suppl*, 393-399.

Suetta, C., Andersen, J.L., Dalgas, U., Berget, J., Koskinen, S., Aagaard, P., Magnusson, S.P. and Kjaer, M. (2008) Resistance training induces qualitative changes in muscle morphology, muscle architecture, and muscle function in elderly postoperative patients. *J Appl Physiol* **105**, 180-186.

Tabor, G. and McGowan, C.M. (2002) Measurement of equine epaxial muscles using ultrasound imaging. In: *EAVDI Annual Conference*, Murcia, Spain.

Thomas JS, France CR, Sha D, Wiele NV. (2008) The influence of pain-related fear on peak muscle activity and force generation during maximal isometric trunk exertions. *Spine (Phila Pa 1976)* **33**(11):E342-8.

Thorstensson, A., Carlson, H., Zomlefer, M.R. and Nilsson, J. (1982) Lumbar back muscle activity in relation to trunk movements during locomotion in man. *Acta Physiol Scand* **116**, 13-20.

Tokuriki, M. (1973a) Electromyographic and joint-mechanical studies in quadrupedal locomotion. I. Walk. *Nippon Juigaku Zasshi* **35**, 433-436.

Tokuriki, M. (1973b) Electromyographic and joint-mechanical studies in quadrupedal locomotion. II. Trot. *Nippon Juigaku Zasshi* **35**, 525-533.

Tokuriki, M. (1974) Electromyographic and joint-mechanical studies in quadrupedal locomotion. 3. Gallop (author's transl). *Nippon Juigaku Zasshi* **36**, 121-132.

Tokuriki, M. and Aoki, O. (1995) Electromyographic activity of the hindlimb muscles during the walk, trot and canter. *Equine Vet J* **18**, 152-155.

Tokuriki, M., Aoki, O., Niki, Y., Kurakawa, Y., Hataya, M. and Kita, T. (1989) Electromyographic activity of cubital joint muscles in horses during locomotion. *Am J Vet Res* **50**, 950-957.

Tokuriki, M., Ohtsuki, R., Kai, M., Hiraga, A., Oki, H., Miyahara, Y. and Aoki, O. (1999) EMG activity of the muscles of the neck and forelimbs during different forms of locomotion. *Equine Vet J Suppl* **30**, 231-234.

Tokuriki, M., Otsuki, R. and Kai, M. (1997) Electromyographic activity of trunk muscles during locomotion on a treadmill. In: *5th WEVA Congress*, J Equine Vet Sci, Padova. p 488.

Townsend, H.G. and Leach, D.H. (1984) Relationship between intervertebral joint morphology and mobility in the equine thoracolumbar spine. *Equine Vet J* **16**, 461-465.

Townsend, H.G., Leach, D.H., Doige, C.E. and Kirkaldy-Willis, W.H. (1986) Relationship between spinal biomechanics and pathological changes in the equine thoracolumbar spine. *Equine Vet J* **18**, 107-112.

Townsend, H.G., Leach, D.H. and Fretz, P.B. (1983) Kinematics of the equine thoracolumbar spine. *Equine Vet J* **15**, 117-122.

Van der Helm, F.C. and Veenbaas, R. (1991) Modelling the mechanical effect of muscles with large attachment sites: application to the shoulder mechanism. *J Biomech* **24**, 1151-1163.

Van Dieën JH, Selen LP, Cholewicki J. (2003) Trunk muscle activation in low-back pain patients, an analysis of the literature. *J Electromyogr Kinesiol.* **13**(4):333-51. Review

Van Eijden, T.M., Korfage, J.A. and Brugman, P. (1997) Architecture of the human jaw-closing and jaw-opening muscles. *Anat Rec* **248**, 464-474.

Van Roy, P., Barbaix, E., Clarijs, J.P. and Mense, S. (2001) Anatomical background of low back pain: variability and degeneration of the lumbar spinal canal and intervertebral disc. *Schmerz* **15**, 418-424.

Von Tscharner, V. (2000) Intensity analysis in time-frequency space of surface myoelectric signals by wavelets of specified resolution. *J Electromyogr Kinesiol* **10**, 433-445.

Wada, N., Akatani, J., Miyajima, N., Shimojo, K. and Kanda, K. (2006a) The role of vertebral column muscles in level versus upslope treadmill walking-an electromyographic and kinematic study. *Brain Res* **1090**, 99-109.

Wada, N., Miyajima, N., Akatani, J., Shimojo, K. and Kanda, K. (2006b) Electromyographic activity of m. longissimus and the kinematics of the vertebral column during level and downslope treadmill walking in cats. *Brain Res* **1103**, 140-144.

Wakeling JM, Nigg BM, Rozitis AI. (2002) Muscle activity damps the soft tissue resonance that occurs in response to pulsed and continuous vibrations. *J Appl Physiol.* **93**(3):1093-103.

Walker, W. and Liem, K. (1994) *Functional anatomy of the vertebrate*, Saunders college Publishing, Fort Worth.

Wallwork, T.L., Hides, J.A. and Stanton, W.R. (2007) Intrarater and interrater reliability of assessment of lumbar multifidus muscle thickness using rehabilitative ultrasound imaging. *J Orthop Sports Phys Ther* **37**, 608-612.

Walton, J.M., Roberts, N. and Whitehouse, G.H. (1997) Measurement of the quadriceps femoris muscle using magnetic resonance and ultrasound imaging. *Br J Sports Med* **31**, 59-64.

Watanabe, K., Miyamoto, K., Masuda, T. and Shimizu, K. (2004) Use of ultrasonography to evaluate thickness of the erector spinae muscle in maximum flexion and extension of the lumbar spine. *Spine* **29**, 1472-1477.

Weaver, M.P., Jeffcott, L.B. and Nowak, M. (1999) Back problems. Radiology and scintigraphy. *Vet Clin North Am Equine Pract* **15**, 113-129, vii-viii.

Weller, R., Pfau, T., Ferrari, M., Griffith, R., Bradford, T. and Wilson, A. (2007) "The determination of muscle volume with a freehand 3D ultrasonography system". *Ultrasound Med Biol.* 33(3):402-7.

Wells, J.B. (1965) Comparison of Mechanical Properties between Slow and Fast Mammalian Muscles. *J Physiol* **178**, 252-269.

Wennerstrand, J., Johnston, C., Roethlisberger-Holm, K., Erichsen, C., Eksell, P. and Drevemo, S. (2004) Kinematic evaluation of the back in the sport horse with back pain. *Equine Vet J* **36**, 707-711.

Wickiewicz, T.L., Roy, R.R., Powell, P.L. and Edgerton, V.R. (1983) Muscle architecture of the human lower limb. *Clin Orthop Relat Res*, 275-283.

Wijnberg, I.D., Back, W., de Jong, M., Zuidhof, M.C., van den Belt, A.J. and van der Kolk, J.H. (2004) The role of electromyography in clinical diagnosis of neuromuscular locomotor problems in the horse. *Equine Vet J* **36**, 718-722.

Wijnberg, I.D., Franssen, H., Jansen, G.H., Back, W. and van der Kolk, J.H. (2003) Quantitative electromyographic examination in myogenic disorders of 6 horses. *J Vet Intern Med* **17**, 185-193.

Woledge, R.C., Curtin, N.A. and Homsher, E. (1985) Energetic aspects of muscle contraction. *Monogr Physiol Soc* **41**, 1-357.

Wood, J.D., Enser, M., Fisher, A.V., Nute, G.R., Richardson, R.I. and Sheard, P.R. (1999) Manipulating meat quality and composition. *Proc Nutr Soc* **58**, 363-370.

Zajac, F.E. (1989) Muscle and tendon: properties, models, scaling, and application to biomechanics and motor control. *Crit Rev Biomed Eng* **17**, 359-411.

Zuberi, S.M., Matta, N., Nawaz, S., Stephenson, J.B., McWilliam, R.C. and Hollman, A. (1999) Muscle ultrasound in the assessment of suspected neuromuscular disease in childhood. *Neuromuscul Disord* **9**, 203-207.

VI. Summary

Back problems are very common in horses but unlike in humans their aetiopathogenesis are poorly understood and their diagnosis and treatment are a challenge. The role of musculature in the development of back problems in humans is well established, but while this has been suggested to be the case in the horse there is no scientific evidence for this to date.

The aim of this thesis was to evaluate the structure and function of the largest muscle of the equine back, the Longissimus dorsi muscle (LD) and investigate the usefulness of ultrasonography in determining LD architecture in live horses.

Dissection of clinically normal horse and pony cadaver backs demonstrated the complex architecture of this muscle with its regional variations in diameter, muscle fibre length and pennation angle. The cranial thoracic LD was characterised by a small diameter, long muscle fibres and small pennation angles which suggested a specialization for high velocity contractions and excursion. Caudally muscle fibre length decreased whereas the pennation angle and the cross-section area increased. This design enables the muscle to exert large forces economically and to experience high tension.

The observed anatomical differences corresponded to regional differences in muscle activity pattern and the intensity of muscle activity in six horses examined. Electromyographic measurements showed significant differences at different anatomical locations, gaits, speeds and inclines.

Ultrasonography was evaluated as a tool to visualize and quantify LD architecture in live horses. In the first ultrasonographic study the ultrasonographic anatomy of the LD was determined by matching ultrasonographic images to corresponding frozen sections in a cadaver. Inter- and intra-operator repeatability of ultrasound based muscle measurements. While muscle thickness measurements were found to be repeatable, pennation angle was not.

The presented thesis contributes to understanding the biomechanics of the equine LD by illustrating the relationship between anatomy and function through integrating cadaveric data with measurements in live horses. In the second part the use of ultrasonography in determining LD architecture and function in live horses as future diagnostic tool was investigated and its usefulness and limitations established.

VII.Zusammenfassung

Rückenprobleme sind ein zunehmendes Problem in der Pferdepraxis, aber anders als beim Menschen ist die Ätiopathogenese nur wenig erforscht, deshalb sind Diagnose und Behandlung oft eine Herausforderung für den Tierarzt. Beim Menschen ist die Rolle der Rückenmuskulatur in der Entwicklung von Rückenproblemen wissenschaftlich erwiesen. Obwohl dies auch beim Pferd vermutet wird, gibt es bis heute keine wissenschaftliche Erkenntnisse hierzu.

Das Ziel dieser Arbeit war die Stuktur und Funktion des grössten Rückenmuskels des Pferdes, des Musculus longissimus dorsi (LD), zu untersuchen und die ultrasonographische Darstellbarkeit der Muskel Architektur an lebenden Pferden zu erforschen.

Anatomische Sektionen von klinisch gesunden Kavaderrücken veranschaulichten eine komplexe Muskelarchitektur mit unterschiedlichen Durchmesser, Muskelfaserlänge und Fiederungswinkel entlang des Muskels. Der kraniale Teil des LD ist charakterisiert durch einen schmallen Durchmesser, lange Muskelfasern und kleinen Fiederungswinkeln, was daraufhindeutet, dass dieser Teil des Muskels zu schnellen Kontraktionen und grosse Exkursionen fähig ist. In kaudaler Richtung verkürzen sich die Muskelfasern, wohingegen sich der Fiederungswinkel und der Durchmesser des Muskels vergrößert. Diese Anordnung ermöglicht dem Muskel grosse Kräfte zu entwickeln und hoher Spannung zu wiederstehen.

Die festgestellten regionalen anatomischen Unterschiede entlang des LD stimmten mit regionalen Unterschieden in der Muskelaktivität überein. Erregbarkeitsmuster und Intensität der Muskelaktivität wurde in sechs Pferden anhand von elektromyographische Messungen untersucht. Diese zeigten signifikante Unterschiede zwischen verschiedenen Muskelbereichen und unter verschiedenen Bedingungen wie unterschiedlichen Gangarten, Geschwindigkeiten und Steigungen.

Ultraschall wurde als non-invasive Technik zur Visualisierung und Quantifizierung der LD Architektur am lebenden Pferd untersucht. In der ersten Ultraschallstudie wurde die ultrasonographische Anatomie des LD mit den korrospondierenden, gefrorenen Kadaverschnitten verglichen. Die Reproduzierbarkeit von Ultraschall basierten Messungen an lebenden Pferden wurde in einer zweiten Studie untersucht. Es wurde festgestellt, daβ Messungen der Muskeldicke reproduzierbar war, Messungen des Fiederungwinkels aber nicht.

Die vorliegende Doktorarbeit trägt zum biomechanischen Verständniss des equinen LD bei, indem der Zusammenhang zwischen Anatomie und Funktion dargestellt wird. Dies geschieht

durch die Verbindung von Daten aus Untersuchungen mit lebenden Pferden und Kadavern. Im zweiten Teil wurde die Bewertung der LD-Architektur und Funktion durch Ultraschall überprüft um Ultraschall als diagnostische Technik zu etablieren und dessen Limitationen aufzuzeigen.

VIII. Acknowledgements

Formost, I would like to thank Dr. Renate Weller for offering me to do this research project and for her and Dr. Thilo Pfau's unfailing support and patience during the last three years. I also would like to thank Alan Wilson and the Structure and Motion Lab at the Royal Veterinary Collage in London to give me the opportunity and support to realize this project. I would also like to thank Dr. Rachel Payne for her help with chapter III.1, Dr. James Wakeling with chapter III.2, Richard Prior with chapter III.3, Pattama Ritruechai with chapter III.4. and Aviva Petrie for her help with the statistics.

Finally, I would like to thank Dr. Johann Maierl for his efforts during the painstaking corrections and for his profound suggestions when submitting this thesis in Munich.

And last but not least I would like to thank Harald Kronseder for his financial support.